DET-04-028-3
Revision 0
April 1982

ENRICO FERMI ATOMIC POWER PLANT
UNIT 2
PLANT UNIQUE ANALYSIS REPORT
VOLUME 3
VENT SYSTEM ANALYSIS

Prepared for:
Detroit Edison Company

Prepared by:
NUTECH Engineers, Inc.

Prepared by:

Robert A Lehnert

R. A. Lehnert, P.E.
Engineering Manager

Reviewed by:

T. J. Wenner

T. J. Wenner, P.E.
Engineering Director

Approved by:

A B Higginbotham

Dr. A. B. Higginbotham, P.E.
General Manager
Engineering Department

N. W. Edwards

Dr. N. W. Edwards, P.E.
Senior Vice-President

Issued by:

R H Kohrs

R. H. Kohrs, P.E.
Project Director

R H Buchholz

R. H. Buchholz
Project General Manager

nutech ENGINEERS

REVISION CONTROL SHEET

TITLE: ENRICO FERMI ATOMIC POWER PLANT, UNIT 2 PLANT UNIQUE ANALYSIS REPORT VOLUME 3

REPORT NUMBER: DET-04-028-3 Revision 0

J. C. Attwood / Senior Consultant	JCA Initial
M. L. Fitzgerald / Eng. Analyst	MLF Initial
V. Kumar / Project Engineer	VK Initial
A. S. Lee / Specialist	ASL Initial
V. K. Lee / Consultant I	VKRL Initial
R. A. Lehnert / Eng. Manager	RAL Initial
T. Lem / Specialist	TL Initial
K. Loo / Specialist	KLO Initial
J. D. Lowe / Eng. Analyst	JDL Initial
S. Mofid / Specialist	SM Initial

nutech ENGINEERS

REVISION CONTROL SHEET
(Continuation)

TITLE: ENRICO FERMI ATOMIC POWER PLANT, UNIT 2 PLANT UNIQUE ANALYSIS REPORT VOLUME 3

REPORT NUMBER: DET-04-028-3 Revision 0

Kevin E. Parzyck K. E. Parzyck / Eng. Analyst	KEP Initial
R. D. Quinn R. D. Quinn / Consultant I	RDQ Initial
Susan P. Quinn S. P. Quinn / Senior Technician	SQ Initial
Stan Rosenblum S. H. Rosenblum / Consultant I	SHR Initial
M. A. Rupersburg M. A. Rupersburg / Specialist	MR Initial
William E. Smith W. E. Smith / Associate Engineer	WES Initial
Steve S. Tang S. S. Tang / Senior Engineer	ST Initial
Cindy S. Teramoto C. S. Teramoto / Consultant I	CST Initial
Yin Yan Cheng Y. C. Yin / Engineer	yyc Initial

nutech ENGINEERS

TITLE: ENRICO FERMI ATOMIC POWER PLANT, UNIT 2 PLANT UNIQUE ANALYSIS REPORT VOLUME 3

REPORT NUMBER: DET-04-028-3 Revision 0

EFFECTIVE PAGE(S)	REV	PREPARED	ACCURACY CHECK	CRITERIA CHECK
3-vi	0	RAL	VK	VK
3-vii		RAL	SQ	VK
3-viii through 3-ix		RAL	RDQ	VK
3-x through 3-xv		SQ	VK	RAL
3-1.1 through 3-1.7		RAL	RDQ	VK
3-2.1		RAL	VK	VK
3-2.2 through 3-2.10		RAL	WES	VK
3-2.11 through 3-2.24		WES	RAL	VK
3-2.25 through 3-2.55		RAL	RDQ	VK
3-2.56 through 3-2.57		RAL	VK	RDQ
3-2.58		MLF	SM	RAL
3-2.59 through 3-2.62		CST	KLO	VK
3-2.63 through 3-2.64		MLF	KLO	VK
3-2.65 through 3-2.66		MLF	RDQ	RDQ
3-2.67	0	SQ	MLF	VK
3-2.68	0	KEP	KLO	VK
3-2.69 through 3-2.72		RAL	VK	RDQ
3-2.73 through 3-2.74		SQ	VK	RDQ
3-2.75 through 3-2.76		KEP	KLO	VK
3-2.77		MLF	KLO	VK
3-2.78		MLF	KLO	VK
3-2.79 through 3-2.84		SQ	MLF	VK
3-2.85		CST	KLO	VK
3-2.86		SQ	CST	VK
3-2.87		SQ	MLF	VK
3-2.88		SQ	VK	VK
3-2.89 through 3-2.97		RAL	RDQ	VK
3-2.98		SQ	RAL	VK
3-2.99 through 3-2.101		RAL	RDQ	VK
3-2.102 through 3-2.104		RDQ	RAL	VK
3-2.105 through 3-2.108	0	RAL	RDQ	VK

QEP-001.4-00

nutech ENGINEERS

REVISION CONTROL SHEET
(Continuation)

TITLE: ENRICO FERMI ATOMIC POWER PLANT, UNIT 2 PLANT UNIQUE ANALYSIS REPORT VOLUME 3

REPORT NUMBER: DET-04-028-3 Revision 0

EFFECTIVE PAGE(S)	REV	PREPARED	ACCURACY CHECK	CRITERIA CHECK
3-2.109 through 3-2.111	0	RDQ	VK	RAL
3-2.112 through 3-2.132		RAL	RDQ	VK
3-2.133 through 3-2.136		MLF	CST	VK
3-2.137 through 3-2.143		MLF	CST	RDQ
3-2.144 through 3-2.148		RAL	RDQ	VK
3-2.149		KEP	CST	RDQ
3-2.150 through 3-2.158		RAL	RDQ	VK
3-2.159		SQ	CST	RDQ
3-2.160		JDL	yay	RAL
3-2.161 through 3-2.162		KEP	CST	RDQ
3-2.163		JJT	TL	CST
3-2.164 through 3-2.167		RAL	RDQ	VK
3-2.168		SQ	RDQ	VK
3-2.169 through 3-2.170		RAL	RDQ	VK
3-2.171	0	MLF	SM	VK
3-2.172	0	MLF	MAR	VK
3-2.173		TL	CST	RDQ
3-2.174		MAR	S.M	RDQ
3-2.175		KEP	MLF	RDQ
3-2.176		ASL	VKRL	CST
3-2.177		MAR	S.M	RDQ
3-2.178		JHR	JCA	JCA
3-2.179 through 3-2.181		SQ	CST	RAL
3-2.182 through 3-2.186		RAL	RDQ	VK
3-3.1		SQ	VK	RAL

QEP-001.4-00

nutech ENGINEERS

ABSTRACT

The primary containment for the Enrico Fermi Atomic Power Plant, Unit 2, was designed, erected, pressure-tested, and ASME Code N-stamped during the early 1970's for the Detroit Edison Company by the Chicago Bridge and Iron Company. Since that time new requirements, defined in the Nuclear Regulatory Commission's Safety Evaluation Report NUREG-0661, which affect the design and operation of the primary containment system have evolved. The requirements to be addressed include an assessment of additional containment design loads postulated to occur during a loss-of-coolant accident or a safety relief valve discharge event, as well as an assessment of the effects that these postulated events have on the operational characteristics of the containment system.

This plant unique analysis report documents the efforts undertaken to address and resolve each of the applicable NUREG-0661 requirements, and demonstrates, in accordance with NUREG-0661 acceptance criteria, that the design of the primary containment system is adequate and that original design safety margins have been restored. The report is composed of five volumes which are:

- Volume 1 - GENERAL CRITERIA AND LOADS METHODOLOGY
- Volume 2 - SUPPRESSION CHAMBER ANALYSIS
- Volume 3 - VENT SYSTEM ANALYSIS
- Volume 4 - INTERNAL STRUCTURES ANALYSIS
- Volume 5 - SAFETY RELIEF VALVE PIPING ANALYSIS

This volume, Volume 3, which documents the evaluation of the vent system, has been prepared by NUTECH Engineers, Incorporated (NUTECH), acting as an agent responsible to the Detroit Edison Company.

TABLE OF CONTENTS

LIST OF ACRONYMS

ADS	Automatic Depressurization System
ACI	American Concrete Institute
AISC	American Institute of Steel Construction
ASME	American Society of Mechanical Engineers
CDF	Cumulative Distribution Function
CO	Condensation Oscillation
DC	Downcomer
DC/VH	Downcomer/Vent Header
DBA	Design Basis Accident
DBE	Design Basis Earthquake
DLF	Dynamic Load Factor
FSAR	Final Safety Analysis Report
FSI	Fluid-Structure Interaction
FSTF	Full-Scale Test Facility
IBA	Intermediate Break Accident
LDR	Load Definition Report
LOCA	Loss-of-Coolant Accident
MC	Midcylinder
MJ	Mitered Joint
MVA	Multiple Valve Actuation
NEP	Non-Exceedance Probability
NOC	Normal Operating Conditions
NRC	Nuclear Regulatory Commission

LIST OF ACRONYMS
(Concluded)

NVB	Non-Vent Line Bay
NWL	Normal Water Level
OBE	Operating Basis Earthquake
PSD	Power Spectral Density
PUA	Plant Unique Analysis
PUAAG	Plant Unique Analysis Application Guide
PUAR	Plant Unique Analysis Report
PULD	Plant Unique Load Definition
QSTF	Quarter-Scale Test Facility
RPV	Reactor Pressure Vessel
RSEL	Resultant-Static-Equivalent Load
SBA	Small Break Accident
SER	Safety Evaluation Report
SRSS	Square Root of the Sum of the Squares
SRV	Safety Relief Valve
SRVDL	Safety Relief Valve Discharge Line
SSE	Safe Shutdown Earthquake
SVA	Single Valve Actuation
TAP	Torus-Attached Piping
VB	Vent Line Bay
VH	Vent Header
VL	Vent Line
VL/VH	Vent Line/Vent Header

LIST OF TABLES

LIST OF TABLES
(Continued)

LIST OF TABLES
(Concluded)

LIST OF FIGURES

LIST OF FIGURES
(Continued)

LIST OF FIGURES
(Concluded)

3-1.0 INTRODUCTION

In conjunction with Volume 1 of the Plant Unique Analysis Report (PUAR), this volume documents the efforts undertaken to address the requirements defined in NUREG-0661 which affect the Fermi 2 vent system. The vent system PUAR is organized as follows:

- o INTRODUCTION
  - Scope of Analysis
  - Summary and Conclusions
- o VENT SYSTEM ANALYSIS
  - Component Description
  - Loads and Load Combinations
  - Analysis Acceptance Criteria
  - Method of Analysis
  - Analysis Results

The INTRODUCTION section contains an overview discussion of the scope of the vent system evaluation, as well as a summary of the conclusions derived from the comprehensive evaluation of the vent system. The VENT SYSTEM ANALYSIS section contains a comprehensive discussion of the vent system loads and load combinations, and a description of the component parts of the vent system

affected by these loads. The section also contains a discussion of the methodology used to evaluate the effects of these loads, the associated evaluation results, and the acceptance limits to which the results are compared.

3-1.1 Scope of Analysis

The criteria presented in Volume 1 are used as the basis for the Fermi 2 vent system evaluation. The modified vent system is evaluated for the effects of LOCA related loads and SRV discharge related loads defined by the NRC Safety Evaluation Report NUREG-0661 (Reference 1) and the Mark I Containment Program Load Definition Report (LDR) (Reference 2).

The LOCA and SRV discharge loads used in this evaluation are formulated using the methodology discussed in Volume 1 of this report. The loads are developed using the plant unique geometry, operating parameters, and test results contained in the Plant Unique Load Definition (PULD) report (Reference 3). The effects of increased suppression pool temperatures which occur during SRV discharge events are also evaluated. These temperatures are taken from the plant's suppression pool temperature response analysis. Other loads and methodology, such as the evaluation for seismic loads, are taken from the plant's Final Safety Analysis Report (FSAR) (Reference 4).

The evaluation includes performing a structural analysis of the vent system for the effects of LOCA and SRV discharge related loads to confirm that the design of the vent system is adequate. Rigorous analytical techniques are used in this evaluation, including use of detailed analytical models for computing the dynamic response of the vent system. Effects such as local penetration and intersection flexibilities are considered in the vent system analysis.

The results of the structural evaluation for each load are used to evaluate load combinations and fatigue effects for the vent system in accordance with the Mark I Containment Program Structural Acceptance Criteria Plant Unique Analysis Application Guide (PUAAG) (Reference 5). The analysis results are compared with the acceptance limits specified by the PUAAG and the applicable sections of the ASME Code (Reference 6).

3-1.2 Summary and Conclusions

The evaluation documented in this volume is based on the modified Fermi 2 vent system described in Section 1-2.1. The overall load-carrying capacity of the modified vent system and its supports is substantially greater than that of the original suppression chamber design described in the plants's FSAR.

The loads considered in the original design of the vent system include dead weight loads, OBE and DBE loads, thrust loads, and pressure and temperature loads associated with Normal Operating Conditions and a postulated LOCA event. Additional loadings which affect the design of the vent system, postulated to occur during SBA, IBA, or DBA LOCA events and during SRV discharge events, are defined generically in NUREG-0661. These events result in impact and drag loads on vent system components above the suppression pool, hydrodynamic internal pressure loadings on the vent system, hydrodynamic drag loadings on the submerged components of the vent system, and in motions and reaction loadings caused by loads acting on structures attached to the vent system.

The methodology used to develop plant unique loadings for the vent system evaluation is discussed in Section 1-4.0. Applying this methodology results in conservative values for each of the significant NUREG-0661 loadings which envelop those postulated to occur during an actual LOCA or SRV discharge event.

The LOCA and SRV discharge related loads are grouped into event combinations using the NUREG-0661 criteria discussed in Section 1-3.2. The event sequencing and event combinations specified and evaluated envelop the actual events postulated to occur throughout the life of the plant.

Some of the loads contained in the postulated event combinations are major contributors to the total response of the vent system. These include pressurization and thrust loads, pool swell impact loads, condensation oscillation downcomer loads, and chugging downcomer lateral loads. Other loadings, such as internal pressure loads, temperature loads, seismic loads, froth impingement and fallback loads, submerged structure loads, and containment motion and reaction loads, although considered in the evaluation, have a lesser effect on the total response of the vent system.

The vent system evaluation is based on the NUREG-0661 acceptance criteria, which are discussed in Section 1-3.2. These acceptance limits are at least as restrictive as those used in the original vent system design documented in the plant's FSAR. Use of this criteria ensures that the original vent system design margins have been restored.

The controlling event combinations for the vent system are those which include the loadings which have been found to be major contributors to the response of the vent system. The evaluation results for these event combinations show that all of the vent system stresses and support reactions are within acceptable limits.

As a result, the modified vent system described in Section 1-2.1 is adequate to restore the margins of safety inherent in the original design of the vent system documented in the plant's FSAR. The intent of the NUREG-0661 requirements as they affect the design adequacy and safe operation of the Fermi 2 vent system are considered to be met.

3-2.0 VENT SYSTEM ANALYSIS

An evaluation of each of the NUREG-0661 requirements which affect the design adequacy of the Fermi 2 vent system is presented in the sections which follow. The criteria used in this evaluation are contained in Volume 1 of this report.

The component parts of the vent system which are examined are described in Section 3-2.1. The loads and load combinations for which the vent system is evaluated are described and presented in Section 3-2.2. The analysis methodology used to evaluate the effects of these loads and load combinations on the vent system is discussed in Section 3-2.4. The acceptance limits to which the analysis results are compared are discussed and presented in Section 3-2.3. The analysis results and the corresponding vent system design margins are presented in Section 3-2.5.

3-2.1 Component Description

The Fermi 2 vent system is constructed from cylindrical shell segments joined together to form a manifold-like structure which connects the drywell to the suppression chamber. The configuration of the vent system is illustrated in Figures 3-2.1-1 and 3-2.1-2. The major components of the vent system include the vent lines, vent header, and downcomers. The proximity of the vent system to other components of the containment is shown in Figures 3-2.1-3 through 3-2.1-6.

The eight vent lines connect the drywell to the vent header in alternate mitered cylinders of the suppression chamber. The vent lines are nominally 1/4" thick and have an inside diameter of 6'-0". The upper ends of the vent lines are 1/2" thick and include a spherical transition segment at the penetration to the drywell, as shown in Figure 3-2.1-7. The drywell shell at each vent line-drywell penetration is 1-1/2" thick and is reinforced with a 3" thick cylindrical nozzle and a 1-1/2" thick annular pad plate. The vent lines are shielded from jet impingement loads at each vent line-drywell penetration location by jet deflectors which span the openings of the vent lines. The lower ends of the vent

lines are connected to the vent header in the manner of a penstock, as shown in Figure 3-2.1-10. The junction of the vent lines and the vent header are reinforced with 3/4" thick stiffener plates.

The vent header is a continuous assembly of mitered cylindrical shell segments joined together to form a ring header, as shown in Figure 3-2.1-1. The vent header is nominally 1/4" thick and has an inside diameter of 4'-3". Near the vent line-vent header intersections, the vent header has an inside diameter of 6'-0". Conical transition segments connect the smaller and larger diameter portions of the vent header. Additional stiffening for the vent line-vent header intersection is provided by 1-1/2" thick ring plates attached to the vent header transition segments.

A total of eighty downcomers penetrate the vent header in pairs, as shown in Figures 3-2.1-1 and 3-2.1-11. Two downcomer pairs are located in each vent line bay and three pairs are located in each non-vent line bay. Each downcomer consists of an inclined segment which penetrates the vent header and a vertical segment which terminates below the surface of the suppression pool, as shown in Figure 3-2.1-12. The inclined segment is 3/8"

thick and the vertical segment is 1/4" inch thick. Both segments are 2'0" in diameter.

Full penetration welds connect the vent lines to the drywell, the vent lines to the vent header, and the downcomers to the vent header. As such, the connections of the major components of the vent system are capable of developing the full capacity of the associated major components themselves.

The intersections of the downcomers and the vent header are reinforced with a system of stiffener plates and bracing members, as shown in Figures 3-2.1-11 and 3-2.1-12. In the plane of the downcomers, the intersections are stiffened by a 1/2" thick crotch plate located between downcomers in a pair. The connection of the top side of each downcomer to the vent header is reinforced by 1/2" thick outer stiffener plates. Downcomer ring plates which are 1" thick connect the associated crotch plate and the outer stiffener plates. This system of stiffener plates is designed to reduce local intersection stresses caused by loads acting on the submerged portion of the downcomers.

In the direction normal to the plane of the downcomer pair, the intersections are braced by 4" diameter Schedule 80 pipes. One pipe member is located on each side of the vent header. The upper ends of these pipe members are connected to a built-up tee-section and 3/4" thick pad plates attached to the vent header. The lower ends of the pipe members are connected to the downcomer ring plates. The ring plates are stiffened locally with a 3/4" thick gusset plate and pad plate assembly. In addition, the adjacent downcomer pairs in the non-vent line bay are joined by 2" diameter rods, one on either side of the vent header. The ends of these rods are connected to the downcomer rings. The bracing system provides an additional load path for the transfer of loads acting on the submerged portion of the downcomers and results in reduced intersection local stresses. The system of downcomer-vent header intersection stiffener plates and bracing members provides a highly redundant mechanism for the transfer of loads which act on the downcomers, thus reducing the magnitude of loads which pass directly through the intersection.

A bellows assembly is provided at the penetration of the vent line to the suppression chamber as shown in Figure 3-2.1-7. The bellows allow differential movement of the

vent system and suppression chamber to occur without developing significant interaction loads. The bellows assemblies consist of a tandem bellows unit with an inside diameter of 6'-9 3/8". A 1-1/2" thick annular plate connects the upper end of the bellows assembly to the vent line. The lower end of the bellows assembly is connected to the suppression chamber by a 1-3/4" thick nozzle. Each of the two bellows units in the assembly contains a section with five convolutions which are alternately connected to 1/2" thick cylindrical sleeves. The total length of the bellows assembly is 8'-0". The annular plates are attached to the vent lines with 3/8" partial penetration welds.

The SRV piping is routed from the drywell down the vent lines and penetrates the vent lines inside the suppression chamber, as shown in Figures 3-2.1-7 and 3-2.1-8. The vent lines and SRV piping nozzles are reinforced at each vent line-SRV piping penetration location by a 3/4" thick insert plate, two 1-1/2" thick ring plates, a system of 1-1/2" thick gusset plates, and a 16" diameter 1-1/2" thick sleeve on each SRV piping nozzle. The penetration nozzles are attached to the sleeves at the top and bottom by partial penetration welds as shown in Figure 3-2.1-9. The vent line-SRV piping penetration

assembly provides an effective means of transferring loads which act on the SRV piping to the vent line.

Vent header deflectors are provided in the vent line bays and the non-vent line bays, as shown in Figures 3-2.1-6, 3-2.1-10, and 3-2.1-12. The deflectors shield the vent header from pool swell impact loads which occur during the initial phase of a DBA event. In the non-vent line bays, the vent header deflectors are constructed from 12" diameter Schedule 120 pipe with 6" rolled tee-sections attached to either side. The non-vent line bay deflectors are supported by the crotch plates at each vent header-downcomer intersection.

In the vent line bays, the vent header deflectors are constructed from 1-1/2" thick plate, rolled to the same shape as the vent header deflectors in the non-vent line bays. The vent line bay deflectors are supported by the ring plates on the vent line-vent header intersections, by the SRV piping support plates on the vent header, and by the crotch plates at each downcomer-vent header intersection location. The vent header deflectors are designed to completely mitigate pool swell impact loads on the vent header. The vent line bay deflectors also

shield the SRV piping under the vent header from pool swell impact loads.

The drywell/wetwell vacuum breakers (not shown) are eighteen inches in size and extend from mounting flanges attached to 1'-6" diameter, 1" thick nozzles. The nozzles penetrate the vent header at the vent line-vent header intersections, as shown in Figure 3-2.1-10. Additional support for the vacuum breakers at each vent line-vent header intersection location is provided by a system of ring plates, pad plates, and a 10" diameter Schedule 120 pipe beam. The vacuum breaker support system is designed to reduce local stresses at the intersections of the vacuum breaker nozzles and the vent header. The stiffening also reduces motions of the vacuum breakers during dynamic events.

The vent system is supported vertically by two column members at each mitered joint location, as shown in Figures 3-2.1-4, 3-2.1-13 and 3-2.1-14. The support column members are constructed from 10" diameter Schedule 120 pipe. Built-up clevis assemblies are attached to each end of the columns. The upper ends of the support columns are attached to 3/4" thick vent header ring plates with 2-3/8" diameter pins. The ring plates are

attached to the vent header with 1/4" fillet welds. The support column ring plates are reinforced at the pin locations by 3/8" thick cover plates which provide additional bearing capacity and by 1" thick gusset and pad plates which provide additional capacity for drag loads acting on the submerged portion of the support columns. The lower ends of the support columns are attached to 1-1/2" thick ring beam pin plates with 2-3/8" diameter pins. The support column assemblies are designed to transfer vertical loads acting on the vent system to the suppression chamber ring beams, while simultaneously resisting submerged drag loads.

The vent system is supported horizontally by the vent lines which transfer lateral loads acting on the vent system to the drywell at the vent line-drywell penetration locations. The vent lines also provide additional vertical support for the vent system, although primary vertical support is provided by the vent system support columns. The support offered by the vent line bellows is negligible, since the relative stiffness of the bellows with respect to other vent system components is small.

The vent system also provides support for a portion of the SRV piping inside the vent line and suppression chamber, as shown in Figures 3-2.1-3 and 3-2.1-6. Loads which act on the SRV piping are transferred to the vent system by the penetration assembly on the vent line, and by support plates located under the vent line and vent header. Conversely, loads acting on the vent system cause motions to be transferred to the SRV piping at these same support locations. The wetwell SRV piping is extensively tied to the vent system and is evaluated accordingly.

The overall load-carrying capacities of the vent system component parts described in the preceding paragraphs are substantially greater than those of the original vent system design described in the plant's FSAR.

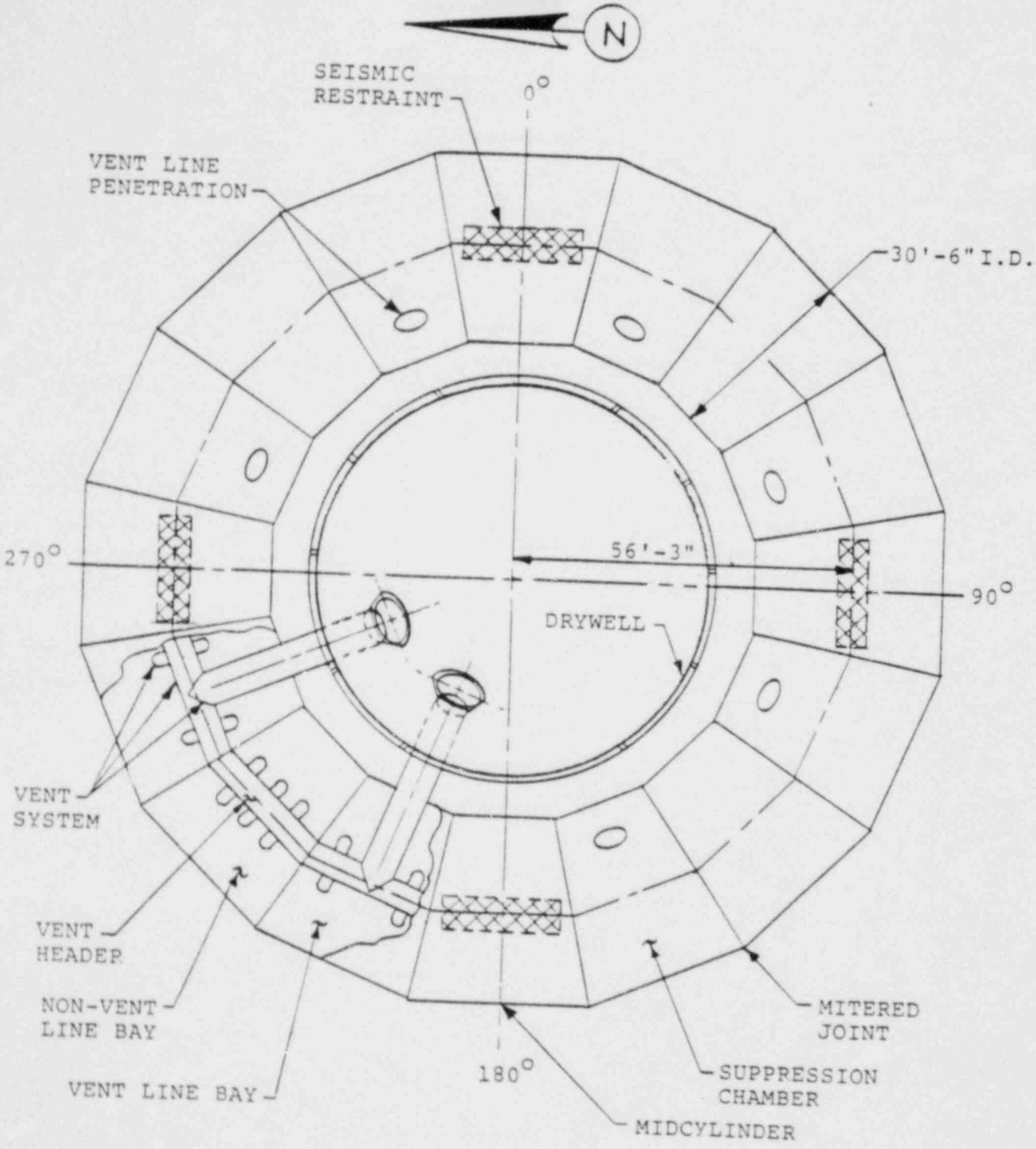

Figure 3-2.1-1

PLAN VIEW OF CONTAINMENT

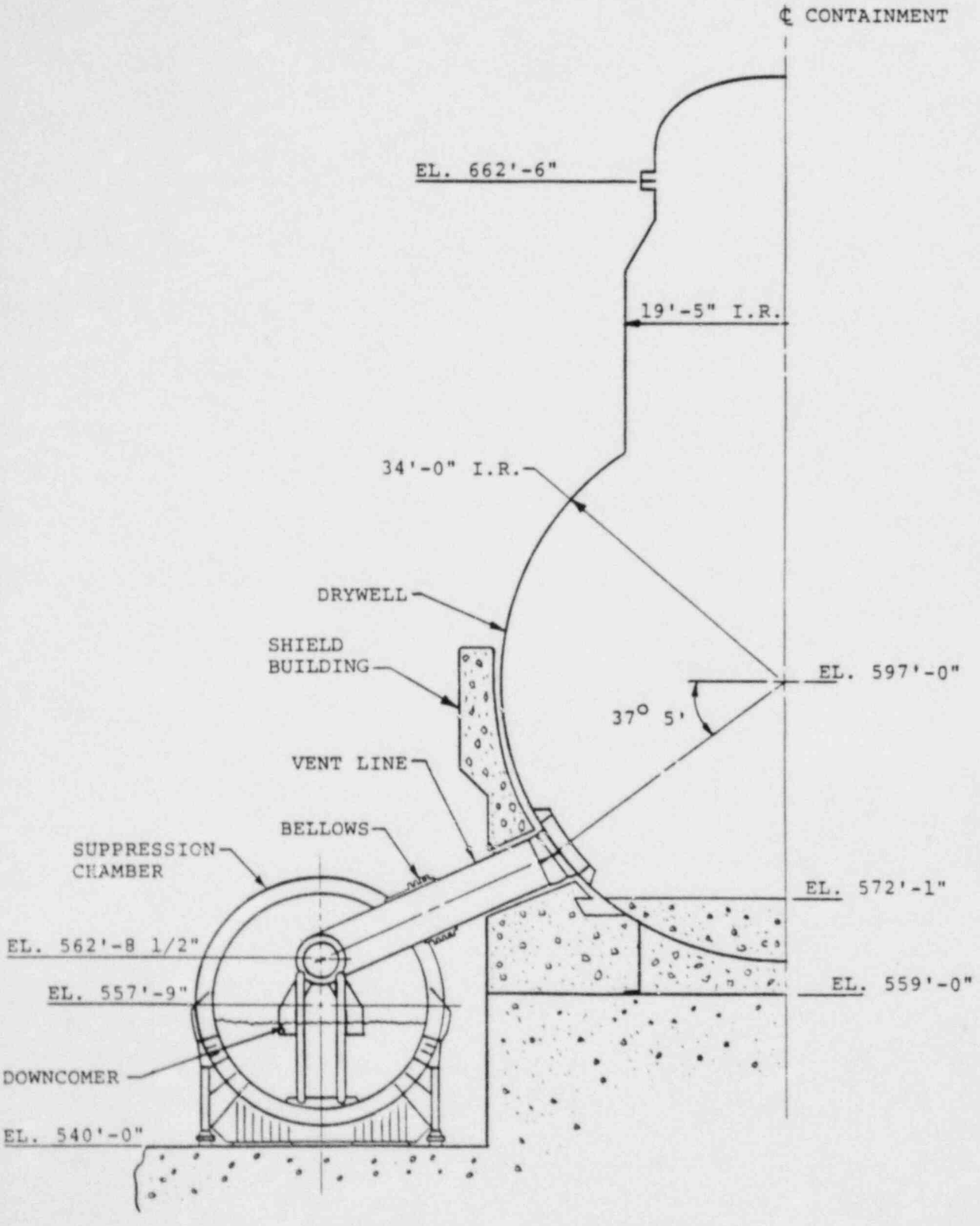

Figure 3-2.1-2

ELEVATION VIEW OF CONTAINMENT

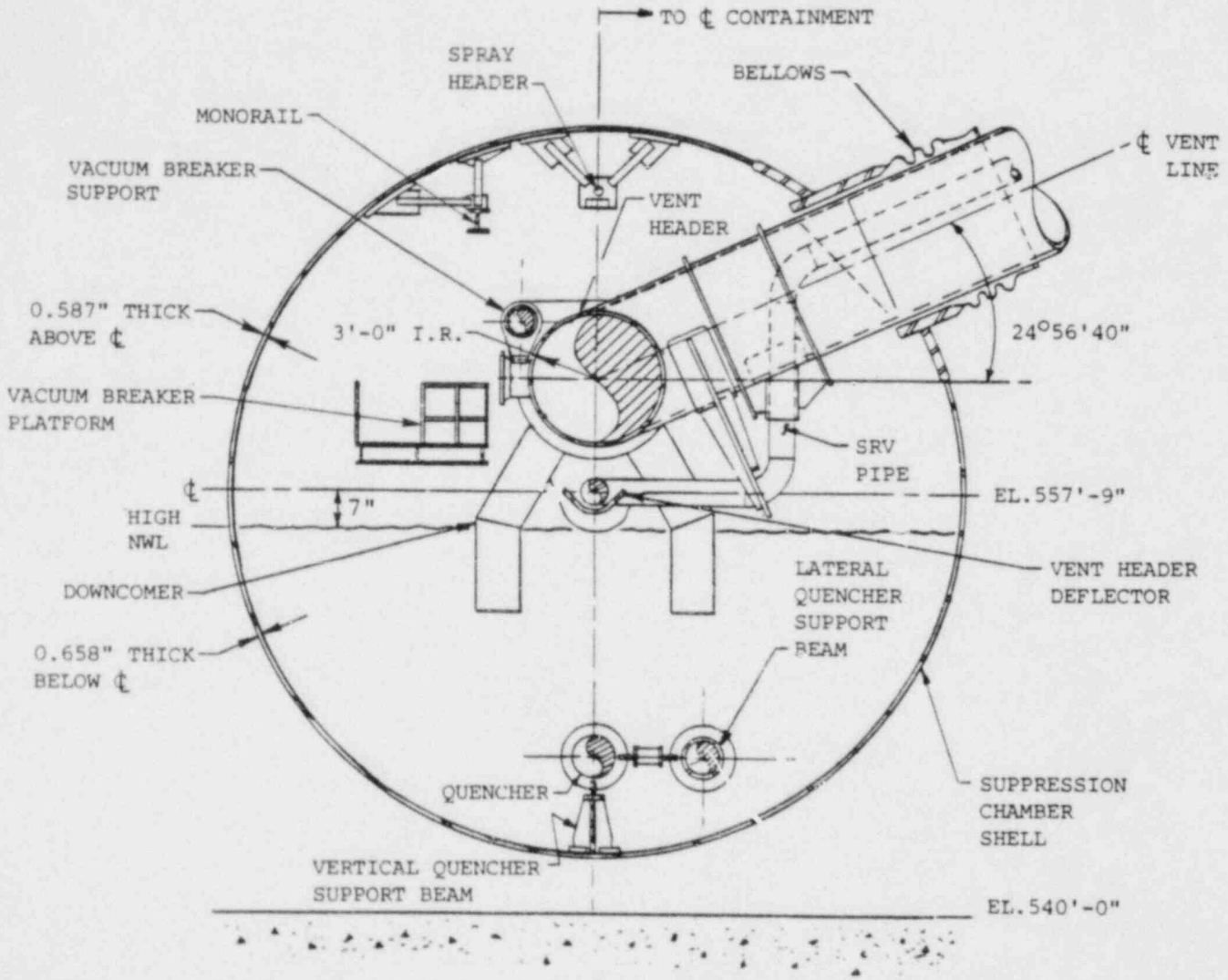

Figure 3-2.1-3

SUPPRESSION CHAMBER SECTION-MIDCYLINDER VENT LINE BAY

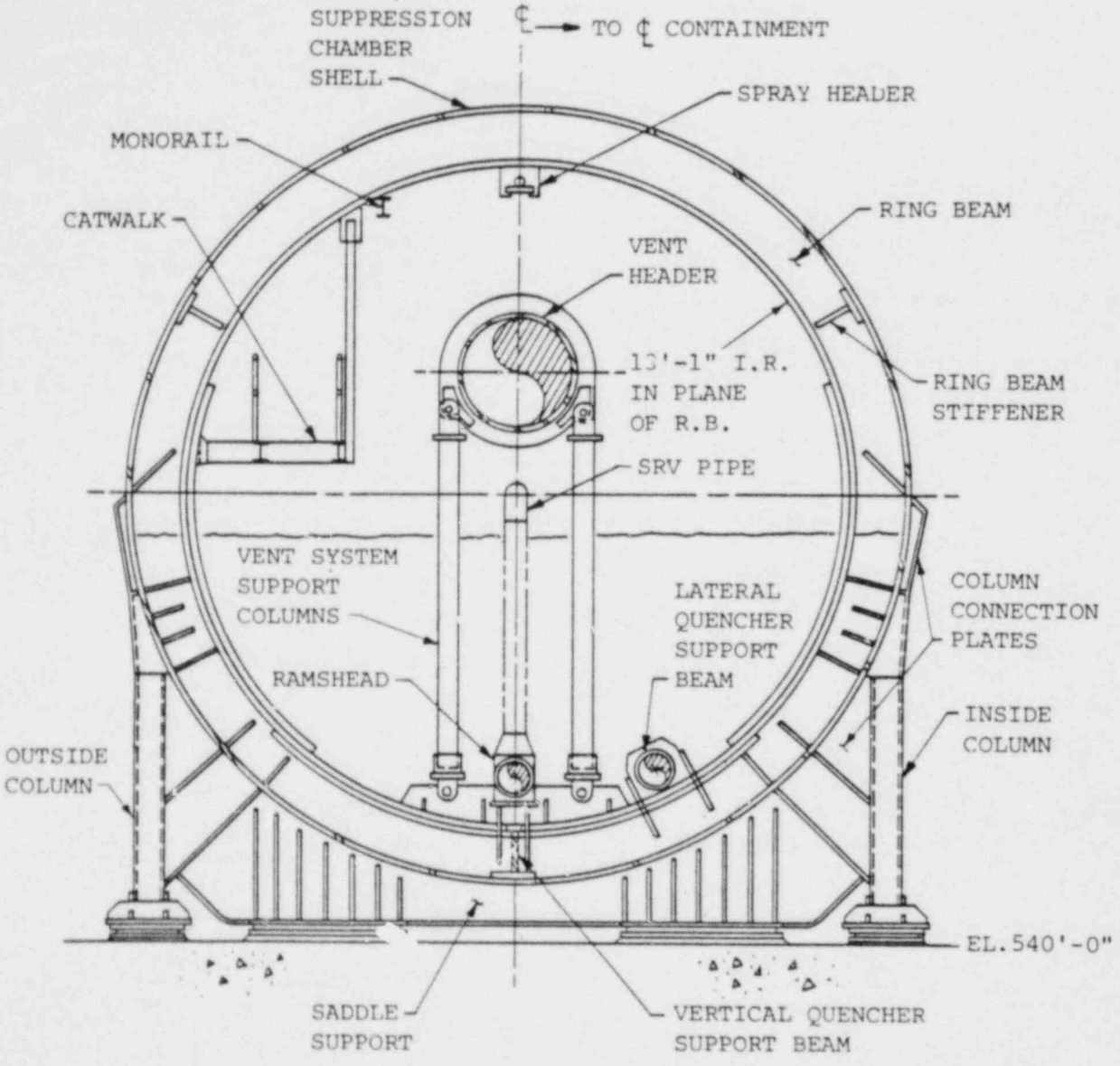

Figure 3-2.1-4

SUPPRESSION CHAMBER SECTION-
MITERED JOINT

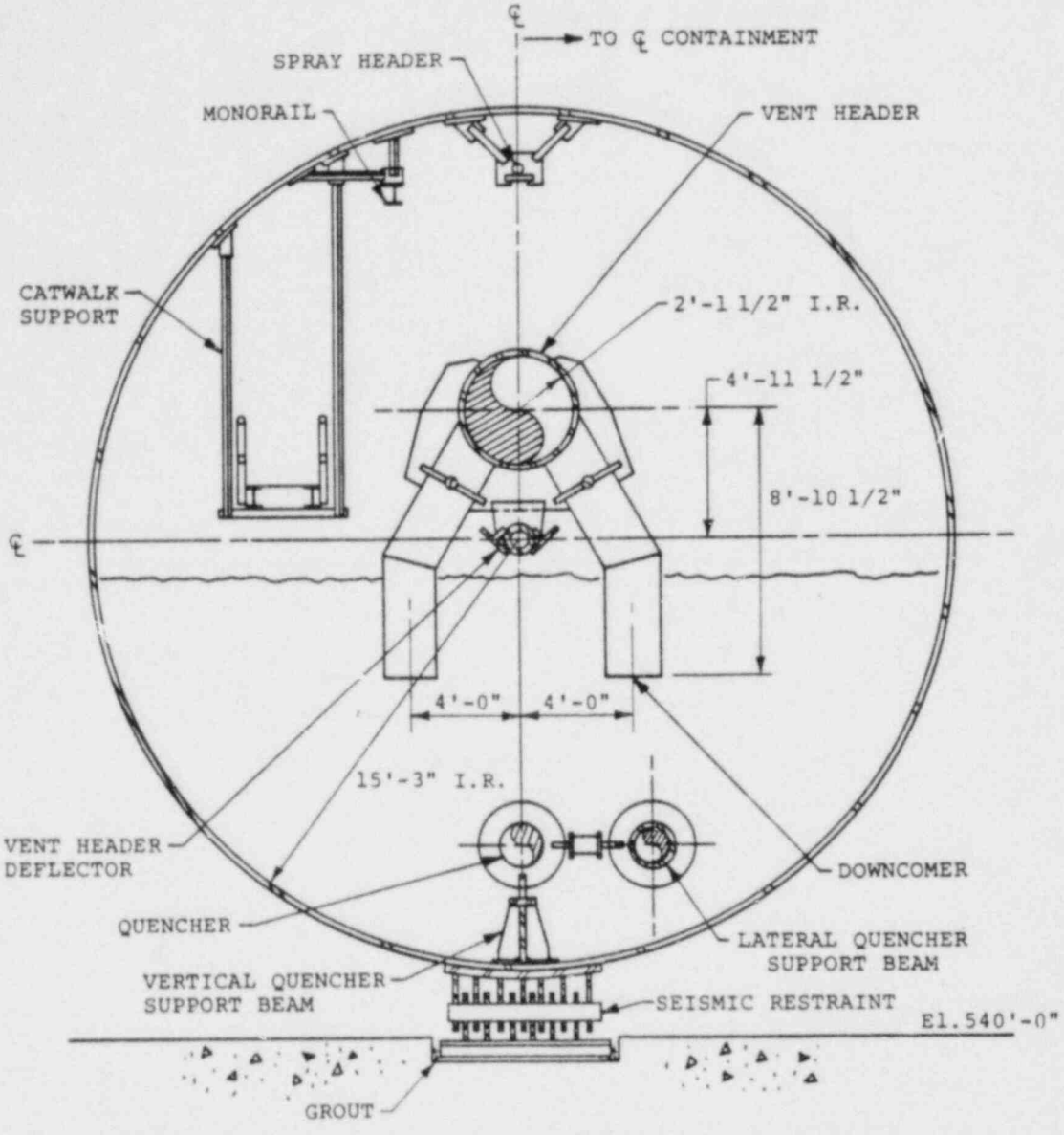

Figure 3-2.1-5

SUPPRESSION CHAMBER SECTION

MIDCYLINDER NON-VENT LINE BAY

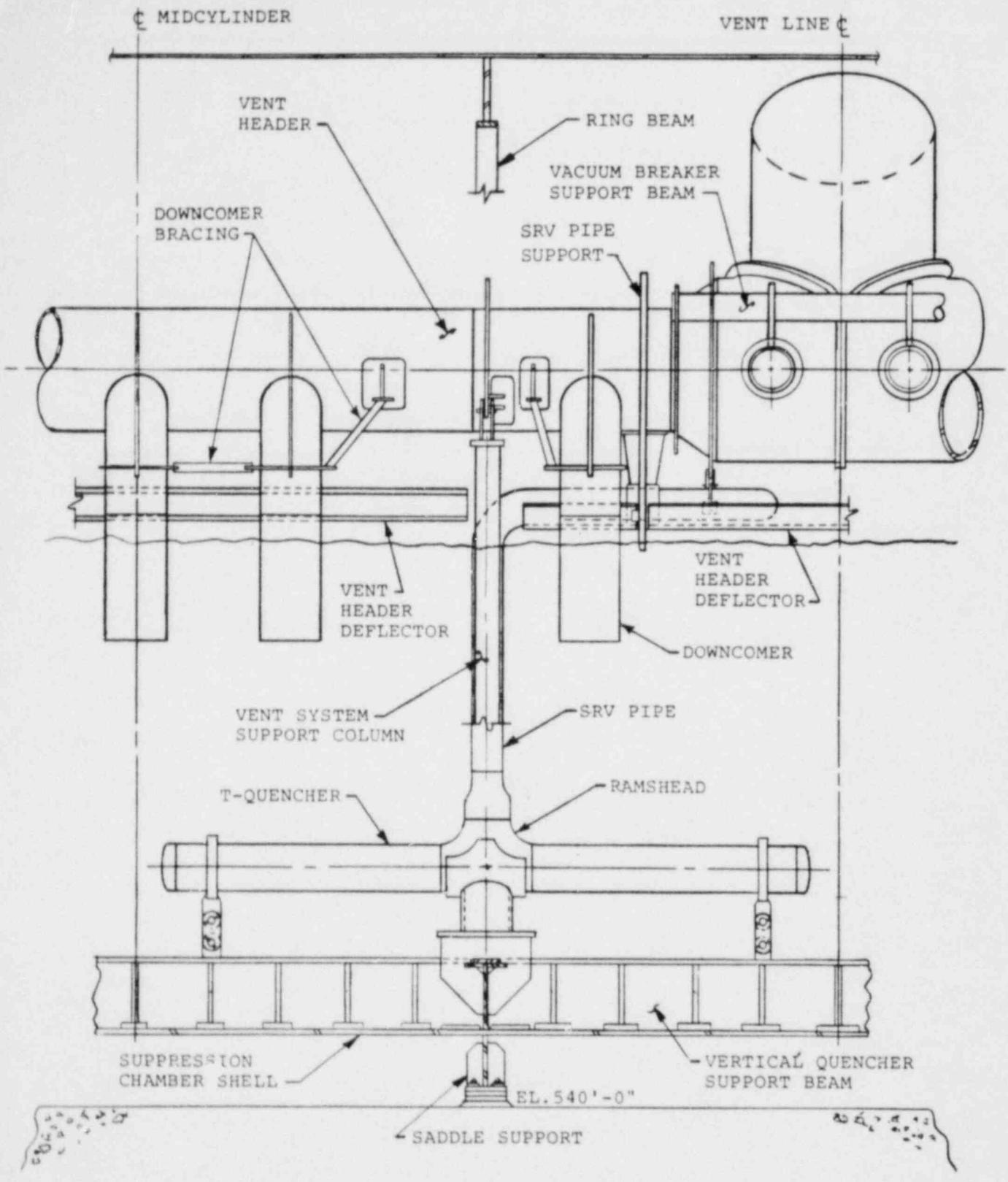

Figure 3-2.1-6

DEVELOPED VIEW OF SUPPRESSION CHAMBER SEGMENT

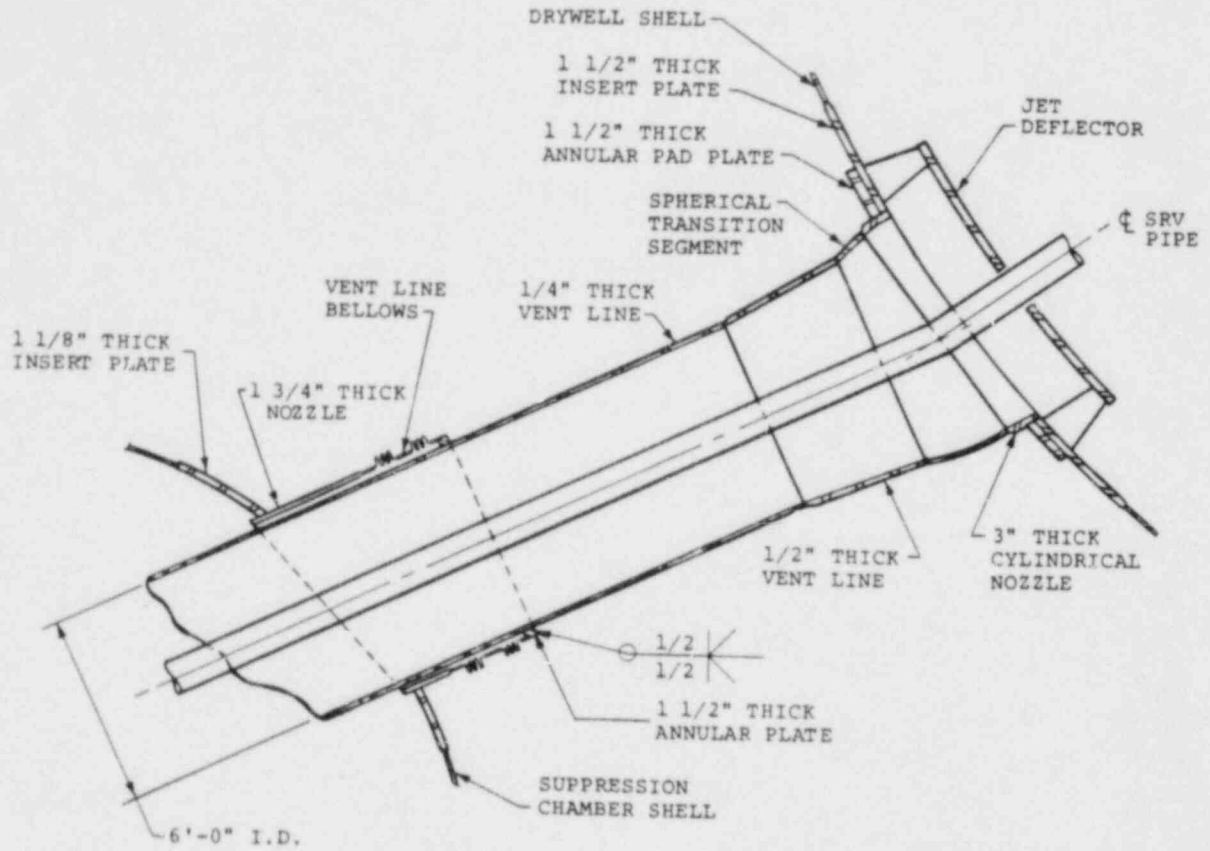

Figure 3-2.1-7

VENT LINE DETAILS - UPPER END

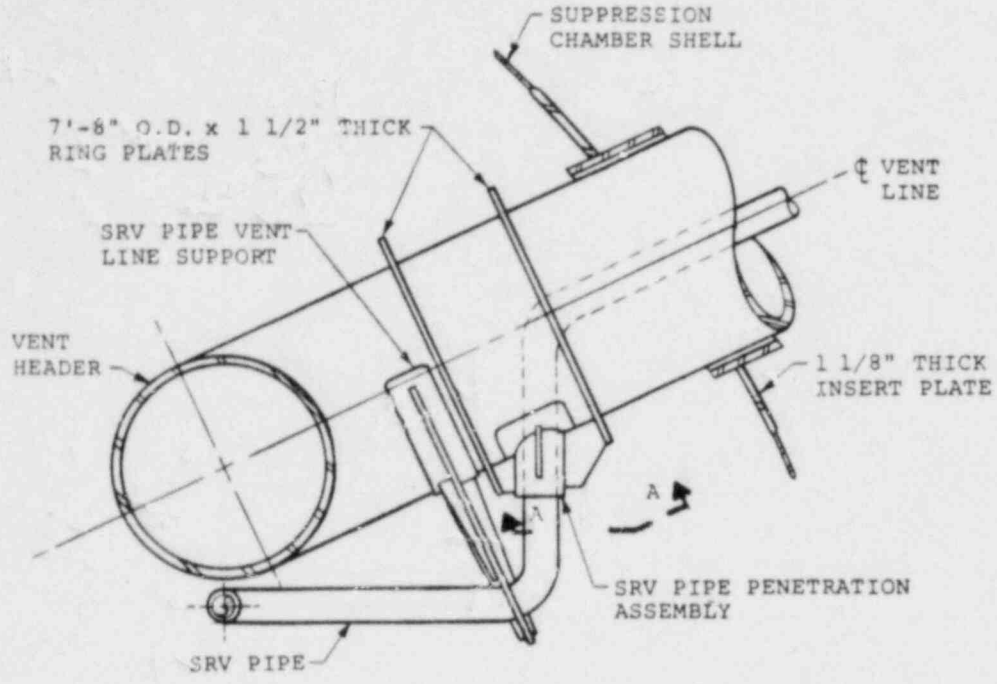

VENT LINE ELEVATION VIEW

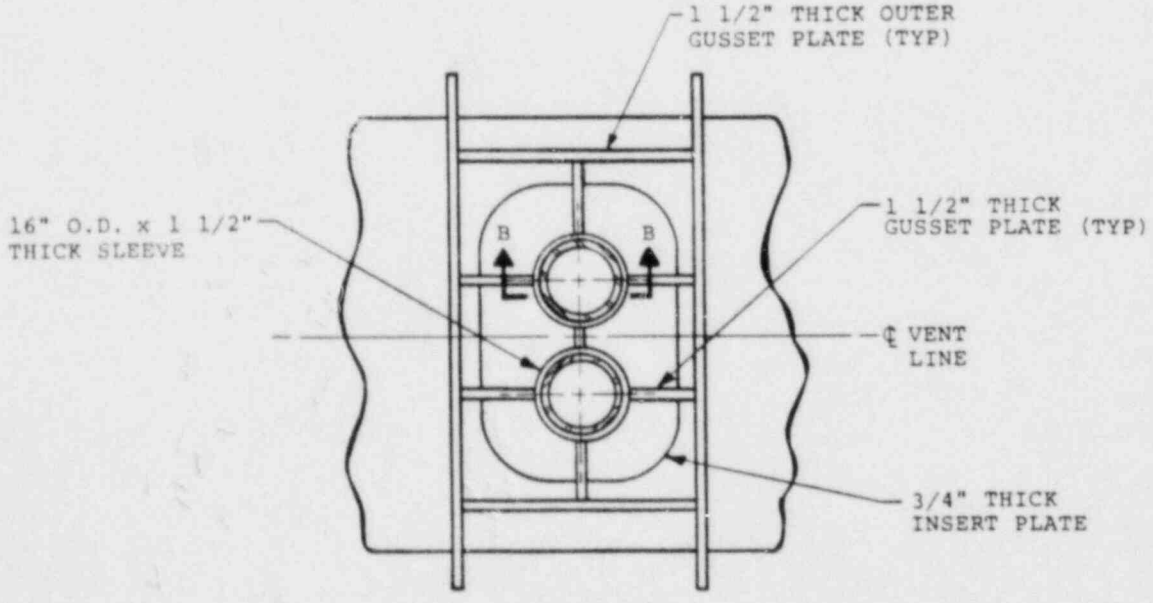

VIEW A-A

Figure 3-2.1-8

VENT LINE DETAILS - LOWER END

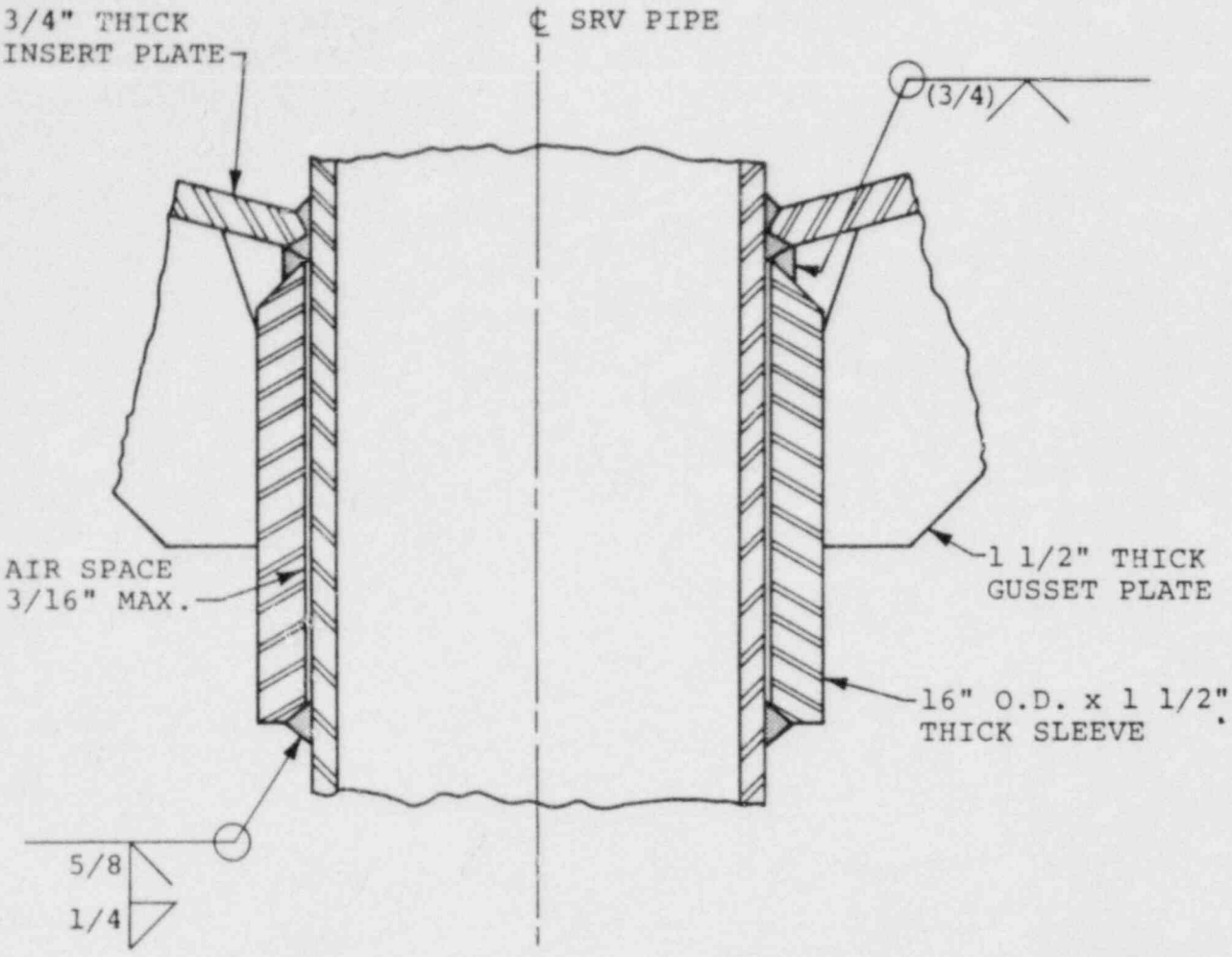

SECTION B-B

Figure 3-2.1-9

VENT LINE-SRV PIPING PENETRATION

NOZZLE DETAILS

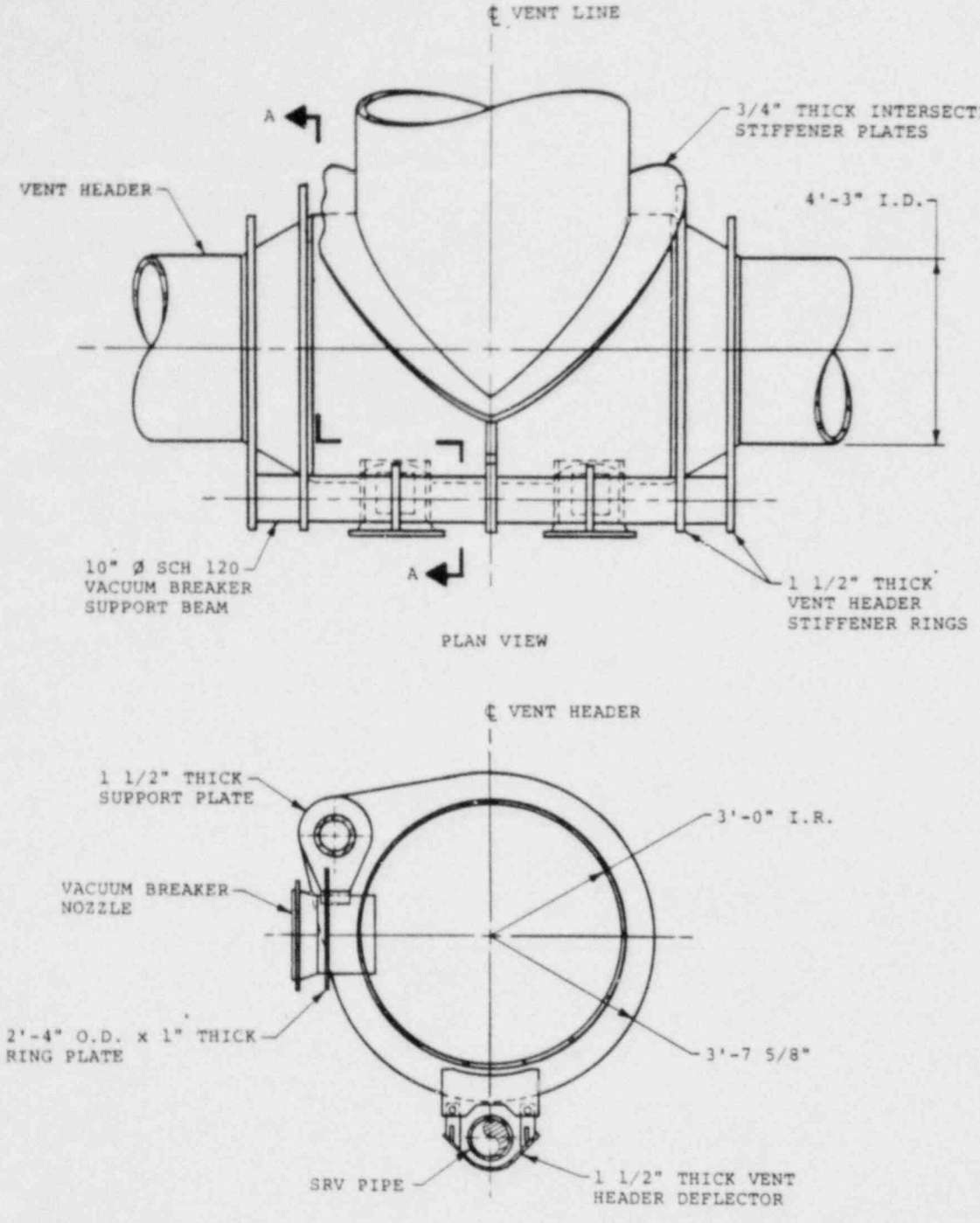

Figure 3-2.1-10

VENT LINE-VENT HEADER INTERSECTIO. DETAILS

nutech ENGINEERS

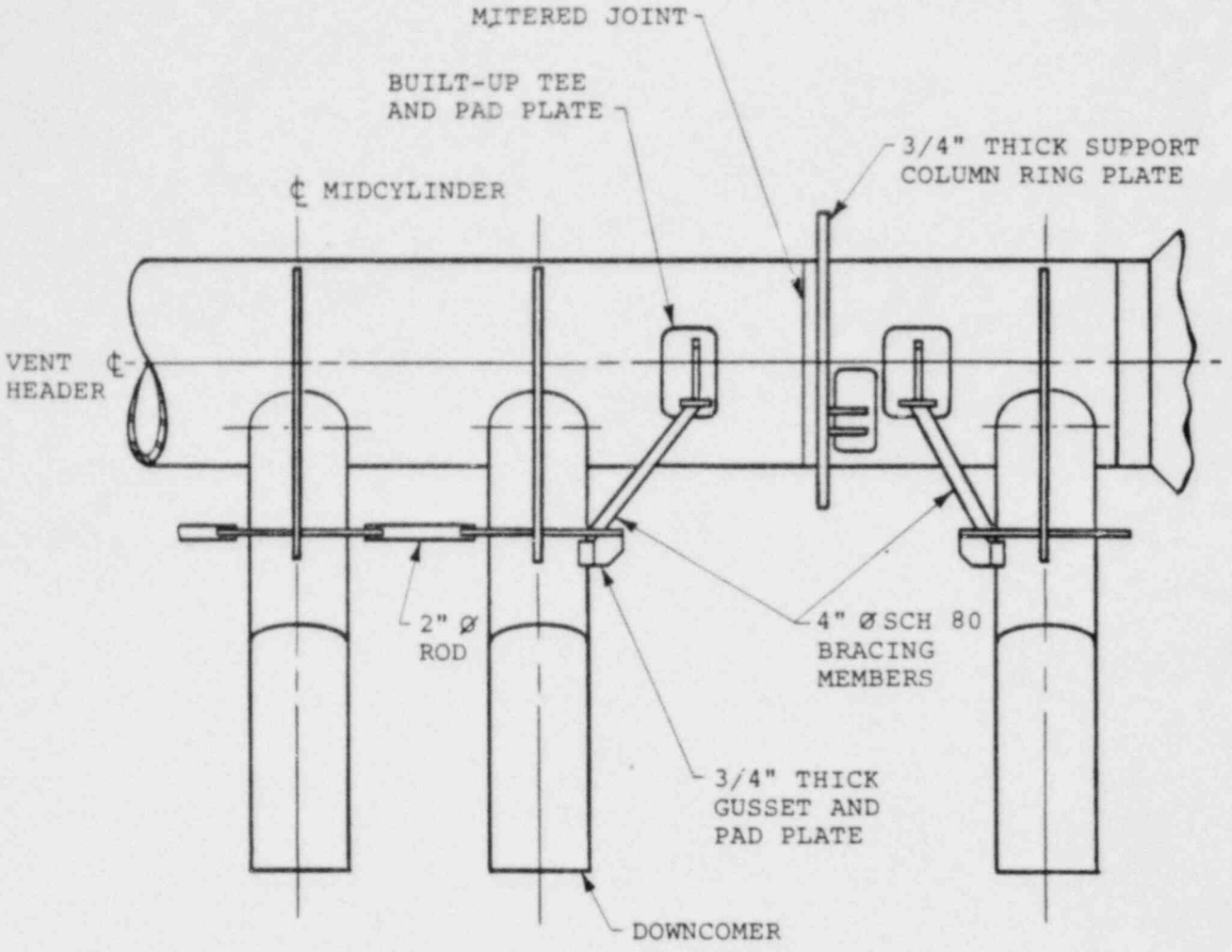

Figure 3-2.1-11

DEVELOPED VIEW OF VENT HEADER
AND DOWNCOMER BRACING SYSTEM

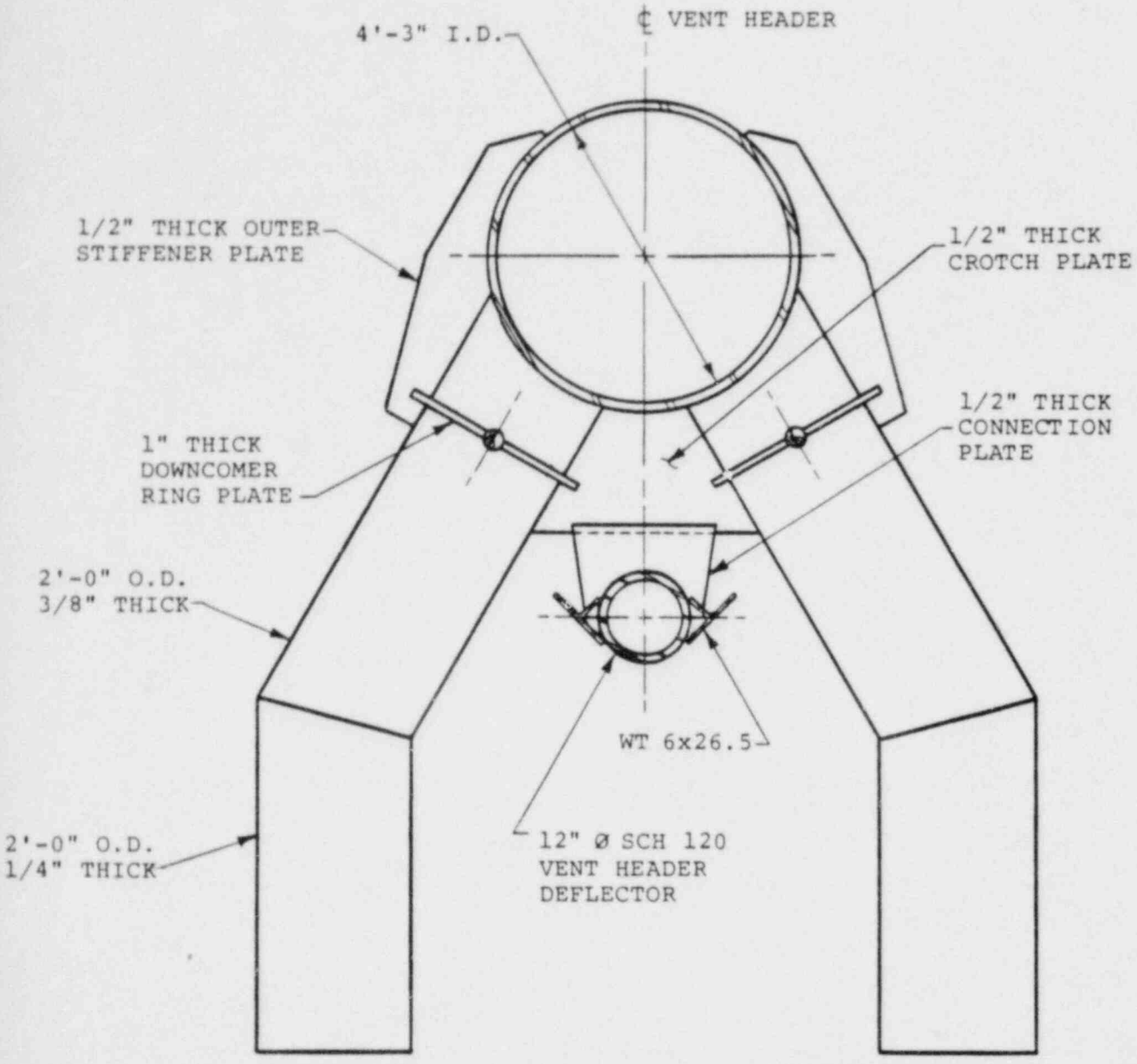

Figure 3-2.1-12

DOWNCOMER - VENT HEADER INTERSECTION DETAILS

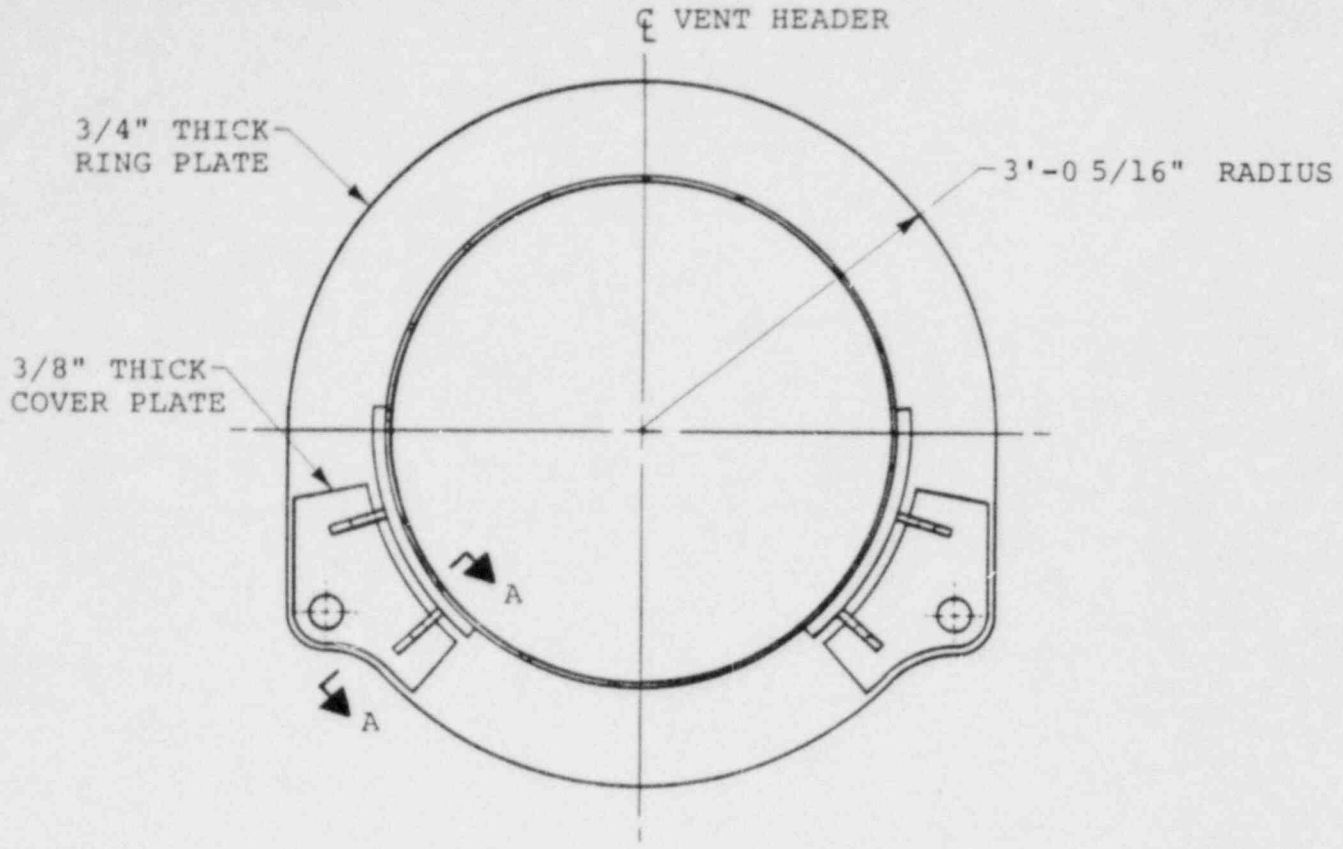

SECTION THRU VENT HEADER AT
COLUMN SUPPORT RING PLATE

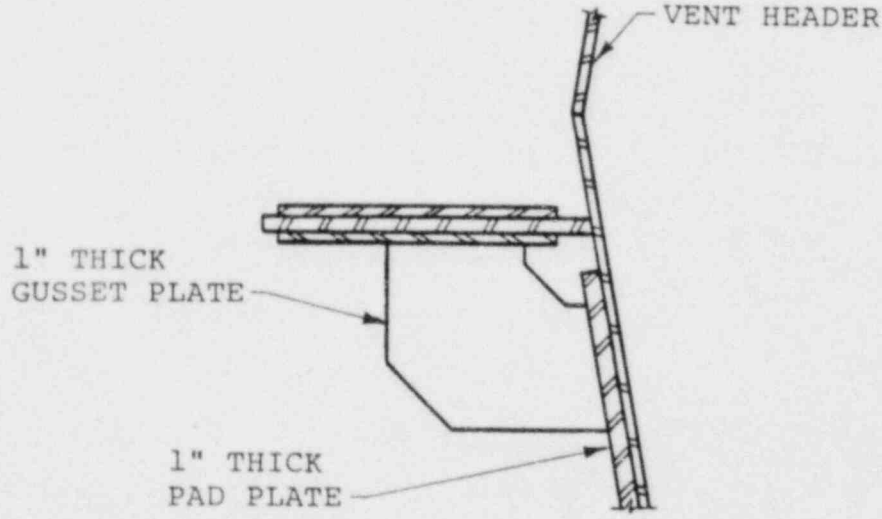

SECTION A-A

Figure 3-2.1-13

SUPPORT COLUMN RING PLATE DETAILS

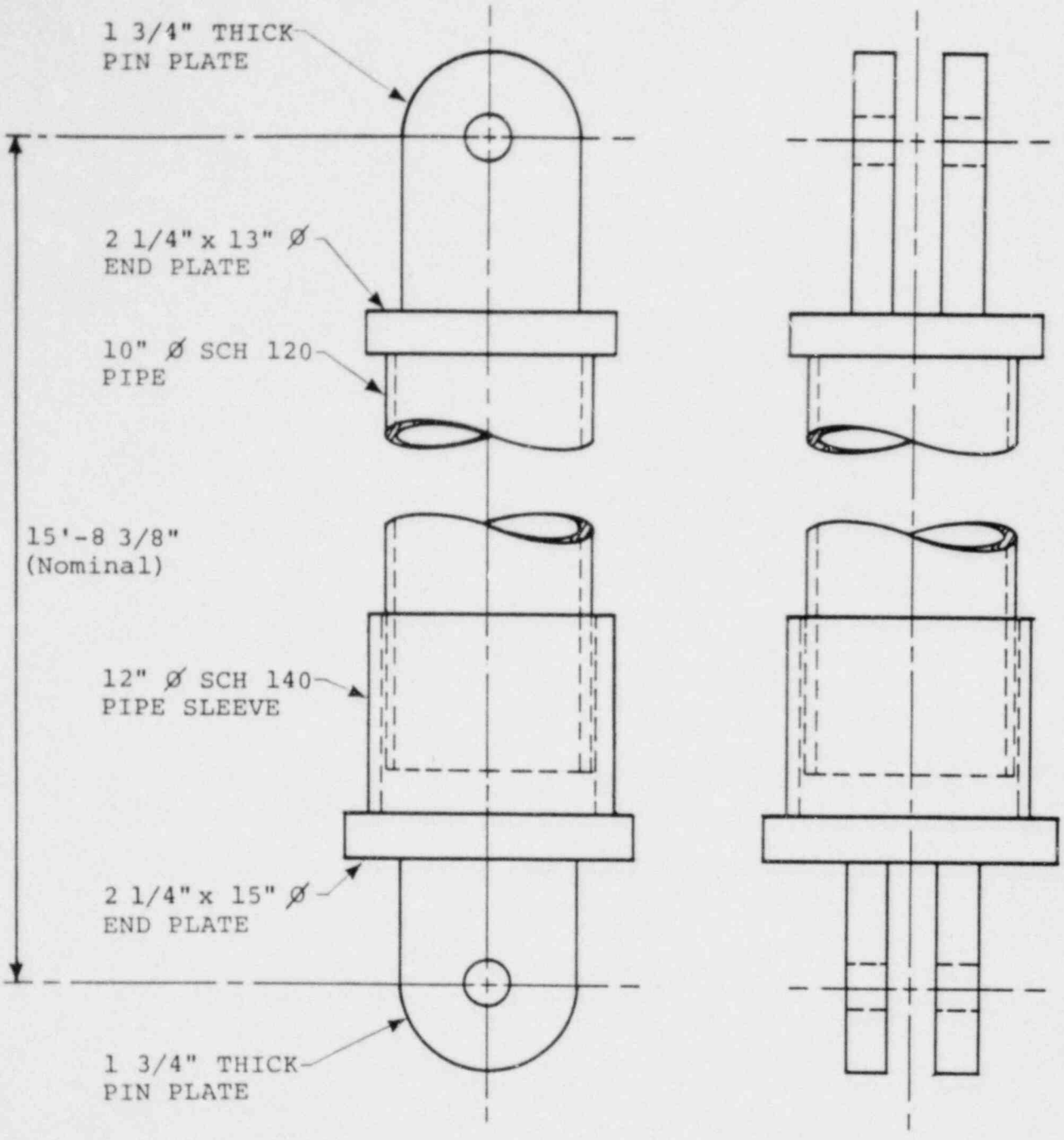

Figure 3-2.1-14

VENT SYSTEM SUPPORT COLUMN DETAILS

3-2.2 Loads and Load Combinations

The loads for which the Fermi 2 vent system is evaluated are defined in NUREG-0661 on a generic basis for all Mark I plants. The methodology used to develop plant unique vent system loads for each load defined in NUREG-0661 is discussed in Section 1-4.0. The results of applying the methodology to develop specific values for each of the governing loads which act on the vent system are discussed and presented in Section 3-2.2.1.

Using the event combinations and event sequencing defined in NUREG-0661 and discussed in Sections 1-3.2 and 1-4.3, the controlling load combinations which affect the vent system are formulated. The controlling vent system load combinations are discussed and presented in Section 3-2.2.2.

3-2.2.1 Loads

The loads acting on the vent system are categorized as follows:

1. Dead Weight Loads
2. Seismic Loads
3. Pressure and Temperature Loads
4. Vent System Discharge Loads
5. Pool Swell Loads
6. Condensation Oscillation Loads
7. Chugging Loads
8. Safety Relief Valve Discharge Loads
9. Piping Reaction Loads
10. Containment Interaction Loads

Loads in categories 1 through 3 were considered in the original containment design as documented in the plant's FSAR. Additional category 3 pressure and temperature loads result from postulated LOCA and SRV discharge events. Loads in categories 4 through 7 result from postulated LOCA events; loads in category 8 result from SRV discharge events; loads in category 9 are reactions which result from loads acting on SRV piping systems; loads in category 10 are motions which result from loads acting on other containment-related structures.

Not all of the loads defined in NUREG-0661 are evaluated in detail since some are enveloped by others or have a negligible effect on the vent system. Only those loads which maximize the vent system response and lead to controlling stresses are fully evaluated and discussed. These loads are referred to as governing loads in subsequent discussions.

Table 3-2.2-1 shows the specific vent system components which are affected by each of the loadings defined in NUREG-0661. The table also lists the section in Volume 1 in which the methodology for developing values for each loading is discussed. The magnitudes and characteristics of each governing vent system load in each load category are identified and presented in the paragraphs which follow.

1. Dead Weight Loads

   a. Dead Weight of Steel: The weight of steel used to construct the modified vent system and its supports is considered. The nominal component dimensions and a density of steel of 490 lb/ft^3 are used in this calculation.

2. Seismic Loads

a. OBE Loads: The vent system is subjected to horizontal and vertical accelerations during an Operating Basis Earthquake (OBE). This loading is taken from the original design basis for the containment documented in the plant's FSAR. The OBE loads have a maximum horizontal spectral acceleration of 0.23g and a maximum vertical spectral acceleration of 0.067g.

b. SSE Loads: The vent system is subjected to horizontal and vertical accelerations during a Safe Shutdown Earthquake (SSE). This loading is taken from the original design basis for the containment documented in the plant's FSAR [termed Design Basis Earthquake (DBE) in the FSAR]. The SSE loads have a maximum horizontal spectral acceleration of 0.46g and a maximum vertical spectral acceleration of 0.133g.

3. Pressure and Temperature Loads

a. Normal Operating Internal Pressure Loads: The vent system is subjected to internal pressure

loads during Normal Operating conditions. This loading is taken from the original design basis for the containment documented in the plant's FSAR. The range of normal operating internal pressures specified is 0.0 to 2.0 psi.

b. LOCA Internal Pressure Loads: The vent system is subjected to internal pressure loads during a Small Break Accident (SBA), Intermediate Break Accident (IBA), and Design Basis Accident (DBA) event. The procedure used to develop LOCA internal pressures for the containment is discussed in Section 1-4.1.1. The resulting vent system internal pressure transients and pressure magnitudes at key times during the SBA, IBA, and DBA events are presented in Figures 3-2.2-1 through 3-2.2-3.

The vent system internal pressures for each event are conservatively assumed to be equal to the corresponding drywell internal pressures, neglecting reductions due to losses. The net internal pressures acting on the components of the vent system inside the suppres-

sion chamber are taken as the difference in pressures between the vent system and suppression chamber.

The pressures specified are assumed to act uniformly over the vent line, vent header, and downcomer shell surfaces. The external or secondary containment pressure for the vent system components outside the suppression chamber for all events is assumed to be zero. The effects of internal pressure on the vent system for the DBA event are included in the pressurization and thrust loads discussed in load case 4a.

c. Normal Operating Temperature Loads: The vent system is subjected to the thermal expansion loads associated with normal operating conditions. This loading is taken from the original design basis for the containment documented in the plant's FSAR. The range of normal operating temperatures for the vent system with a concurrent SRV discharge event is 50 to 150°F. The temperature of the SRV

piping with a concurrent SRV discharge event is conservatively taken as 363°F.

Additional normal operating temperatures for the vent system inside the suppression chamber are taken from the suppression pool temperature response analysis. The resulting vent system temperatures are summarized in Table 3-2.2-2.

d. LOCA Temperature Loads: The vent system is subjected to thermal expansion loads associated with the SBA, IBA, and DBA events. The procedure used to develop LOCA containment temperatures is discussed in Section 1-4.1.1. The resulting vent system temperature transients and temperature magnitudes at key times during the SBA, IBA, and DBA events are presented in Figures 3-2.2-4 through 3-2.2-6.

Additional vent system SBA event temperatures are taken from the suppression pool temperature response analysis. The resulting vent system temperatures are summarized in Table 3-2.2-2. The greater of the temperatures

specified in Figure 3-2.2-4 and Table 3-2.2-2 is used in evaluating the effects of SBA event temperatures.

The temperatures of the major components of the vent system, such as the vent line, vent header, and downcomers, are conservatively assumed to be equal to the corresponding drywell temperatures for the IBA and DBA events. For the SBA event, the temperature of the major components of the vent system is assumed to be equal to the maximum saturation temperature of the drywell, which is 270°F.

The temperatures of the external components of the vent system such as the support columns, downcomer bracing, vent header deflectors, vacuum breaker supports, and associated ring plates and stiffeners are assumed to be equal to the corresponding suppression chamber temperatures for each event.

The temperatures specified are assumed to be representative of the major component and

external component metal temperatures throughout the vent system. The temperature of the SRV piping for those SBA, IBA, and DBA events which include SRV discharge loads is taken as 363°F. The ambient or initial temperature of the vent system for all events is assumed to be equal to the arithmetic mean of the minimum and maximum vent system operating temperatures.

4. Vent System Discharge Loads

   a. Pressurization and Thrust Loads: The vent system is subjected to pseudo-static pressurization and thrust loads during a DBA event. The procedure used to develop vent system pressurization and thrust forces, applied to the unreacted areas of the major components of the vent system, is discussed in Section 1-4.1.2. The resulting maximum forces for each of the major component unreacted areas at key times during the DBA event are shown in Table 3-2.2-3. The pressurization loads acting on the vent line-drywell penetrations are obtained by multiplying the corresponding drywell internal pressures for the DBA event by the penetration unreacted area.

The vent system discharge loads shown include the effects of zero drywell/wetwell pressure differential. The vent system discharge loads specified for the DBA event include the effects of DBA internal pressure loads as discussed in load case 3a. The vent system discharge loads which occur during the SBA or IBA events are negligible.

5. Pool Swell Loads

a. Vent System Impact and Drag Loads: During the initial phase of a DBA event, transient impact and drag pressures are postulated to act on major components of the vent system above the suppression pool. The major components affected include the vent line inside the suppression chamber below the maximum bulk pool height and the inclined portion of the downcomers below the downcomer rings. The upper portion of the downcomers is shielded from pool swell impact loads by the downcomer rings. The vent header in the vent line bay and non-vent line bay is shielded from pool swell impact loads by the vent header deflectors.

The procedure used to develop the transient forces and the spatial distribution of pool swell impact loads on these components is discussed in Section 1-4.1.4. The resulting magnitudes and distribution of pool swell impact loads on the vent line, downcomers, and vent header deflector are summarized in Table 3-2.2-4, and Figures 3-2.2-7 and 3-2.2-8. The results shown are based on plant unique QSTF test data contained in the PULD (Reference 3) and include the effects of the main vent orifice tests. Pool swell loads do not occur during the SBA and IBA events.

b. Impact and Drag Loads on Other Structures: During the initial phase of a DBA event, transient impact and drag pressures are postulated to act on the components of the vent system other than the major components. The components affected include the downcomer bracing members and ring plates, the vacuum breaker and vacuum breaker supports, and the SRV piping and supports located beneath the vent line. The portion of the SRV piping

located under the vent header is shielded from pool swell impact loads by a vent header deflector.

The procedure used to develop the transient forces and the spatial distribution of pool swell impact loads on these components is discussed in Section 1-4.1.4. The resulting magnitudes and distribution of pool swell impact pressures on the downcomer bracing members and ring plates, and the vacuum breaker and vacuum breaker supports are summarized in Table 3-2.2-5. The pool swell impact loads on the SRV piping and supports located beneath the vent line are presented in Volume 5 of this report. The results shown are based on plant unique QSTF test data contained in the PULD which are used to determine the impact velocities and arrival times. Pool swell loads do not occur during the SBA and IBA events.

c. Froth Impingement and Fallback Loads: During the initial phase of a DBA event, transient impingement pressures are postulated to act on

components of the vent system located in specified regions above the rising suppression pool. The components located in Region I which are affected include the downcomer bracing members and ring plates, the vacuum breaker and vacuum breaker supports and the SRV piping supports beneath the vent line. The components located in Region II which are affected include the vacuum breaker and vacuum breaker supports.

The procedure used to develop the transient forces and spatial distribution of froth impingement and fallback loads on these components is discussed in Section 1-4.1.4. The resulting magnitudes and distribution of froth impingement and fallback pressures on the downcomer bracing members and ring plates, and the vacuum breaker and vacuum breaker supports are summarized in Table 3-2.2-6. The froth impingement loads acting on the SRV piping and supports located beneath the vent line are presented in Volume 5 of this report. The results shown include the effects of using the plant unique QSTF movies to determine the

source velocity, departure angle, and froth density. Pool swell loads do not occur during the SBA and IBA events.

d. Pool Fallback Loads: During the later portion of the pool swell event, transient drag pressures are postulated to act on selected components of the vent system located between the maximum bulk pool height and the downcomer exit. The components affected include the downcomer bracing members and ring plates, and the SRV piping and supports located beneath the vent line. The procedure used to develop transient drag pressures and spatial distribution of pool fallback loads on these components is discussed in Section 1-4.1.4.

The resulting magnitudes and distribution of pool fallback loads on the downcomer bracing members and ring plates are summarized in Table 3-2.2-7. The pool fallback loads on the SRV piping and supports located beneath the vent line are presented in Volume 5 of this report. The results shown include the effects of maximum pool displacements measured in

plant unique QSTF tests. Pool swell loads do not occur during the SBA and IBA events.

e. LOCA Air Clearing Submerged Structure Loads: Transient drag pressures are postulated to act on the submerged components of the vent system during the air clearing phase of a DBA event. The components affected include the downcomers, the support columns, and the submerged portion of the SRV piping. The procedure used to develop the transient forces and spatial distribution of DBA air clearing drag loads on these components is discussed in Section 1-4.1.6.

The resulting magnitudes and distribution of drag pressures acting on the downcomers and the vent system support columns for the controlling DBA air clearing load case are shown in Tables 3-2.2-8 and 3-2.2-9. The controlling DBA air clearing loads on the submerged portion of the SRV piping are presented in Volume 5 of this report. The results shown include the effects of velocity drag, acceleration drag, and interference effects. The

LOCA air clearing submerged structure loads which occur during an SBA or IBA event are negligible.

6. Condensation Oscillation Loads

a. IBA Condensation Oscillation Downcomer Loads: Harmonic internal pressure loads are postulated to act on the downcomers during the condensation oscillation phase of an IBA event. The procedure used to develop the harmonic pressures and spatial distribution of IBA condensation oscillation downcomer loads is discussed in Section 1-4.1.7. The loading consists of a uniform internal pressure component acting on all downcomers and a differential internal pressure component acting on one downcomer in a downcomer pair. The resulting pressure amplitudes and associated frequency range for each of the three harmonics in the IBA condensation oscillation downcomer loading are shown in Table 3-2.2-10. The corresponding distribution of differential downcomer internal pressure loadings are shown in Figure 3-2.2-9.

The IBA condensation oscillation downcomer load harmonic in the range of the dominant downcomer frequency for the uniform and the differential pressure components is applied at the dominant downcomer frequency. The remaining two downcomer load harmonics are applied at frequencies which are multiples of the dominant frequency. The results of the three harmonics for the uniform and differential IBA condensation oscillation downcomer load components are summed absolutely.

b. DBA Condensation Oscillation Downcomer Loads: Harmonic internal pressure loads are postulated to act on the downcomers during the condensation oscillation phase of a DBA event. The procedure used to develop the harmonic pressures and spatial distribution of DBA condensation oscillation downcomer loads is the same as that discussed for IBA condensation oscillation downcomer loads in load case 6a. The resulting pressure amplitudes and associated frequency range for each of the three harmonics in the DBA condensation oscillation downcomer loading are shown in Table

3-2.2-11. The corresponding distribution of differential downcomer internal pressure loadings are shown in Figure 3-2.2-9.

c. IBA Condensation Oscillation Vent System Pressure Loads: Harmonic internal pressure loads are postulated to act on the vent system during the condensation oscillation phase of an IBA event. The components affected include the vent line, the vent header, and the downcomers. The procedure used to develop the harmonic pressures and spatial distribution of IBA condensation oscillation vent system pressures is discussed in Section 1-4.1.7. The resulting pressure amplitudes and associated frequency range for the vent line and vent header are shown in Table 3-2.2-12. The loading is applied at the frequency within a specified range which maximizes the vent system response.

The effects of IBA condensation oscillation vent system pressures on the downcomers are included in the IBA condensation oscillation downcomer loads discussed in load case 6a. An

additional static internal pressure of 1.5 psi is applied uniformly to the vent line, vent header, and downcomers to account for the effects of nominal downcomer submergence. The IBA condensation oscillation vent system pressures act in addition to the IBA containment internal pressures discussed in load case 3a.

d. DBA Condensation Oscillation Vent System Pressure Loads: Harmonic internal pressure loads are postulated to act on the vent system during the condensation oscillation phase of a DBA event. The components affected include the vent line, vent header, and the downcomers. The procedure used to develop the harmonic pressures and spatial distribution of the DBA condensation oscillation vent system pressures is the same as that discussed for the IBA in load case 6c. The resulting pressure amplitudes and associated frequency range for the vent line and vent header are shown in Table 3-2.2-12. The DBA condensation oscillation vent system pressures act in addition to the DBA vent system pressurization and thrust loads discussed in load case 4a.

e. IBA Condensation Oscillation Submerged Structure Loads: Harmonic pressure loads are postulated to act on the submerged components of the vent system during the condensation oscillation phase of an IBA event. In accordance with NUREG-0661, the submerged structure loads specified for pre-chug are used in lieu of IBA condensation oscillation submerged structure loads. Pre-chug submerged structure loads are discussed in load case 7c.

f. DBA Condensation Oscillation Submerged Structure Loads: Harmonic drag pressures are postulated to act on the submerged components of the vent system during the condensation oscillation phase of a DBA event. The components affected include the support columns and the submerged portions of the SRV piping. The procedure used to develop the harmonic forces and spatial distribution of DBA condensation oscillation drag loads on these components is discussed in Section 1-4.1.7.

Loads are developed for the case with the average source strength at all downcomers and the case with twice the average source strength at the nearest downcomer. The results of these two cases are evaluated to determine the controlling loads.

The resulting magnitudes and distribution of drag pressures acting on the support columns for the controlling DBA condensation oscillation drag load case are shown in Table 3-2.2-13. The controlling DBA condensation oscillation drag loads on the submerged portion of the SRV piping are presented in Volume 5 of this report. The effects of DBA condensation oscillation submerged structure loads on the downcomers are included in the loads discussed in load case 6b.

The results shown in Table 3-2.2-13 include the effects of velocity drag, acceleration drag, torus shell FSI acceleration drag, interference effects, and acceleration drag volumes. A typical pool acceleration profile from which the FSI accelerations are derived

is shown in Figure 3-2.2-10. The results of each harmonic in the loading are combined using the methodology discussed in Section 1-4.1.7.

7. Chugging Loads

a. Chugging Downcomer Lateral Loads: Lateral loads are postulated to act on the downcomers during the chugging phase of an SBA, IBA, and DBA event. The procedure used to develop chugging downcomer lateral loads is discussed in Section 1-4.1.8. The maximum lateral load acting on any one downcomer in any direction is obtained using the maximum downcomer lateral load and chugging pulse duration measured at FSTF, the frequency of the tied downcomers for FSTF, and the plant unique downcomer frequency calculated for Fermi. This information is summarized in Table 3-2.2-14. The resulting ratio of Fermi to FSTF Dynamic Load Factors (DLF) is used in subsequent calculations to determine the magnitude of multiple downcomer loads and to determine the load magnitude used for evaluating fatigue. The methodology used to determine the plant unique

downcomer frequency is discussed in Section 3-2.4.1.

The magnitude of chugging lateral loads acting on multiple downcomers simultaneously is determined using the methodology described in Section 1-4.1.8. The methodology involves calculation of the probability of exceeding a given downcomer load magnitude once per LOCA as a function of the number of downcomers loaded. The chugging load magnitudes, shown in Table 3-2.2-15, are determined using the resulting non-exceedance probabilities and the ratio of the DLF's taken for the maximum downcomer load calculation. The distributions of chugging downcomer lateral loads which are considered include those cases which maximize local effects in the vent system and those cases which maximize overall effects in the vent system. These distributions are summarized in Tables 3-2.2-16 and 3-2.2-17.

The maximum downcomer lateral load magnitude used for evaluating fatigue is obtained using the maximum downcomer lateral load measured at

FSTF with a 95% NEP, and the ratio of DLF's taken from maximum downcomer load calculations. The stress reversal histograms provided for FSTF are converted to plant unique stress reversal histograms using the postulated plant unique chugging duration as shown in Table 3-2.2-18.

b. Chugging Vent System Pressures: Transient and harmonic internal pressures are postulated to act on the vent system during the chugging phase of an SBA, IBA, and DBA event. The components affected include the vent line, the vent header, and the downcomers. The procedure used to develop chugging vent system pressures is discussed in Section 1-4.1.8. The load consists of a gross vent system pressure oscillation component, an acoustic vent system pressure oscillation component, and an acoustic downcomer pressure oscillation component. The resulting pressure magnitudes and characteristics of the chugging vent system pressure loading are shown in Table 3-2.2-19. The three load components are evaluated individually and are not combined.

The overall effects of chugging vent system pressures on the downcomers are included in the loads discussed in load case 7a. The downcomer pressures shown in Table 3-2.2-19 are used to evaluate downcomer hoop stresses. The chugging vent system pressures act in addition to the SBA and IBA containment internal pressures discussed in load case 3a and the DBA pressurization and thrust loads discussed in load case 4a.

c. Pre-Chug Submerged Structure Loads: During the chugging phase of an SBA, IBA, or DBA event, harmonic drag pressures associated with the pre-chug portion of a chug cycle are postulated to act on the submerged components of the vent system. The components affected include the support columns and the submerged portion of the SRV piping. The procedure used to develop the harmonic forces and spatial distribution of pre-chug drag loads on these components is discussed in Section 1-4.1.8.

Loads are developed for the case with the average source strength at all downcomers and the case with twice the average source strength at the nearest downcomer. The results of these two cases are evaluated to determine the controlling loads. The resulting magnitudes and distribution of drag pressures acting on the support columns for the controlling pre-chug drag load case are shown in Table 3-2.2-20. The controlling pre-chug drag loads on the submerged portion of the SRV piping are presented in Volume 5 of this report. The effects of pre-chug submerged structure loads on the downcomers are included in the loads discussed in load case 7a.

The results shown include the effects of velocity drag, acceleration drag, torus shell FSI acceleration drag, interference effects, and acceleration drag volumes. A typical pool acceleration profile from which the FSI accelerations are derived is shown in Figure 3-2.2-10.

d. Post-Chug Submerged Structure Loads: During the chugging phase of an SBA, IBA, or DBA event, harmonic drag pressures associated with the post-chug portion of a chug cycle are postulated to act on the submerged components of the vent system. The components affected include the support columns and the submerged portion of the SRV piping. The procedure used to develop the harmonic forces and spatial distribution of pre-chug drag loads on these components is discussed in Section 1-4.1.8.

Loads are developed for the cases with the average source strength at the nearest two downcomers acting both in-phase and out-of-phase. The results of these cases are evaluated to determine the controlling loads. The resulting magnitudes and distribution of drag pressures acting on the vent system support columns for the controlling post-chug drag load case are shown in Table 3-2.2-21. The controlling post-chug drag loads on the submerged portion of the SRV piping are presented in Volume 5 of this

report. The effects of post-chug submerged structure loads acting on the downcomers are included in the chugging downcomer lateral loads discussed in load case 7a.

The results shown include the effects of velocity drag, acceleration drag, torus shell FSI acceleration drag, interference effects, and acceleration drag volumes. A typical pool acceleration profile from which the FSI accelerations are derived is shown in Figure 3-2.2-10. The results of each harmonic are combined using the methodology described in Section 1-4.1.8.

8. Safety Relief Valve Discharge Loads

a. SRV Discharge Air Clearing Submerged Structure Loads: Transient drag pressures are postulated to act on the submerged components of the vent system during the air clearing phase of an SRV discharge event. The components affected include the downcomers, support columns, and the submerged portion of the SRV piping. The procedure used to develop the transient forces and spatial distribution of

the SRV discharge air clearing drag loads on these components is discussed in Section 1-4.2.4.

Loads are developed for the case with four bubbles from quenchers in three consecutive bays acting in-phase and the case with four bubbles from quenchers in two adjacent bays acting in-phase. These results are evaluated to determine the controlling loads. A calibration factor is applied to the resulting downcomer loads developed using the methodology discussed in Section 1-4.2.4. The magnitudes and distribution of drag pressures acting on the downcomers and the support columns for the controlling SRV discharge drag load case are shown in Tables 3-2.2-22 and 3-2.2-23.

These results include the effects of velocity drag, acceleration drag, interference effects, acceleration drag volumes, and the additional load mitigation effects of the 20" diameter T-quencher.

9. Piping Reaction Loads

a. SRV Piping Reaction Loads: Reaction loads are induced on the vent system due to loads acting on the drywell and wetwell SRV piping systems. These reaction loads occur at the vent line-SRV piping penetrations and at the SRV piping supports located beneath the vent lines and vent header. The SRV piping reaction loads consist of those caused by motions of the vent system and loads acting on the drywell and wetwell portions of the SRV piping systems. Loads acting on the SRV piping systems include pressurization and thrust loads, elevated structure loads, submerged structure loads, and other operating or design basis loads.

The effects of the SRV piping reaction loads on the vent system are included in the vent system analysis. The reaction loads for the drywell portion of the SRV piping are taken from Volume 5 of this report.

10. Containment Interaction Loads

a. Containment Structure Motions: Loads acting on the drywell, suppression chamber and vent

system cause interaction effects between these structures. The interaction effects result in vent system motions applied at the attachment points of the vent system to the drywell and the suppression chamber. The effects of these motions on the vent system are considered in the vent system analysis.

The values of the loads presented in the preceding paragraphs envelop those which could occur during the LOCA and SRV discharge events postulated. An evaluation for the effects of the above loads results in conservative estimates of the vent system responses and leads to bounding values of vent system stresses.

Volume 3 Load Designation			PUAR Section Reference
Category	Load Type	Case Number	
Dead Weight Loads	Dead Weight of Steel	1a	1-3.1
Seismic Loads	OBE Seismic Loads	2a	1-3.1
	SSE Seismic Loads	2b	1-3.1
Pressure and Temperature Loads	Normal Operating Internal Pressure	3a	1-3.1
	LOCA Internal Pressure	3b	1-4.1.1
	Normal Operating Temperature Loads	3c	1-3.1
	LOCA Temperature Loads	3d	1-4.1.1
Vent System Discharge	Pressurization and Thrust Loads	4a	1-4.1.2
Pool Swell Loads	Vent System Impact and Drag Loads	5a	1-4.1.4.1
	Impact and Drag Loads on other Structures	5b	1-4.1.4.2
	Froth Impingement & Fallback Loads	5c	1-4.1.4.3
	Pool Fallback Loads	5d	1-4.1.4.4
	LOCA Water Clearing Submerged Structure Loads	N/A	1-4.1.5
	LOCA Air Clearing Submerged Structure Loads	5e	1-4.1.6
Condensation Oscillation Loads	IBA C.O. Downcomer Loads	6a	1-4.1.7.2
	DBA C.O. Downcomer Loads	6b	1-4.1.7.2
	IBA C.O. Vent System Pressure Loads	6c	1-4.1.7.2
	DBA C.O. Vent System Pressure Loads	6d	1-4.1.7.2
	IBA C.O. Submerged Structure Loads	6e	1-4.1.7.3
	DBA C.O. Submerged Structure Loads	6f	1-4.1.7.3
Chugging Loads	Chugging Downcomer Lateral Loads	7a	1-4.1.8.2
	Chugging Vent System Pressures	7b	1-4.1.8.2
	Pre-Chug Submerged Structure Loads	7c	1-4.1.8.3
	Post-Chug Submerged Structure Loads	7d	1-4.1.8.3
SRV Discharge Loads	SRV Discharge Water Clearing Submerged Structure Loads	N/A	1-4.2.4
	SRV Discharge Air Clearing Submerged Structure Loads	8a	1-4.2.4
Piping Reaction Loads	SRV Piping Reaction Loads	9a	Vol. 5
Containment Interaction Loads	Containment Structure Motions	10a	Vol. 2

ADING INFORMATION

Component Part Loaded									Remarks
Drywell Penetration	Vent Line	Vent Line Bellows	Vent Header	Vent Header Deflector	Downcomers	Downcomer Bracing	Support Columns	Vacuum Breaker/ Supports	
X	X	X	X	X	X	X	X	X	As-modified geometry
X	X	X	X	X	X	X	X	X	0.23g horizontal, 0.067g vertical
X	X	X	X	X	X	X	X	X	0.46g horizontal, 0.133g vertical
X	X	X	X		X				0.0 to 2.0 psi
X	X	X	X		X				SBA, IBA, & DBA pressures
X	X	X	X	X	X	X	X	X	50 to 150 ^{O}F
X	X	X	X	X	X	X	X	X	SBA, IBA & DBA temperatures
X	X		X		X				Forces on unreacted areas
	X			X	X				Header shielded by deflectors
						X		X	Components below max pool height
						X		X	Two regions specified
						X			Major components not affected
							X		Effects negligible
					X		X		Primarily local effects
					X				Uniform & differential components
					X				Uniform & differential components
X	X		X						Downcomer pressures included in 6a
X	X		X						Downcomer pressures included in 6b
							X		Downcomer loads included in 6a
							X		Downcomer loads included in 6b
					X				RSEL based on FSTF
X	X		X		X				Three loading alternates
							X		Downcomer loads included in 7a
							X		Downcomer loads included in 7a
							X		Effects negligible
					X		X		Primarily local effects
	X		X						Reactions on vent line & header
X		X					X		Drywell & torus motions

Table 3-2.2-2

SUPPRESSION POOL TEMPERATURE RESPONSE

ANALYSIS RESULTS-MAXIMUM TEMPERATURES

Condition	Case Number (1)	Number of SRV's Actuated	Maximum Bulk Pool Temperature (^{O}F)
Normal Operating	1A	1	154.0
	1B	1	172.0
	2A	5	165.0
	2B	1	162.0
	2C	5	168.0
SBA Event	3A	5(ADS)	171.0
	3B	5	169.0

Note:

1. See Section 1-5.1 for a description of SRV discharge events.

Table 3-2.2-3

VENT SYSTEM PRESSURIZATION AND THRUST LOADS FOR

DBA EVENT

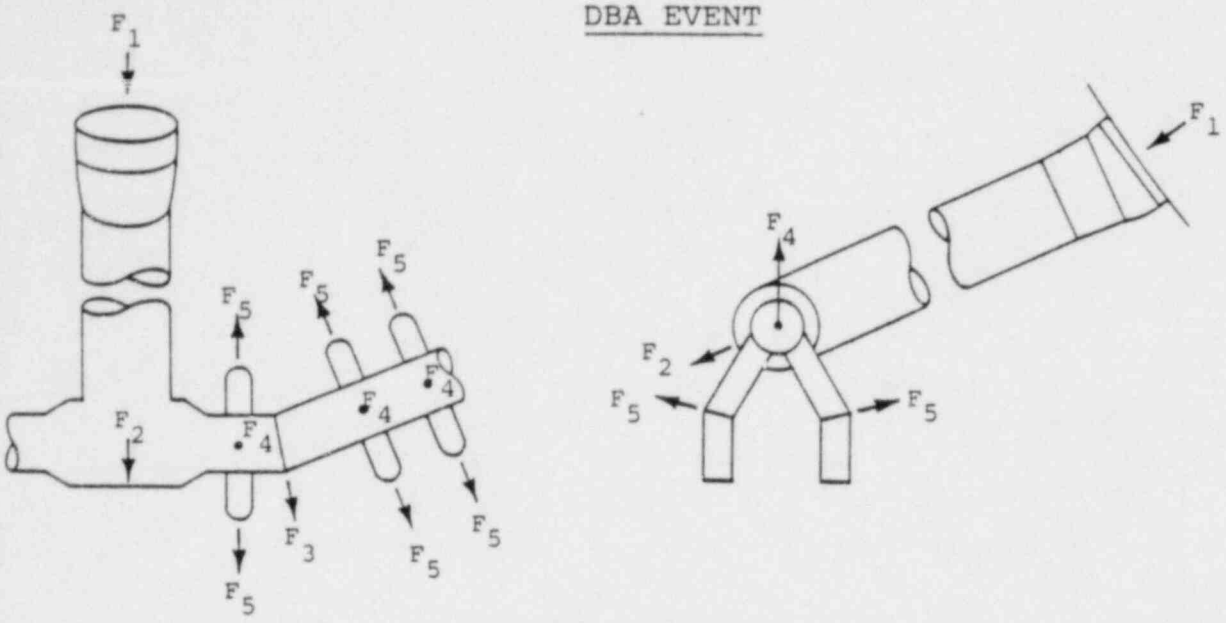

Key Diagram

Time During DBA Event (sec)	Maximum Component Force Magnitude (kips)				
	F_1(2)	F_2	F_3	F_4	F_5
Pool Swell 0.0 to 1.5	50.6	137.4	20.0	20.0	4.1
Condensation Oscillation 5.0 to 35.0	46.4	126.2	16.7	17.3	3.6
Chugging 35.0 to 65.0	6.6	19.3	5.0	3.3	0.6

Notes:

1. Loads shown include the effects of the DBA internal pressures in Figure 3-2.2-3.
2. Values shown are equal to product of penetration unreacted area and DBA internal pressure.

Table 3-2.2-4

POOL SWELL IMPACT LOADS FOR VENT LINE

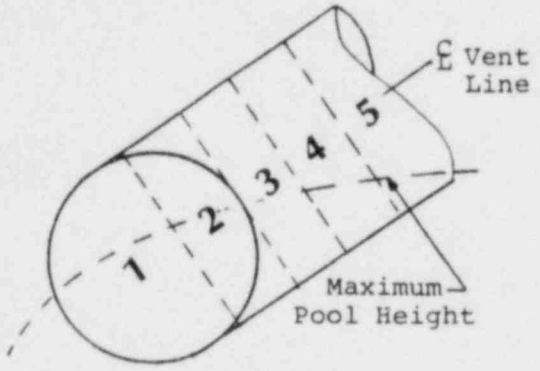

Key Diagram

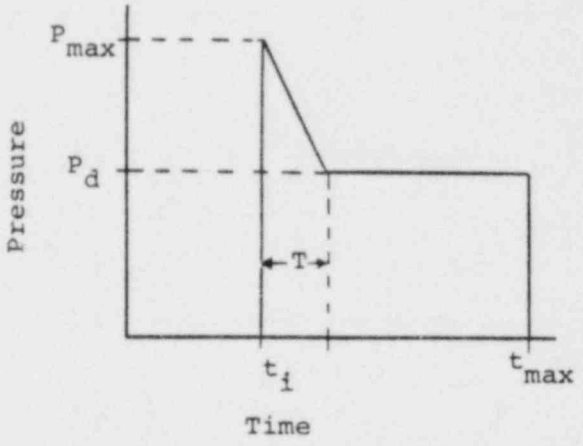

Pressure Transient

Segment Number	Time (msec)			Pressure (psi)	
	Impact (t_i)	Impact Duration (T)	Maximum Pool Height (t_{max})	Impact (P_{max})	Drag (P_d)
1	0.00	0.00	0.00	0.00	0.00
2	0.00	0.00	0.00	0.00	0.00
3	604.00	25.00	890.00	20.85	2.13
4	750.00	73.00	890.00	6.00	1.31
5	850.00	40.00	890.00	0.78	0.00

Notes:

1. For structure geometry, see Figure 3-2.1-8.
2. Pressures shown are applied to vertical projected areas in a direction normal to vent line surface.
3. Loads are symmetric with respect to vertical centerline of vent line.

Table 3-2.2-5

POOL SWELL IMPACT LOADS FOR OTHER VENT SYSTEM COMPONENTS

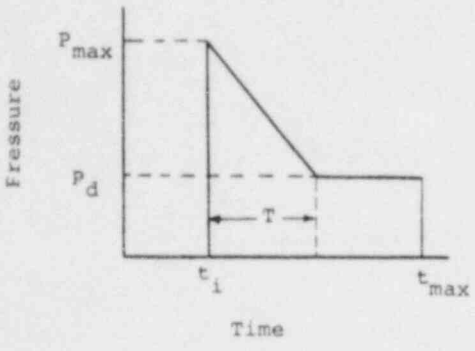

Cylindrical Structures

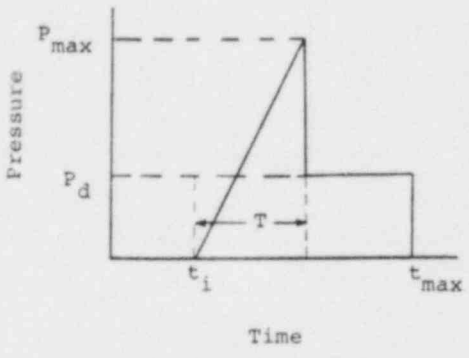

Flat Structures

PRESSURE TRANSIENTS

Item	(1) Segment Number	Time (msec)			Pressure (psi)	
		Arrival (t_i)	Impact Duration (T)	Maximum Pool Height (t_{max})	Impact (P_{max})	Drag (P_d)
DOWNCOMER BRACING - NON VENT BAY						
2" ϕ Rod	1	475.00	0.50	890.00	81.06	9.26
	2	476.00	0.50	890.00	75.78	8.41
	3	477.00	0.50	890.00	72.36	7.91
Ring Plates	1	461.00	0.14	890.00	33.52	33.52
	1	470.00	0.14	890.00	25.93	25.93
4" ϕ Pipe	1	477.00	2.10	890.00	20.75	2.85
	2	510.00	1.60	890.00	38.70	2.76
	3	N/A	N/A	N/A	N/A	N/A
DOWNCOMER BRACING - VENT BAY						
Ring Plate	1	478.00	0.16	890.00	18.06	18.06
4" ϕ Pipe	1	484.00	2.90	890.00	11.59	1.78
	2	N/A	N/A	N/A	N/A	N/A
	3	N/A	N/A	N/A	N/A	N/A
VACUUM BREAKER (5)						
Vacuum Breaker	1	650.00	30.10	890.00	4.95	1.46

Notes:

1. Segment numbers represent nodalization of structures for loads calculations.
2. For structure geometry see Figures 3-2.1-10 through 3-2.1-12.
3. Pressures shown are applied to vertical projected areas in direction normal to structure.
4. Loads are symmetric with respect to vertical centerline of vent header.
5. Pool swell impact loads do not act on vacuum breaker supports.

Table 3-2.2-6

VENT SYSTEM FROTH IMPINGEMENT AND FALLBACK LOADS

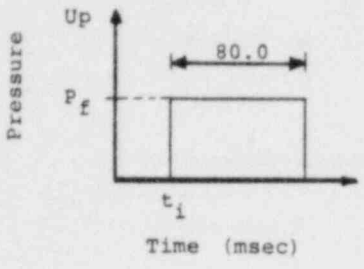

Region I Transient

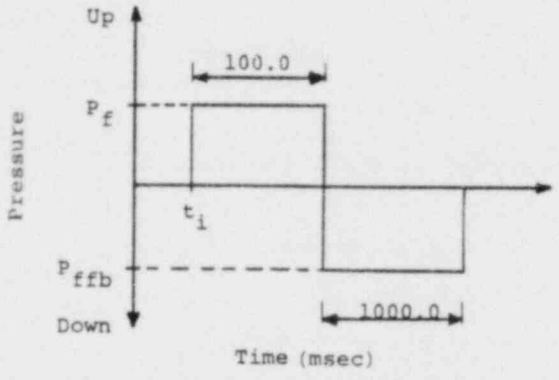

Region II Transient

DOWNCOMER BRACING REGION I FROTH (msec, psi)					
Item	Segment Number (1)	Non-Vent Bay		Vent Bay	
		Impact Time (t_i)	Froth Pressure (P_f)	Impact Time (t_i)	Froth Pressure (P_f)
2" ϕ Rod	1	365.00	2.679	N/A	N/A
	2	368.00	2.656	N/A	N/A
	3	370.00	2.629	N/A	N/A
Ring Plates	1	374.00	3.494	379.00	1.966
	1	376.00	2.770	N/A	N/A
4" ϕ Pipe	1	371.00	2.204	385.00	2.505
	2	374.00	2.301	381.00	2.260
	3	376.00	2.199	380.00	2.057

VACUUM BREAKER AND SUPPORTS FROTH (msec, psi)						
Item	Segment Number (1)	Region I		Region II		
		Impact Time (t_i)	Froth Pressure (P_f)	Impact Time (t_i)	Froth Pressure (P_f)	Fallback Pressure (P_{ffb})
Vacuum Breaker	1	400.00	0.829	N/A	N/A	N/A
Nozzle	1	400.00	1.481	N/A	N/A	N/A
Support Beam	1	384.00	0.993	N/A	N/A	N/A
	2	380.00	1.077	663.00	.130	N/A
	3	376.00	1.103	565.00	.605	N/A
	4	372.00	1.099	513.00	1.041	0.065

Notes:

1. Segment numbers represent nodalization of structures for loads calculations.
2. For structure geometry see Figures 3-2.1-10 through 3-2.1-12.
3. Pressures shown are applied to vertical projected areas in direction normal to structure.
4. Loads are symmetric with respect to vertical centerline of vent header.

Table 3-2.2-7

VENT SYSTEM POOL FALLBACK LOADS

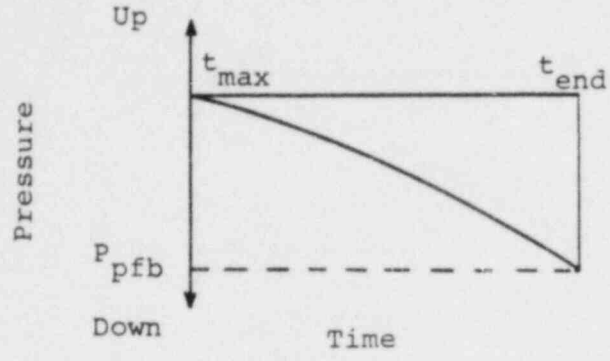

Pressure Transient

Item	Segment Number	Time (msec)		Fallback Pressure (P_{pfb}) (psi)
		Arrival (t_{max})	End of Fallback (t_{end})	
DOWNCOMER BRACING - NON-VENT BAY				
2" ϕ Rod	1	890.00	1165.00	0.38
	2	890.00	1158.00	0.15
	3	890.00	1124.00	0.12
Ring Plates	1	890.00	1166.00	3.11
	1	890.00	1132.00	2.54
4" ϕ Pipe	1	890.00	1110.00	0.19
	2	890.00	991.00	0.14
	3	N/A	N/A	N/A
DOWNCOMER BRACING - VENT BAY				
Ring Plate	1	890.00	1075.00	1.76
4" ϕ Pipe	1	890.00	1076.00	0.14
	2	N/A	N/A	N/A
	3	N/A	N/A	N/A

Notes:

1. Segment numbers represent nodalization of structures for load calculations.
2. For structure geometry see Figures 3-2.1-11 and 3-2.1-12.
3. Pressures shown are applied to vertical projected areas in direction normal to structure.
4. Loads are symmetric with respect to vertical centerline of vent header.

Table 3-2.2-8

DOWNCOMER LOCA AIR CLEARING SUBMERGED STRUCTURE

LOAD DISTRIBUTION

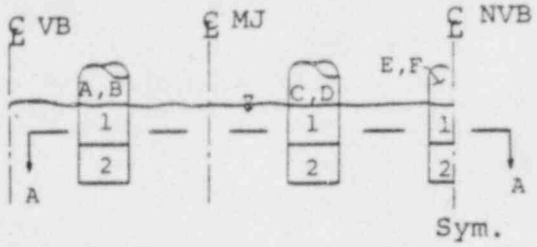

Elevation View-Downcomers

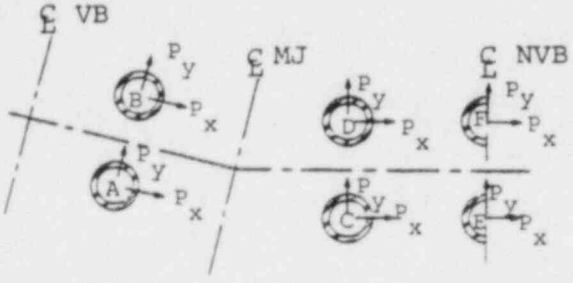

Section A-A

Item		Segment Number	Pressure Magnitude (psi)	
			P_x	P_y
Downcomer	A	1	-0.09	-0.44
		2	-0.25	-1.22
	B	1	-0.38	0.31
		2	-1.05	0.87
	C	1	-0.90	-0.56
		2	-2.61	-1.57
	D	1	-0.75	0.46
		2	-2.20	1.28
	E	1	0.00	-0.29
		2	0.00	-0.81
	F	1	0.00	0.27
		2	0.00	0.75

Note:

1. Loads shown include DLF's of 2.0.

Table 3-2.2-9

SUPPORT COLUMN LOCA AIR CLEARING SUBMERGED STRUCTURE

LOAD DISTRIBUTION

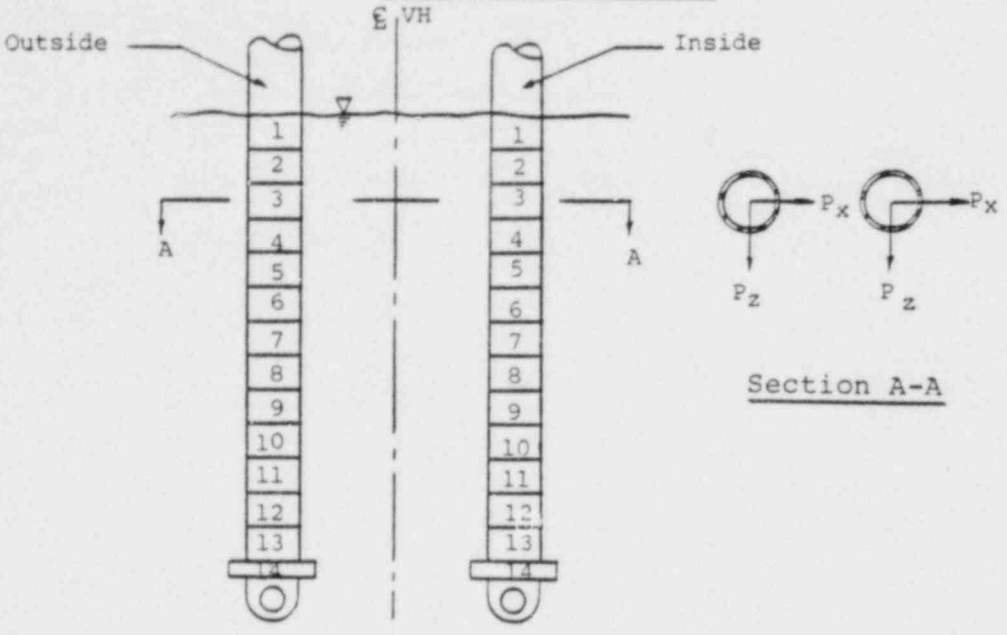

Elevation View - Mitered Joint

Section A-A

Segment Number	Pressure Magnitude (psi)			
	Inside Column		Outside Column	
	P_x	P_z	P_x	P_z
1	-0.19	0.18	-0.09	0.16
2	-0.60	0.60	-0.27	0.49
3	-1.09	1.15	-0.43	0.83
4	-1.62	1.78	-0.56	1.16
5	-1.86	2.08	-0.67	1.37
6	-1.88	2.08	-0.74	1.38
7	-1.55	1.63	-0.81	1.19
8	-1.10	1.01	-0.84	0.88
9	-0.68	0.51	-0.85	0.56
10	-0.41	0.12	-0.84	0.27
11	-0.22	-0.19	-0.80	0.07
12	-0.12	-0.29	-0.76	-0.07
13	-0.09	-0.44	-0.92	-0.18
14	-0.08	-0.58	-1.12	-0.27

Note:

1. Loads shown include DLF's of 2.0

Table 3-2.2-10

IBA CONDENSATION OSCILLATION

DOWNCOMER LOADS

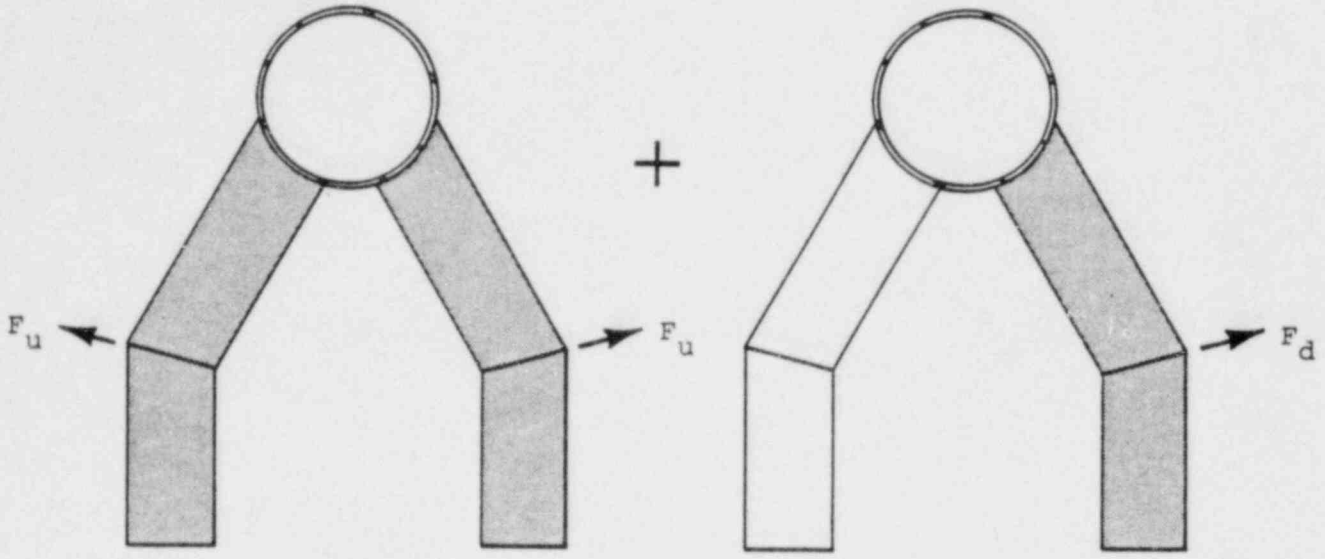

Uniform Pressure

Differential Pressure

Frequency Interval (Hz)	Downcomer Load Amplitudes (1)			
	Uniform (F_u)		Differential (F_d) (2)	
	Pressure (psi)	Force (lb)	Pressure (psi)	Force (lb)
6.0 - 10.0	1.10	241.75	0.20	43.95
12.0 - 20.0	0.80	175.82	0.20	43.95
18.0 - 30.0	0.20	43.95	0.20	43.95

Notes:

1. Effects of uniform and differential pressures summed to obtain total load.
2. See Figure 3-2.2-9 for downcomer differential pressure load distributions.

Table 3-2.2-11

DBA CONDENSATION OSCILLATION DOWNCOMER LOADS

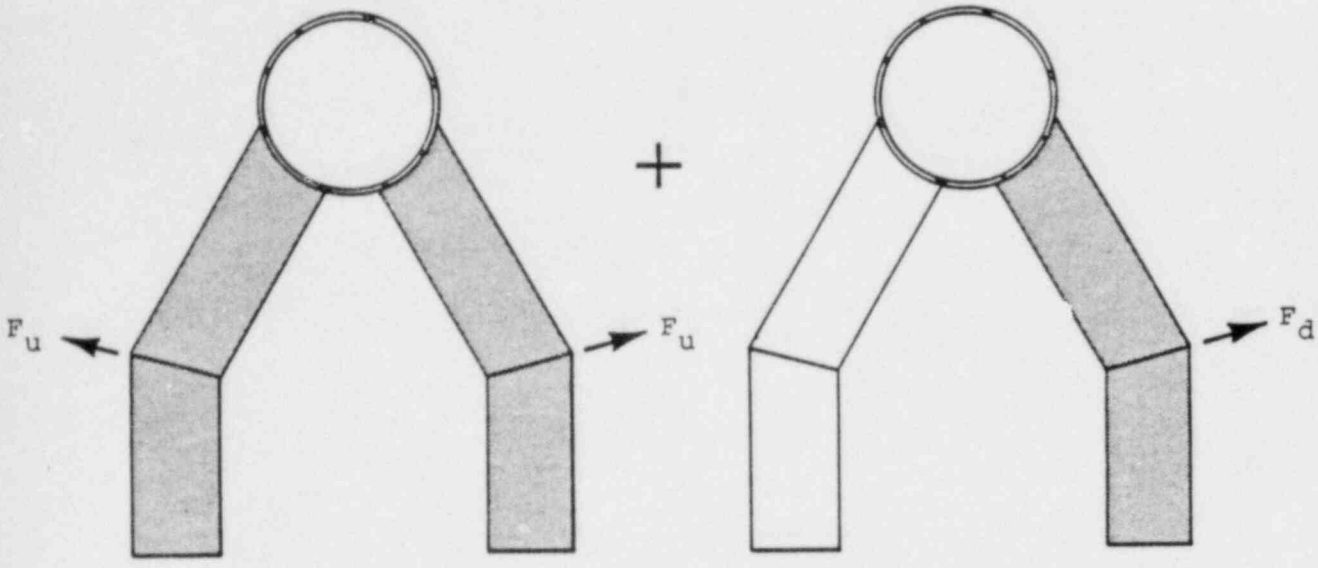

Uniform Pressure

Differential Pressure

Frequency Interval (Hz)	Downcomer Load Amplitudes (1)			
	Uniform (F_u)		Differential (F_d) (2)	
	Pressure (psi)	Force (lb)	Pressure (psi)	Force (lb)
4.0 - 8.0	3.60	791.18	2.85	626.35
8.0 - 16.0	1.30	285.70	2.60	571.41
12.0 - 24.0	0.60	131.86	1.20	263.73

Notes:

1. Effects of uniform and differential pressures summed to obtain total load.
2. See Figure 3-2.2-9 for downcomer differential pressure load distribution.

Table 3-2.2-12

IBA AND DBA CONDENSATION OSCILLATION

VENT SYSTEM INTERNAL PRESSURES

Load Characteristics	Component Load			
	Vent Line		Vent Header	
	IBA	DBA	IBA	DBA
Type	Single Harmonic	Single Harmonic	Single Harmonic	Single Harmonic
Magnitude (psi)	± 2.5	± 2.5	± 2.5	± 2.5
Distribution	Uniform	Uniform	Uniform	Uniform
Frequency Range (Hz)	6 - 10	4 - 8	6 - 10	4 - 8

Notes:

1. Downcomer CO internal pressure loads are included in loads shown in Tables 3-2.2-10 and 3-2.2-11.
2. Loads shown act in addition to vent system internal pressures in Figures 3-2.2-2 and 3-2.2-3.
3. Additional static internal pressure of 1.5 psi applied to the entire vent system to account for nominal submergence of downcomers.

Table 3-2.2-13

SUPPORT COLUMN DBA CONDENSATION OSCILLATION SUBMERGED

STRUCTURE LOAD DISTRIBUTION

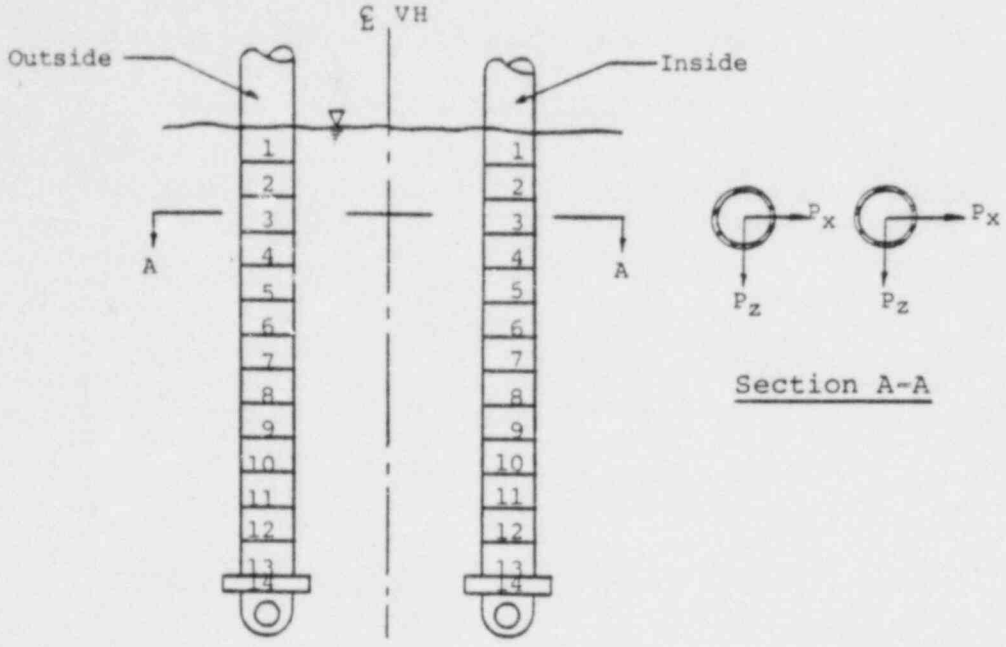

Section A-A

Elevation View-Mitered Joint

Segment Number	Pressure Magnitude (psi)			
	Inside Column		Outside Column	
	P_x	P_z	P_x	P_z
1	5.90	-5.05	34.95	-5.65
2	17.38	-15.08	50.53	-12.84
3	28.01	-24.36	54.76	-18.28
4	35.19	-30.56	53.38	-21.51
5	33.54	-28.91	49.80	-22.17
6	29.41	-24.99	45.42	-20.51
7	23.26	-19.24	40.97	-17.51
8	17.66	-13.98	36.99	-14.21
9	13.48	-10.00	33.49	-11.24
10	10.67	-7.24	30.53	-8.82
11	9.04	-5.39	27.62	-6.91
12	8.15	-4.19	25.28	-5.47
13	11.93	-5.31	36.31	-6.87
14	17.74	-7.27	52.14	9.29

Note:

1. Loads shown include FSI effects and DLF's.

Table 3-2.2-14

MAXIMUM DOWNCOMER CHUGGING LOAD MAGNITUDE DETERMINATION

Maximum Chugging Load for Single Downcomer
FSTF Maximum Load Magnitude: P_1=3.046 kips Tied Downcomer Frequency: f_1=2.9 Hz Pulse Duration: t_d= 0.003 sec. Dynamic Load Factor: $DLF_1 = \pi f_1 t_d$=0.027 Fermi 2 Downcomer Frequency: f=12.4 Hz Dynamic Load Factor: $DLF=\pi f t_d$=0.117 Maximum Load Magnitude (In any direction): $P_{max}=P_1(\frac{DLF}{DLF_1})=(3.046)(4.276)=13.02$ kips

Note:

1. See Figure 3-2.4-6 for Fermi downcomer frequency determination.

Table 3-2.2-15

MULTIPLE DOWNCOMER CHUGGING LOAD MAGNITUDE DETERMINATION

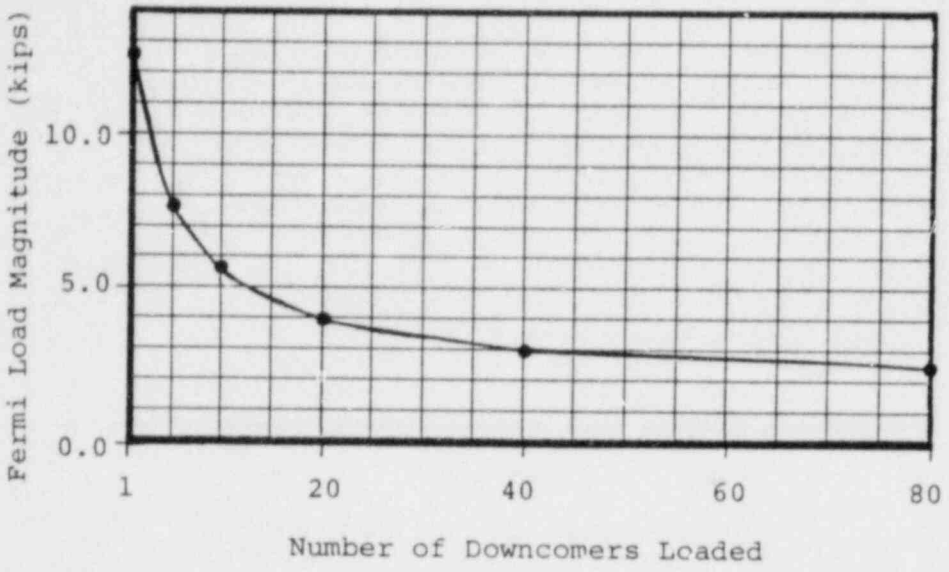

Chugging Loads for Multiple Downcomers (kips)				
Number of Downcomers	Number of Chugs	Probability of Exceedance	FSTF Load Per Downcomer	Fermi Load Per Downcomer
5	344	2.91×10^{-3}	1.77	7.57
10	688	1.45×10^{-3}	1.26	5.39
20	1375	7.27×10^{-4}	0.91	3.89
40	2751	3.64×10^{-4}	0.68	2.91
80	5502	1.82×10^{-4}	0.57	2.44

FSTF

Chugging duration: $T_{c_1} = 512$ sec
Number of downcomers: $n_{dc_1} = 8$
Number of chugs: $N_{c_1} = 313$

Fermi

Chugging duration: $T_c = 900$ sec
Number of downcomers: $n_{dc} = 2$ to 80
Number of chugs: $N_c = \frac{N_{c_1}}{T_{c_1} \times n_{dc_1}} \times T_c \times n_{dc}$
Probability of exceedance: $P_{ex} = 1/N_c$

Table 3-2.2-16

CHUGGING LATERAL LOADS FOR MULTIPLE DOWNCOMERS-MAXIMUM OVERALL EFFECTS

Case Number	Number of Downcomers Loaded	Description/Distribution	(1) Magnitude (kips)
1	80	All downcomers, parallel to MC plane, same direction, maximize overall lateral load	2.44
2	80	All downcomers, parallel to one VL, same direction, maximize overall lateral load	2.44
3	80	All downcomers, parallel to VH, same direction, maximize VL bending	2.44
4	80	All downcomers perpendicular to VH, same direction, maximize VH torque	2.44
5	10	Downcomers centered on one VL, perpendicular to VH, opposing directions, maximize VL bending	5.39
6	10	Downcomers centered on one VL, perpendicular to VH, same directions, maximize VL axial loads	5.39
7	10	All downcomers between two VL's, perpendicular to VH, same direction maximize VH bending	5.39
8-10	4	NVB downcomers near miter, parallel to VH, permutate directions, maximize DC bracing loads	8.51

Note:

1. Magnitudes obtained from Table 3-2.2-15.

Table 3-2.2-17

CHUGGING LATERAL LOADS FOR TWO DOWNCOMERS LOADED-

MAXIMIZE LOCAL EFFECTS

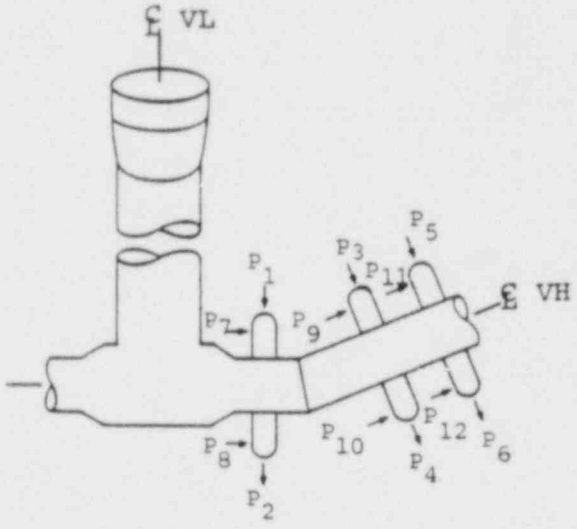

Key Diagram-Plan View

Downcomer Load Cases for Maximum Local Effects					
Case Number	Active[1] Loads (P_i)	Magnitude[2] (kips)	Case Number	Active[1] Loads(P_i)	Magnitude[2] (kips)
11	$+P_1, -P_2$	11.16	17	$-P_9, +P_{10}$	11.16
12	$+P_1, +P_2$	11.16	18	$+P_9, +P_{10}$	11.16
13	$-P_7, +P_8$	11.16	19	$+P_5, -P_6$	11.16
14	$+P_7, +P_8$	11.16	20	$+P_5, +P_6$	11.16
15	$+P_3, -P_4$	11.16	21	$-P_{11}, +P_{12}$	11.16
16	$+P_3, +P_4$	11.16	22	$+P_{11}, +P_{12}$	11.16

Notes:

1. Signs designate direction.
2. Magnitudes obtained from Table 3-2.2-15.

Table 3-2.2-18

LOAD REVERSAL HISTOGRAM FOR CHUGGING

DOWNCOMER LATERAL LOAD FATIGUE EVALUATION

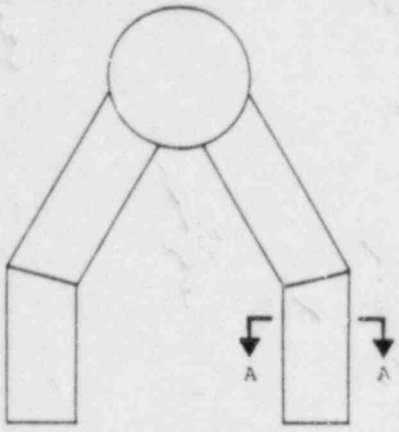

Elevation View

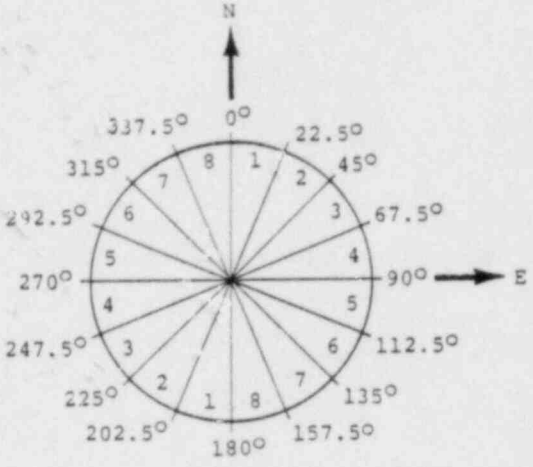

Section A-A

KEY DIAGRAM

Percent of Maximum Load Range[2]	Angular Sector Load Reversals (cycles)[1]							
	1	2	3	4	5	6	7	8
5 - 10	4706	2573	2839	3076	3168	2673	2563	4629
10 - 15	2696	1206	1100	1104	1096	1052	1163	2545
15 - 20	1399	727	653	572	769	708	679	1278
20 - 25	676	419	452	377	370	398	368	621
25 - 30	380	250	252	225	192	255	197	334
30 - 35	209	187	139	121	97	114	162	208
35 - 40	157	62	84	86	62	60	90	150
40 - 45	113	53	28	39	48	44	58	86
45 - 50	63	33	32	26	18	23	33	67
50 - 55	65	26	14	11	9	7	16	40
55 - 60	51	26	11	5	11	11	23	28
60 - 65	44	9	2	4	0	5	9	26
65 - 70	32	16	7	5	0	2	9	21
70 - 75	12	9	11	5	0	4	7	19
75 - 80	26	4	2	0	2	4	7	18
80 - 85	7	5	2	0	0	0	0	12
85 - 90	4	1	0	0	0	0	5	11
90 - 95	7	4	0	0	2	0	0	9
95 - 100	2	5	0	0	0	2	4	7

Notes:

1. Values shown are for chugging duration of 900 sec.
2. The maximum single downcomer load magnitude range used for fatigue is 3.936 x 4.276 = 16.8 kips (see Table 3-2.2-14).

nutech ENGINEERS

Table 3-2.2-19

CHUGGING VENT SYSTEM INTERNAL PRESSURES

Load Type		Load Description	Component Load Magnitude (psi)		
Number	Description		Vent Line	Vent Header	Downcomer
1	Gross Vent System Pressure Oscillation	Transient pressure. Uniform distribution.	± 2.5	± 2.5	± 5.0
2	Acoustic Vent System Pressure Oscillation	Single harmonic in 6.9 to 9.5 Hz range. Uniform distribution.	± 2.5	± 3.0	± 3.5
3	Acoustic Downcomer Pressure Oscillation	Single harmonic in 40.0 to 50.0 Hz range. Uniform distribution.	N/A	N/A	± 13.0

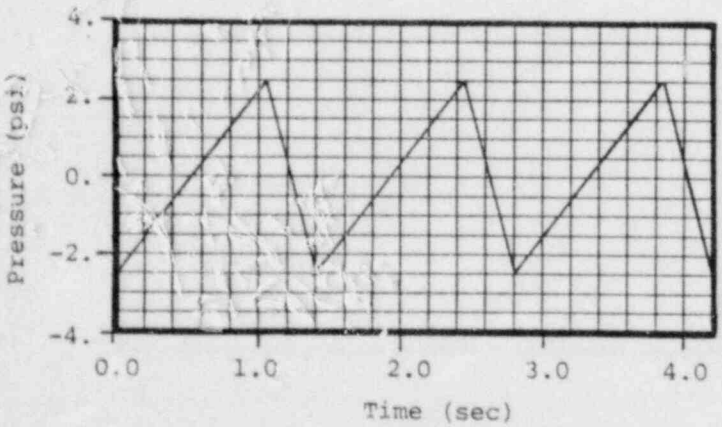

Forcing Function for Load Type 1

Loading Information
1. Downcomer loads shown used for hoop stress calculations only.
2. Loads act in addition to internal pressure loads shown in Figures 3-2.2-2 and 3-2.2-3.

Table 3-2.2-20

SUPPORT COLUMN PRE-CHUG SUBMERGED STRUCTURE

LOAD DISTRIBUTION

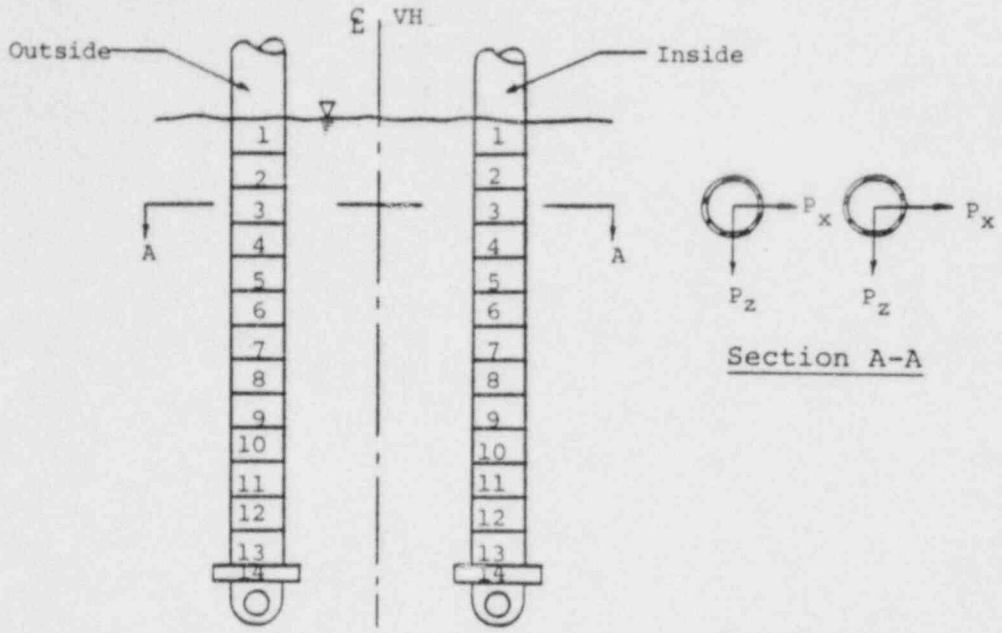

Section A-A

Elevation View - Filtered Joint

Segment Number	Pressure Magnitude (psi)			
	Inside Column		Outside Column	
	P_x	P_z	P_x	P_z
1	0.26	-0.19	0.34	-0.17
2	0.78	-0.59	0.59	-0.43
3	1.25	-0.98	0.74	-0.62
4	1.56	-1.23	0.83	-0.72
5	1.47	-1.07	0.89	-0.69
6	1.25	-0.74	0.92	-0.54
7	0.93	-0.34	0.93	-0.34
8	0.66	-0.03	0.92	-0.14
9	0.46	-0.18	0.89	-0.10
10	0.33	-0.30	0.85	-0.20
11	0.26	-0.35	0.80	-0.25
12	0.22	-0.37	0.74	-0.28
13	0.32	-0.58	1.08	-0.45
14	0.47	-0.86	1.55	-0.67

Note:

1. Loads shown include FSI effects and DLF's.

Table 3-2.2-21

SUPPORT COLUMN POST-CHUG SUBMERGED STRUCTURE

LOAD DISTRIBUTION

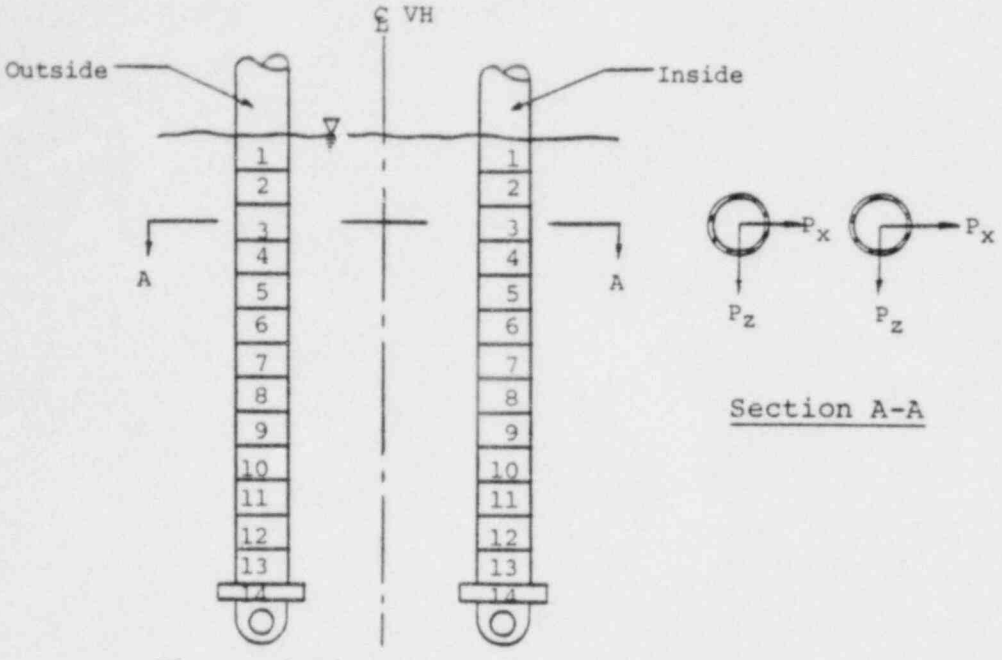

Section A-A

Elevated View-Mitered Joint

Segment Number	Pressure Magnitude (psi)			
	Inside Column		Outside Column	
	P_x	P_z	P_x	P_z
1	17.05	-3.07	11.20	-2.44
2	50.77	-9.23	22.92	-6.53
3	81.49	-14.99	31.23	-9.89
4	102.44	-18.76	36.41	-11.98
5	98.63	-17.49	38.60	-12.44
6	88.70	-14.63	38.16	-11.39
7	72.54	-10.66	35.85	-9.48
8	56.83	-7.14	32.60	-7.40
9	44.18	-4.57	29.07	-5.57
10	34.71	-2.87	25.70	-4.13
11	27.81	-1.80	22.57	-3.06
12	22.85	-1.14	19.96	-2.29
13	30.01	-1.17	27.74	-2.75
14	41.67	-1.44	39.28	-3.64

Note:

1. Loads shown include FSI effects and DLF's.

Table 3-2.2-22

DOWNCOMER SRV DISCHARGE SUBMERGED STRUCTURE LOAD DISTRIBUTION

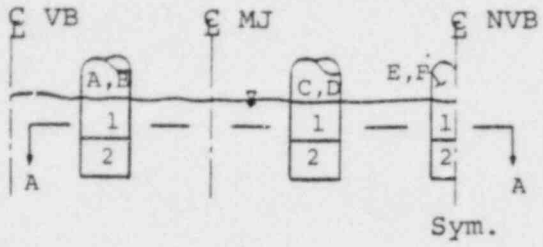

Elevation View-Downcomers

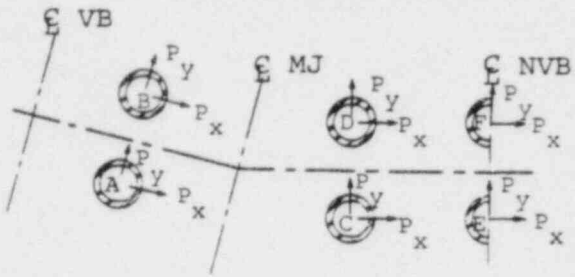

Section A-A

Item		Segment Number	Pressure Magnitude (psi)	
			P_x (1)	P_y (1)
Downcomer	A	1	1.55	-0.08
		2	2.69	-0.27
	B	1	1.57	0.27
		2	2.69	0.53
	C	1	-0.17	-2.30
		2	-0.37	-4.19
	D	1	-0.92	2.06
		2	-1.59	3.76
	E	1	0.70	0.10
		2	1.58	-0.29
	F	1	1.22	0.12
		2	2.64	0.29

Note:

1. Loads in X and Y direction include DLF's of 2.0 and 3.0, respectively.

Table 3-2.2-23

SUPPORT COLUMN SRV SUBMERGED STRUCTURE LOAD DISTRIBUTION

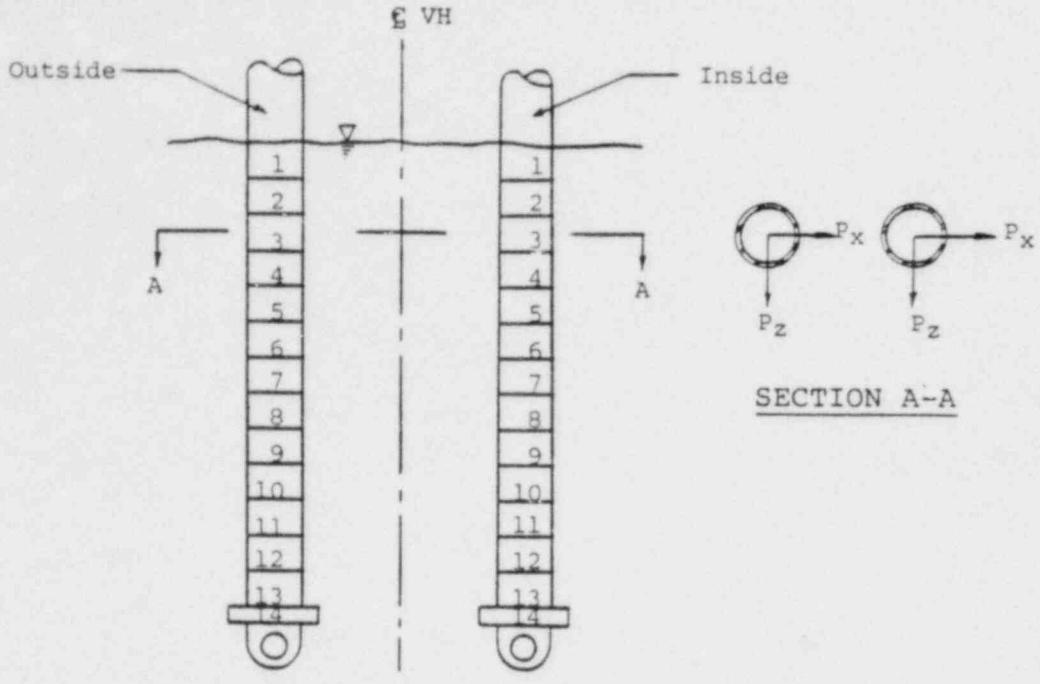

SECTION A-A

Elevation View-Mitered Joint

Segment Number	Pressure Magnitude (psi)			
	Inside Column		Outside Column	
	P_x	P_z	P_x	P_z
1	0.12	0.21	0.12	0.21
2	0.12	0.21	0.12	0.21
3	0.28	0.45	0.28	0.45
4	0.28	0.45	0.28	0.45
5	0.33	0.50	0.33	0.50
6	0.39	0.54	0.39	0.54
7	0.46	0.52	0.46	0.52
8	0.46	0.52	0.46	0.52
9	0.49	0.44	0.49	0.44
10	0.49	0.44	0.49	0.44
11	0.25	0.80	0.25	0.80
12	0.25	0.80	0.25	0.80
13	0.46	1.13	0.46	1.13
14	0.58	1.50	0.58	1.50

Note:

1. Loads shown include DLF of 3.0.

P_o = 0.0 psi

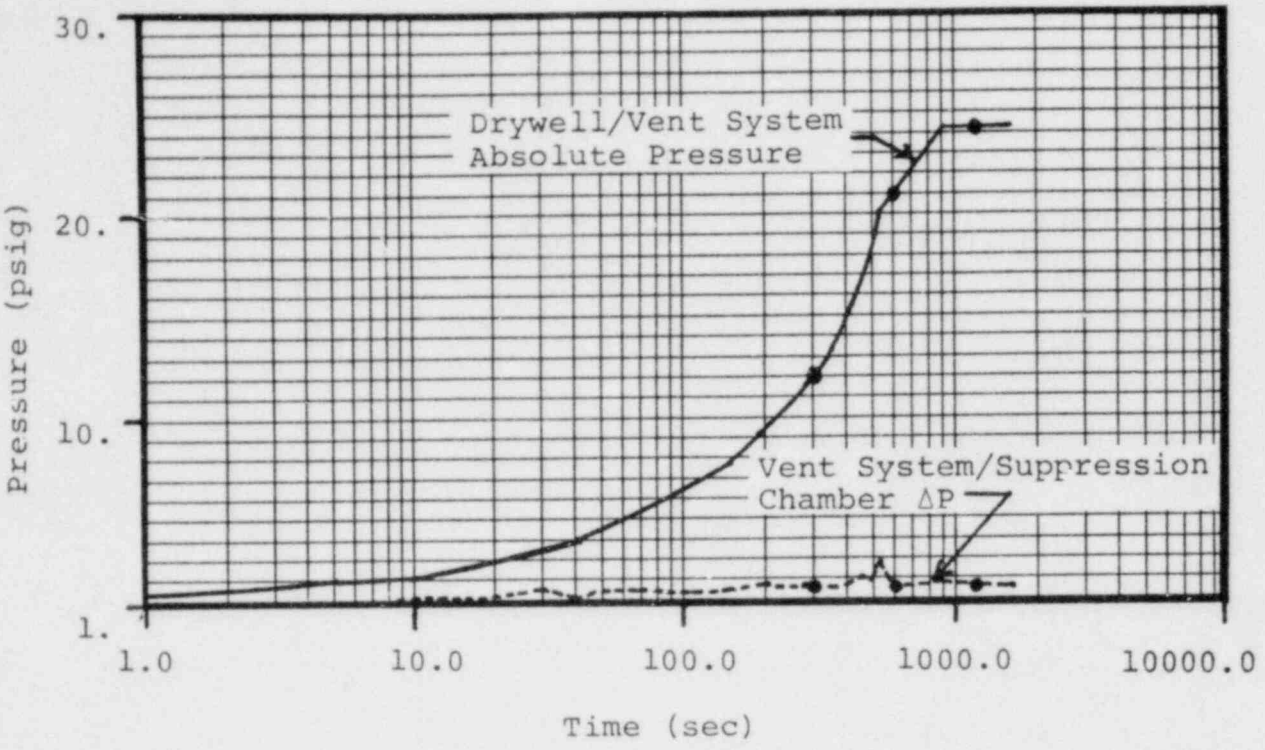

Event Description	Pressure Designation	Time (sec)		Pressure (psig)			
		t_{min}	t_{max}	P_{min}	ΔP_{min}	P_{max}	ΔP_{max}
Instant of Break to Onset of Chugging	P_1	0.	300.	0.750	0.175	11.7	1.7
Onset of Chugging to Initiation of ADS	P_2	300.	600.	11.7	1.7	20.9	1.5
Initiation of ADS to RPV Depressurization	P_3	600.	1200.	20.9	1.5	24.2	1.8

Figure 3-2.2-1

VENT SYSTEM INTERNAL PRESSURES FOR SBA EVENT

P_o = 0.0 psi

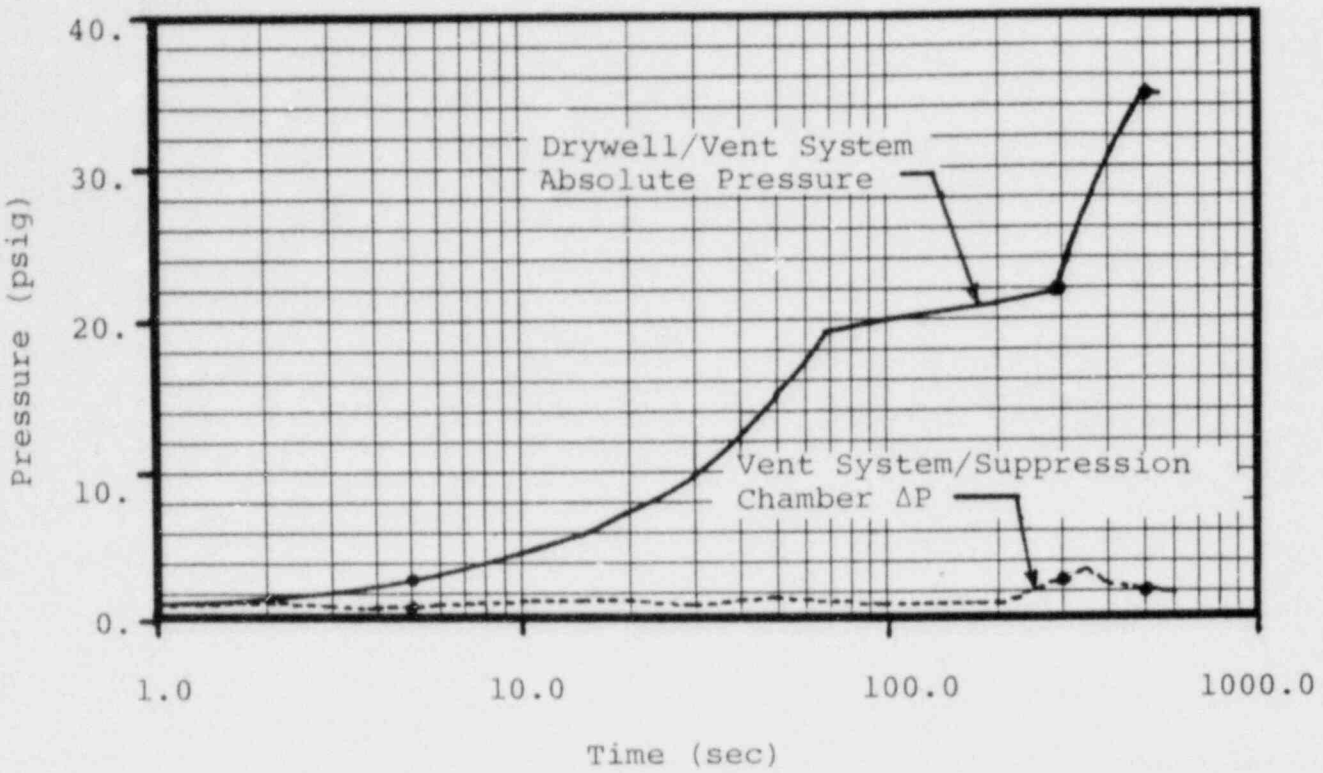

Event Description	Pressure Designation	Time (sec)		Pressure (psig)			
		t_{min}	t_{max}	P_{min}	ΔP_{min}	P_{max}	ΔP_{max}
Instant of Break to Onset of CO and Chugging	P_1	0.	5.	0.750	0.175	3.0	1.5
Onset of CO and Chugging to Initiation of ADS	P_2	5.	300.	3.0	1.5	21.7	1.4
Initiation of ADS to RPV Depressurization	P_3	300.	500.	21.7	1.4	34.7	2.0

Figure 3-2.2-2

VENT SYSTEM INTERNAL PRESSURES FOR IBA EVENT

P_o = 0.0 psi

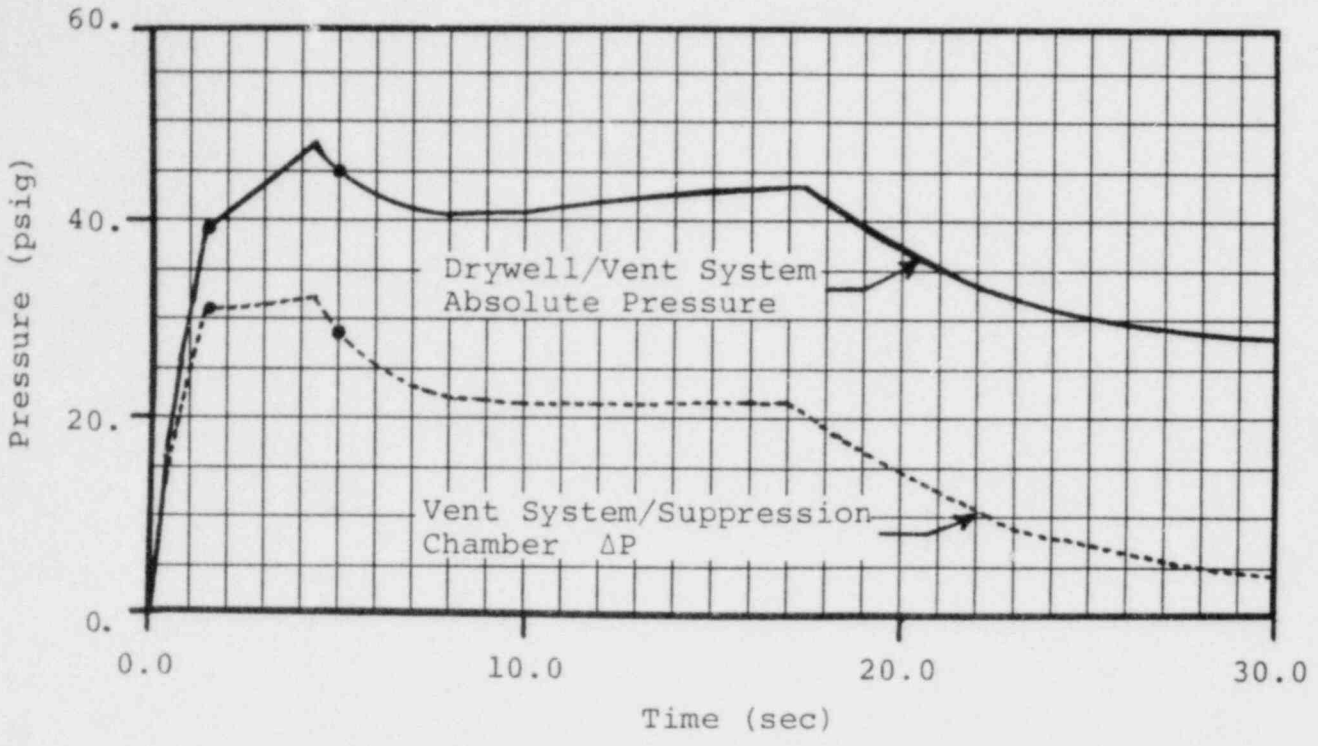

Event Description	Pressure Designation	Time (sec)		Pressure (psig)			
		t_{min}	t_{max}	P_{min}	ΔP_{min}	P_{max}	ΔP_{max}
Instant of Break to Termination of Pool Swell	P_1	0.0	1.5	0./50	0.175	39.6	31.6
Termination of Pool Swell to Onset of CO	P_2	1.5	5.0	39.6	31.6	48.0	32.5
Onset of CO to Onset of Chugging	P_3	5.0	35.0	28.0	4.1	45.0	29.0
Onset of Chugging to RPV Depressurization	P_4	35.0	65.0	28.0	4.1	28.0	4.1

Note:

1. DBA vent system internal pressure loads are included in vent system pressurization and thrust loads shown in Table 3-2.2-3.

Figure 3-2.2-3

VENT SYSTEM INTERNAL PRESSURES FOR DBA EVENT

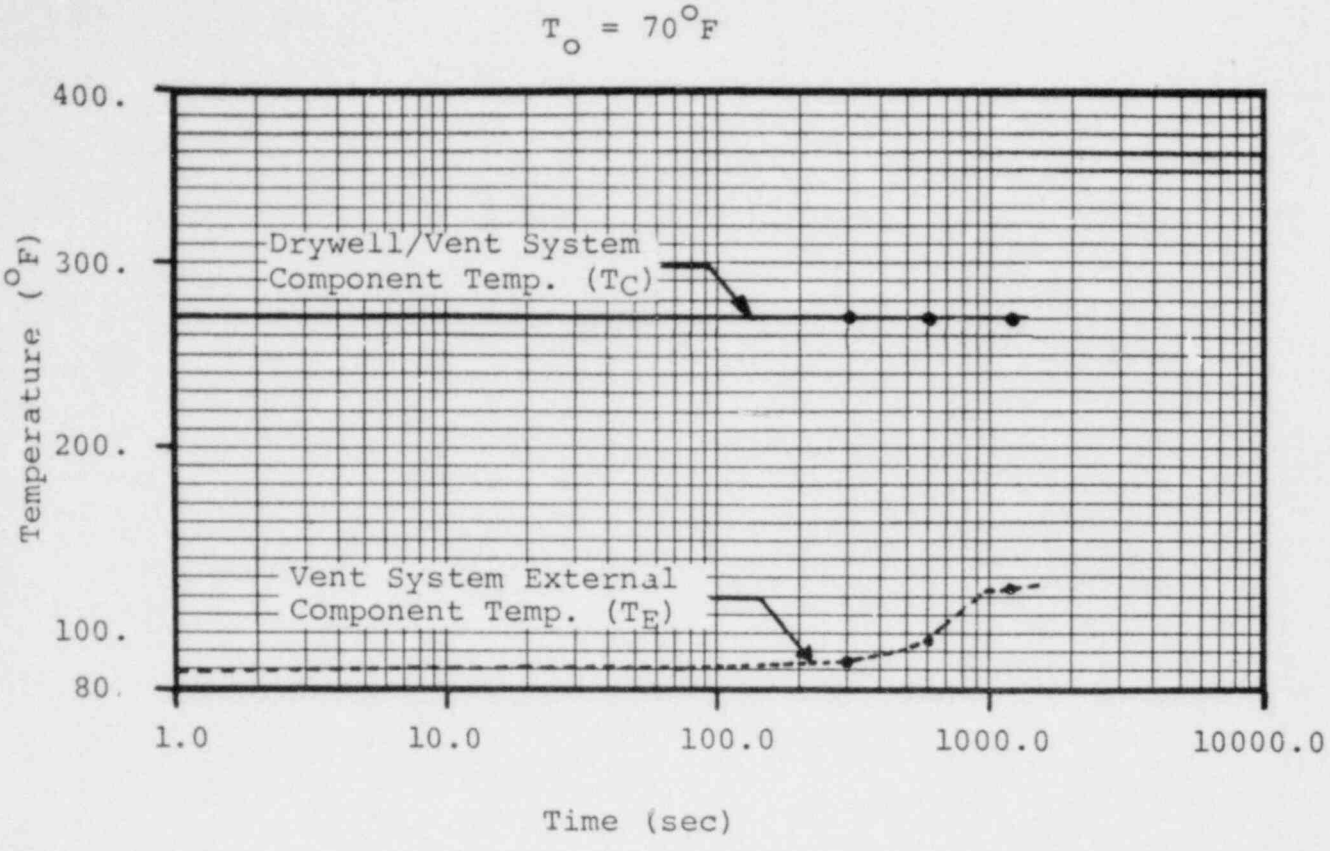

Note:

1. See Table 3-2.2-2 for additional SBA event temperatures.

Event Description	Temperature Designation	Time (sec)		Temperature (^oF)			
		t_{min}	t_{max}	$T_{C_{min}}$	$T_{E_{min}}$	$T_{C_{max}}$	$T_{E_{max}}$
Instant of Break to Onset of Chugging	T_1	0.	300.	135.0	95.0	270.0	98.0
Onset of Chugging to Initiation of ADS	T_2	300.	600.	270.0	98.0	270.0	103.0
Initiation of ADS to RPV Depressurization	T_3	600.	1200.	270.0	103.0	270.0	134.0

Figure 3-2.2-4

VENT SYSTEM TEMPERATURES

FOR SBA EVENT

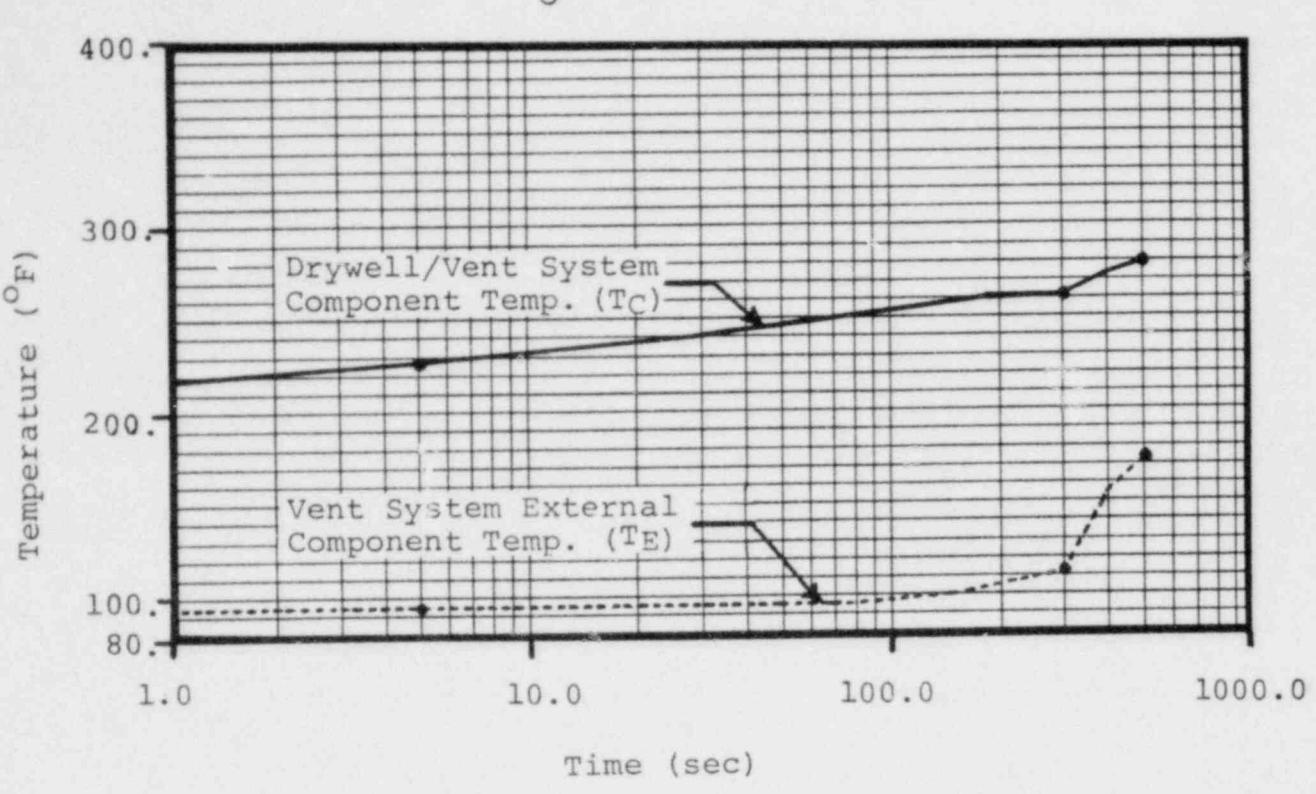

Event Description	Temperature Designation	Time (sec)		Temperature (^oF)			
		t_{min}	t_{max}	$T_{C_{min}}$	$T_{E_{min}}$	$T_{C_{max}}$	$T_{E_{max}}$
Instant of Break to Onset of CO and Chugging	T_1	0.	5.	135.0	95.0	228.0	95.0
Onset of CO and Chugging to Initiation of ADS	T_2	5.	300.	228.0	95.0	262.0	112.0
Initiation of ADS to RPV Depressurization	T_3	300.	500.	262.0	112.0	280.0	173.0

Figure 3-2.2-5

VENT SYSTEM TEMPERATURES

FOR IBA EVENT

nutech ENGINEERS

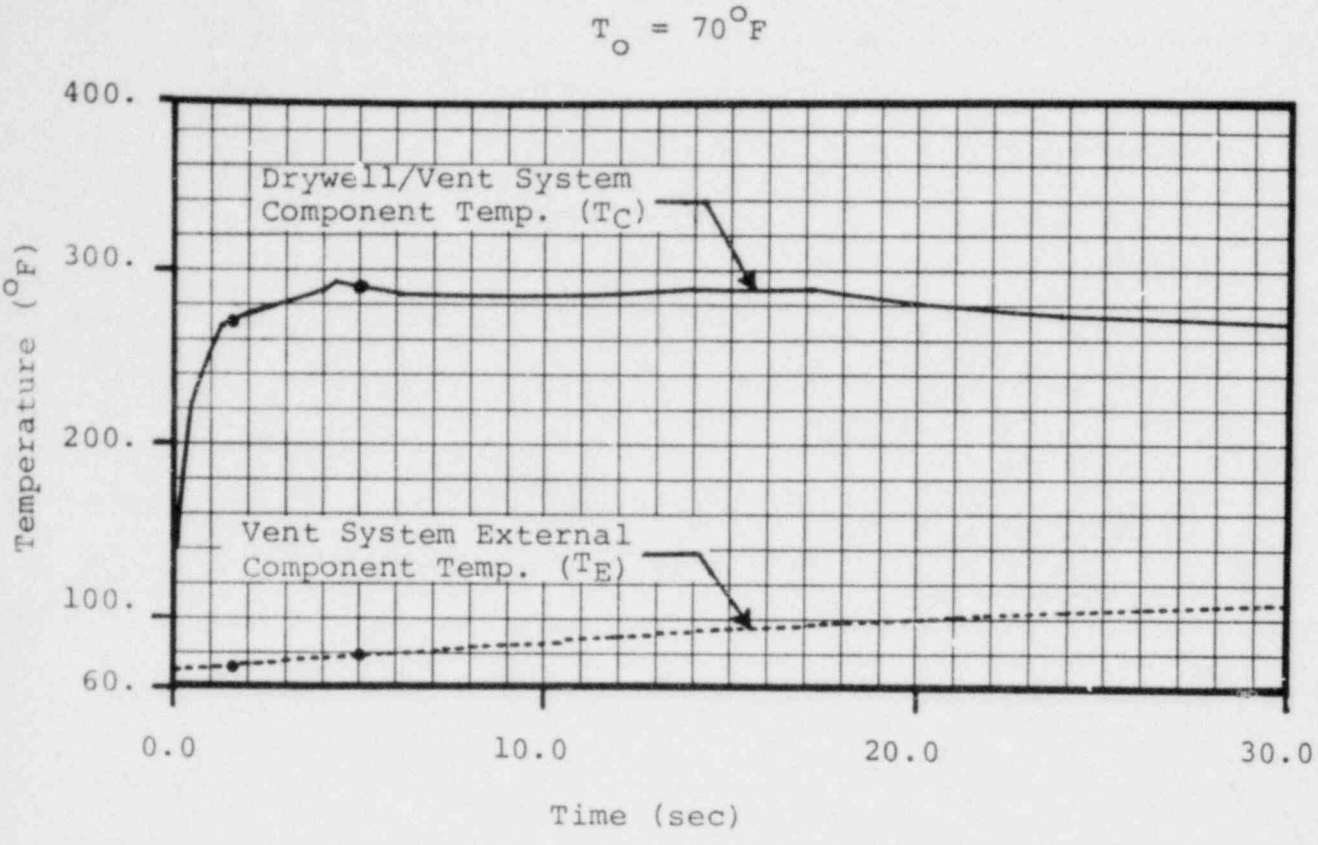

Event Description	Temperature Designation	Time (sec)		Temperature (^oF)			
		t_{min}	t_{max}	$T_{C_{min}}$	$T_{E_{min}}$	$T_{C_{max}}$	$T_{E_{max}}$
Instant of Break to Termination of Pool Swell	T_1	0.0	1.5	135.0	70.0	276.0	73.5
Termination of Pool Swell to Onset of CO	T_2	1.5	5.0	276.0	73.5	292.0	78.8
Onset of CO to Onset of Chugging	T_3	5.0	35.0	292.0	78.8	270.0	109.0
Onset of Chugging to RPV Depressurization	T_4	35.0	65.0	270.0	109.0	270.0	109.0

Figure 3-2.2-6

VENT SYSTEM TEMPERATURES

FOR DBA EVENT

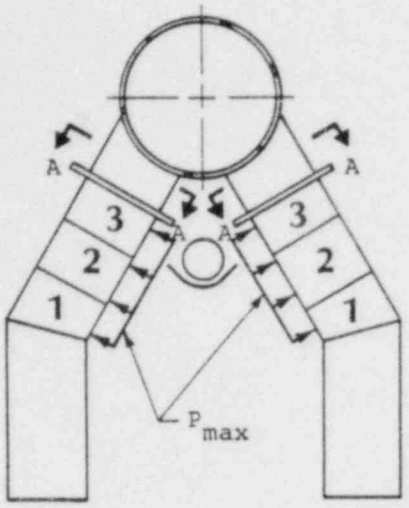

Elevation View

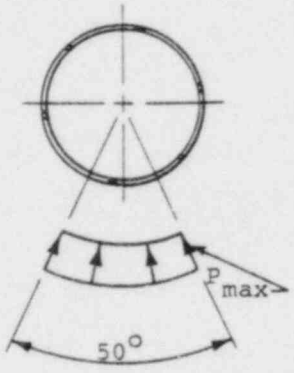

Section A-A

Pressure Distribution

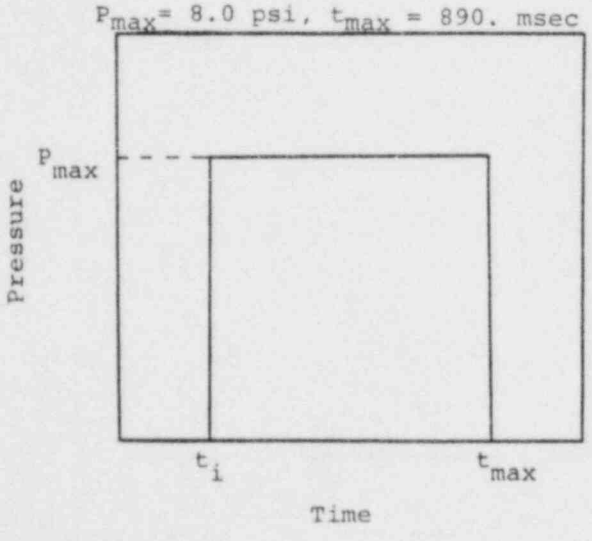

Pressure Transient

Load Information		
Downcomer Pair Location	Segment Number	Impact Time t_i (msec)
Vent Bay	1	343.00
	2	410.00
	3	459.00
Non-Vent Bay Near Miter	1	343.00
	2	406.00
	3	452.00
Midcylinder Non-Vent Bay	1	337.00
	2	402.00
	3	450.00

Note:

1. Pressures shown are applied in a direction normal to downcomers surface.

Figure 3-2.2-7

DOWNCOMER POOL SWELL IMPACT LOADS

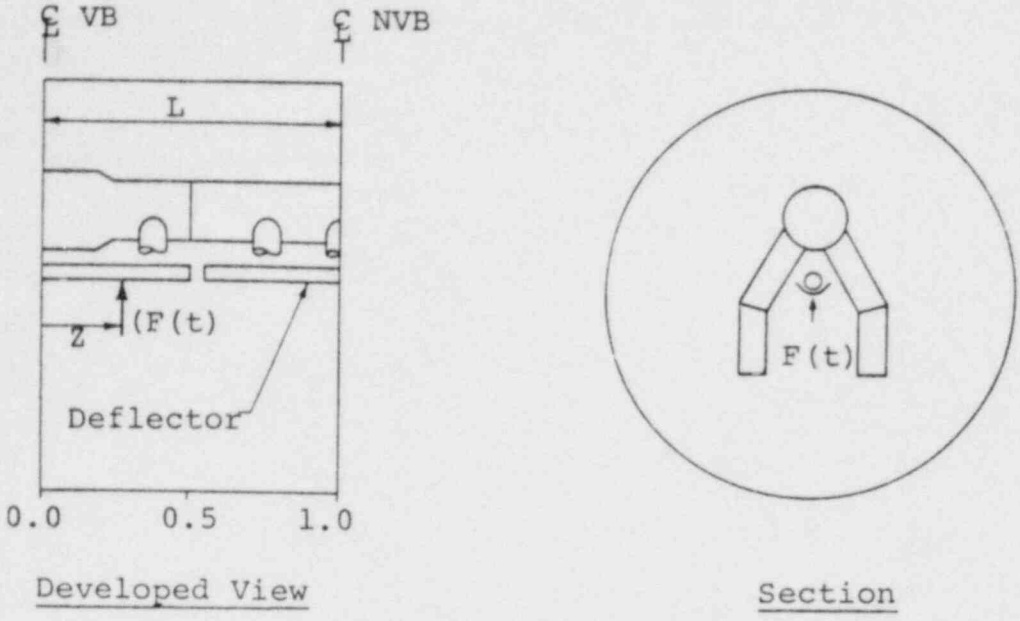

Developed View

Section

KEY DIAGRAM

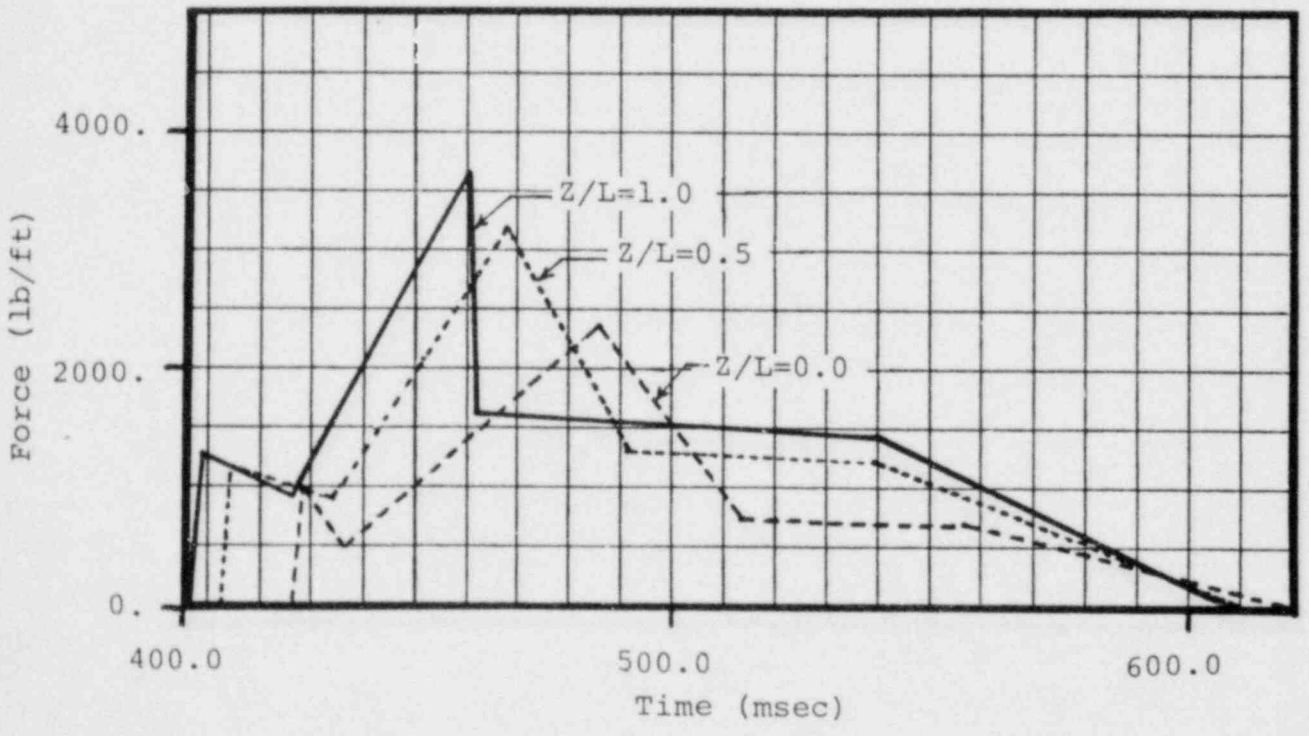

Note:

1. Loads at discrete locations along deflector obtained by linear interpolation.

Figure 3-2.2-8

POOL SWELL IMPACT LOADS FOR VENT HEADER DEFLECTORS AT SELECTED LOCATIONS

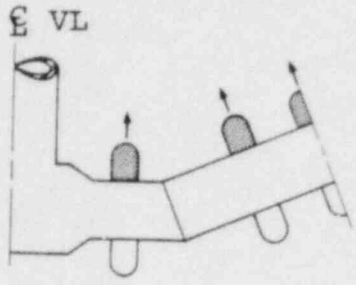

Case 1

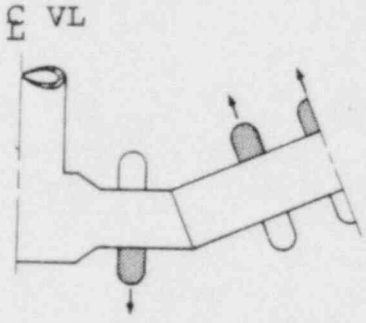

Case 2

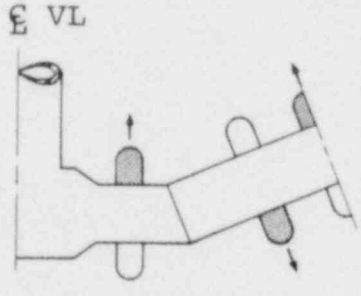

Case 3

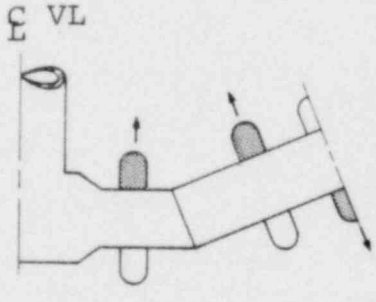

Case 4

Notes:

1. See Table 3-2.2-10 for IBA pressure amplitudes and frequencies.
2. See Table 3-2.2-11 for DBA pressure amplitudes and frequencies.
3. Four additional cases with pressures in downcomers opposite those shown are also considered.

Figure 3-2.2-9

IBA AND DBA CONDENSATION OSCILLATION DOWNCOMER DIFFERENTIAL PRESSURE LOAD DISTRIBUTION

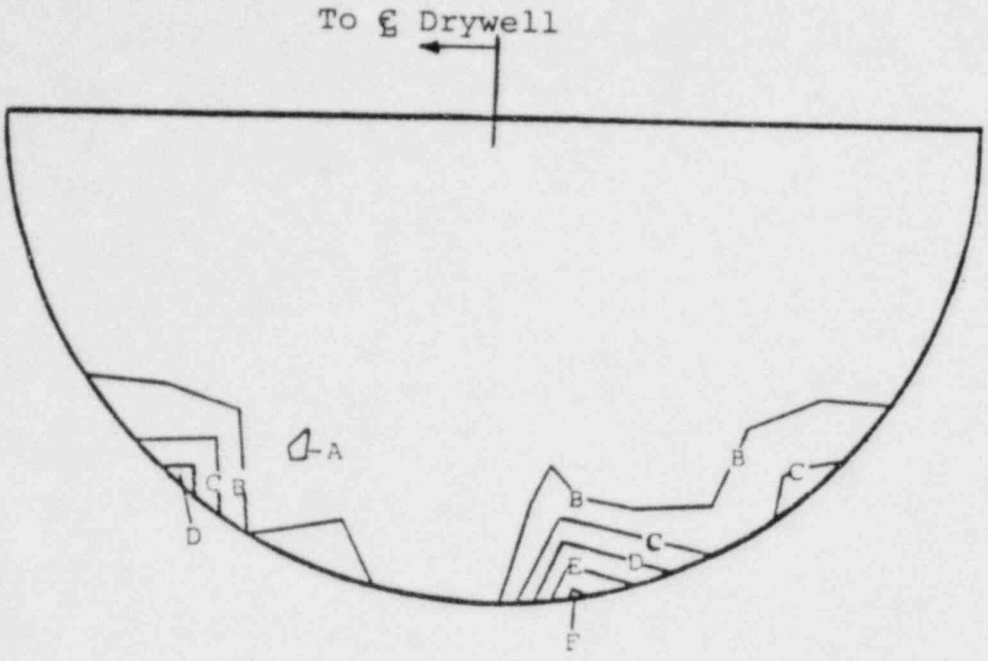

Key Diagram

Loading Information	
Profile	Pool Acceleration (ft/sec^2)
A	10.0
B	20.0
C	30.0
D	40.0
E	50.0
F	60.0
Pool accelerations due to harmonic application of torus shell pressures shown in Figure 2-2.2-10 at a suppression chamber frequency of 20.39hz.	

Figure 3-2.2-10

POOL ACCELERATION PROFILE FOR DOMINANT

SUPPRESSION CHAMBER FREQUENCY

AT MIDCYLINDER LOCATION

3-2.2.2 Load Combinations

The load categories and associated load cases for which the vent system is evaluated are presented in Section 3-2.2.1. The general NUREG-0661 criteria for grouping the respective loads and load categories into event combinations are discussed in Section 1-3.2 and presented in Table 3-2.2-24.

The 27 general event combinations shown in Table 3-2.2-24 are expanded to form a total of 69 specific vent system load combinations for the Normal Operating, SBA, IBA, and DBA events. The specific load combinations reflect a greater level of detail than is contained in the general event combinations, including distinction between SBA and IBA, distinction between pre-chug and post-chug, and consideration of multiple cases of particular loadings. The total number of vent system load combinations consists of 3 for the Normal Operating event, 18 for the SBA event, 24 for the IBA event, and 24 for the DBA event. Several different service level limits and corresponding sets of allowable stresses are associated with these load combinations.

Not all of the possible vent system load combinations are evaluated since many are enveloped by others and do not lead to controlling vent system stresses. The enveloping load combinations are determined by examining the possible vent system load combinations and comparing the respective load cases and allowable stresses. The results of this examination are shown in Table 3-2.2-25, where each enveloping load combination is assigned a number for ease of identification.

The enveloping load combinations are reduced further by examining relative load magnitudes and individual load characteristics to determine which load combinations lead to controlling vent system stresses. The load combinations which have been found to produce controlling vent system stresses are separated into two groups. The SBA II, IBA I, DBA I, DBA II, and DBA III combinations are used to evalute stresses in all vent system components except those associated with the vent line-SRV piping penetrations. The NOC I, SBA II, IBA I, and DBA III combinations are use to evaluate stresses in the vent line-SRV piping penetrations. An explanation of the logic used to conclude that these are the controlling vent system load combinations is presented

in the paragraphs which follow. Table 3-2.2-26 summarizes the controlling load combinations and identifies which load combinations are enveloped by each of the controlling combinations.

Many of the general event combinations shown in Table 3-2.2-24 have the same allowable stresses and are enveloped by others which contain the same or additional load cases. There is no distinction between Service Level A and B conditions for the vent system, since the Service Level A and B allowable stress values are the same.

Many pairs of load combinations contain identical load cases except for seismic loads. One of the load combinations in the pair contains OBE loads and has Service Level A or B allowables, while the other contains SSE loads with Service Level C allowables. It is evident from examining the load magnitudes presented in Section 3-2.2.1 that both the OBE and SSE vertical accelerations are small compared to gravity. As a result, vent system stresses and support column reactions due to vertical seismic loads are small compared to those caused by other loads in the load combination. The horizontal loads for OBE and SSE are less than 50%

of gravity and also result in small vent system stresses compared to those caused by other loads in the load combinations, except at the vent line-drywell penetrations which provide horizontal support for the vent system. The Service Level C primary stress allowables for the load combinations containing SSE loads are 40 to 80% higher than the Service Level B allowables for the corresponding load combination containing OBE loads. It is apparent, therefore, that the controlling load combinations for evaluation of vent system components, except the vent line-drywell penetration, are those containing OBE loads and Service Level B allowables.

For the vent line-drywell penetration, evaluation of both OBE and SSE combinations is necessary, since seismic loads are a large contributor to the total lateral load acting on the vent system for which the penetrations provide support.

By applying the above reasoning to the total number of vent system load combinations, a reduced number of enveloping load combinations for each event is obtained. The resulting vent system load combinations for the Normal Operating, SBA, IBA and DBA events are shown in Table 3-2.2-25, along with the associated service level

assignments. For ease of identification, each load combination in each event is assigned a number. The reduced number of enveloping load combinations shown in Table 3-2.2-25 consists of 1 for the Normal Operating event, 4 for the SBA event, 5 for the the IBA event, and 6 for the DBA event. The load case designations for the loads which make up the combinations are the same as those presented in Section 3-2.2.1.

It is evident from an examination of Table 3-2.2-25 that further reductions in the number of vent system load combinations requiring evaluation are possible. Any of the SBA or IBA combinations envelop the NOC I combination, since they contain the same loadings as the NOC I combination and in addition, contain condensation oscillation or chugging loads. The NOC I combination does, however, result in local thermal effects in the vent line-SRV piping penetration for the condition when the penetration assembly is cold and the corresponding SRV piping is hot during an SRV discharge. The SBA and IBA combinations, therefore, envelop the NOC I combination for all vent system components except the vent line-SRV piping penetration. The NOC I combination is evaluated for the vent line-SRV piping penetration since it may result in controlling penetration stresses. The

effects of the NOC I combination are also considered in the vent system fatigue evaluation.

The SBA II combination is the same as the IBA III combination except for negligible differences in internal pressure loads. Thus IBA III can be eliminated from consideration. The SBA II combination envelops the SBA I and IBA II combinations, since the submerged structure loads due to post-chug are more severe than those due to pre-chug. It also follows, from the reasoning presented earlier for OBE and SSE seismic loads, that the SBA II combination envelops the SBA III, SBA IV, IBA IV, and IBA V combinations, except when the effects of lateral loads on the vent line-drywell penetration are evaluated. Similarly, the SBA II combination envelops the DBA V and DBA VI combinations, except that these combinations contain vent system discharge loads which are somewhat larger than the pressure loads for the SBA II combination. This effect is accounted for by substituting the vent system discharge loads which occur during the chugging phase of a DBA event for the SBA II pressure loads when the SBA II load combination is evaluated.

By examination of Table 3-2.2-25, it is evident that the load combinations which result in maximum lateral loads on the vent line-drywell penetration are SBA IV, IBA V, and DBA VI. All of these contain SSE loads and chugging downcomer lateral loads which when combined, result in the maximum possible lateral load on the vent system. As previously discussed, the SBA II combination envelops the above combinations except for seismic loads. The effects of seismic loads are accounted for by substituting SSE loads for OBE loads when evaluating the SBA II combination.

The DBA II combination envelops the DBA IV combination, since the SRV discharge loads which occur late in the DBA event have a negligible effect on the vent system. The DBA II combination also has more restrictive allowables than the DBA IV combination.

The controlling vent system load combinations evaluated in the remaining report sections can now be summarized. The SBA II, IBA I, DBA I, DBA II, and DBA III combinations are evaluated for all vent system components except those associated with the vent line-SRV piping penetration. The DBA I and DBA II combinations do not need to be examined when evaluating the vent line-SRV

piping penetration, since they do not contain SRV discharge loads which are a large contributor to loads on the penetration. Thus, the NOC I, SBA II, IBA I and DBA III combinations are evaluated for the vent line-SRV piping penetration. As previously noted, SSE loads and the vent system discharge loads which occur during the chugging phase of the DBA event are conservatively substituted for OBE loads and the SBA pressure loads when evaluating the SBA II load combination.

To ensure that fatigue is not a concern for the vent system over the life of the plant, the combined effects of fatigue due to Normal Operating plus SBA events and Normal Operating plus IBA events are evaluated. The relative sequencing and timing of each loading in the SBA, IBA, and DBA events used in this evaluation are shown in Figures 3-2.2-11, 3-2.2-12 and 3-2.2-13. The fatigue effects for Normal Operating plus DBA events are enveloped by the Normal Operating plus SBA or IBA events, since the combined effects of SRV discharge loads and other loads for the SBA and IBA events are more severe than those for DBA. Additional information used in the vent system fatigue evaluation is summarized at the bottom of Table 3-2.2-25.

The load combinations and event sequencing described in the preceding paragraphs envelop those which could actually occur during a LOCA or SRV discharge event. An evaluation of these load combinations results in a conservative estimate of the vent system response and leads to bounding values of vent system stresses and fatigue effects.

Table 3-2.2-24

MARK I CONTAINMENT EVENT COMBINATIONS

	SRV	SRV + EQ		SBA IBA		SBA + EQ IBA + EQ				SBA+SRV IBA+SRV		SBA+SRV+EQ IBA+SRV+EQ				DBA		DBA + EQ				DBA+SRV		DBA+SRV+EQ			
Earthquake Type		O	S			O	S	O	S			O	S	O	S			O	S	O	S			O	S	O	S
LOADS	1	2	3	4	5	6	7	8	9	10	11	12	13	14	15	16	17	18	19	20	21	22	23	24	25	26	27
Normal	X	X	X	X	X	X	X	X	X	X	X	X	X	X	X	X	X	X	X	X	X	X	X	X	X	X	X
Earthquake		X	X			X	X	X	X			X	X	X	X			X	X	X	X			X	X	X	X
SRV Discharge	X	X	X							X	X	X	X	X	X							X	X	X	X	X	X
LOCA Thermal				X	X	X	X	X	X	X	X	X	X	X	X	X	X	X	X	X	X	X	X	X	X	X	X
LOCA Reactions				X	X	X	X	X	X	X	X	X	X	X	X	X	X	X	X	X	X	X	X	X	X	X	X
LOCA Quasi-Static Pressure				X	X	X	X	X	X	X	X	X	X	X	X	X	X	X	X	X	X	X	X	X	X	X	X
LOCA Pool Swell																X		X	X			X		X	X		
LOCA Condensation Oscillations					X			X	X		X			X	X		X			X	X		X			X	X
LOCA Chugging					X			X	X		X			X	X		X			X	X		X			X	X

Note:

1. See Section 1-3.2 for additional event combination information.

CONTROLLING VENT SYSTE

Section 3-2.2.1 Load Designation	Condition/Event	NOC	SBA					
	Volume 3 Load Combination Number	I	I	II	III	IV	I	
	Table 3-2.2-24 Load Combination Number	2	14	14	15	15	14	
1) Dead Weight		1a ←						
2) Seismic	OBE	2a ←		→ 2a			2a ←	
	SSE				2b	2b		
3) Pressure[1]		p[2]	P_2, P_3	P_2, P_3	P_2, P_3	P_2, P_3	P_2, P_3	P
3) Temperature[3]		T[4]	T_2, T_3	T_2, T_3	T_2, T_3	T_2, T_3	T_2, T_3	T
4) Vent System Discharge								
5) Pool Swell								
6) Condensation Oscillation							6a,6c 6e	
7) Chugging	Pre-Chug		7a-7c		7a-7c			7a
	Post-Chug			7a,7b 7d		7a,7b 7d		
8) SRV Discharge		8a ←						
9) Piping Reactions		9a ←						
10) Containment Interaction		10a ←						
Service Level		B	B	B	C	C	B	
Number of Event Occurences[8]		150	1 ←					
Number of SRV Actuations[9]		2804	50 ←			→ 50	25 ←	

LOAD COMBINATIONS

IBA				DBA					
	III	IV	V	I	II	III	IV	V	VI
	14	15	15	18	20	25	27	27	27
									1a
	2a			2a	2a				
		2b	2b			2b			2b
P_3	P_2,P_3	P_2,P_3	P_2,P_3	P_1	P_3	P_1	P_3	P_4	P_4
T_3	T_2,T_3	T_2,T_3	T_2,T_3	T_1	T_3	T_1	T_3	T_4	T_4
				4a					4a
				5a-5e		5a-5e			
					6b,6d 6f		6b,6d 6f		
7c		7a-7c						7a-7c	
	7a,7b 7d		7a,7b 7d						7a,7b 7d
			8a			8a	8a(5)	8a(5)	8a(5)
									9a
									10a
	B	C	C	B(6,7)	B(7)	C	C	C	C
									1
			25	0	0	1			1

nutech ENGINEERS

Table 3-2.2-25

(Concluded)

CONTROLLING VENT SYSTEM LOAD COMBINATIONS

Notes for Table 3-2.2-25

1. See Figures 3-2.2-1 through 3-2.2-3 for SBA, IBA, and DBA internal pressure values.

2. The range of normal operating internal pressures is 0.0 to 2.0 psi as specified by the FSAR.

3. See Figures 3-2.2-4 through 3-2.2-6 for SBA, IBA, and DBA temperature values.

4. The range of normal operating temperatures is 50.0 to 150.0°F as specified by the FSAR. See Table 3-2.2-2 for additional normal operating temperatures.

5. The SRV discharge loads which occur during this phase of the DBA event have a negligible effect on the vent system.

6. Evaluation of primary-plus-secondary stress range or fatigue not required.

7. The allowable stress value for local primary membrane stress at penetrations increased by 1.3.

8. The number of seismic load cycles used for fatigue is 1000.

9. The values shown are conservative estimates of the number of actuations expected for a BWR 4 plant with a reactor size of 251.

Table 3-2.2-26

ENVELOPING LOGIC FOR CONTROLLING

VENT SYSTEM LOAD COMBINATIONS

Condition/Event			NOC	SBA				IBA					DBA					
Table 3-2.2-24 Enveloping Load Combinations			2	14	14	15	15	14	14	14	15	15	18	20	25	27	27	27
Table 3-2.2-24 Load Combinations Enveloped			1	4-6, 8, 10-12	4-6, 8, 10-12	3,7, 9, 13	3,7, 9, 13	4-6, 8, 10-12	4-6, 8, 10-12	4-6, 8, 10-12	3,7, 9, 13	3,7, 9, 13	16	17	19, 22, 24	21, 23, 26	21, 23, 26	21, 23, 26
Volume 3 Load Combination Designation			I	I	II	III	IV	I	II	III	IV	V	I	II	III	IV	V	VI
Controlling Load Combinations Evaluated	Vent System Components and Supports	SBA II[1]	X	X		X	X		X	X	X	X					X	X
		IBA I	X															
		DBA I																
		DBA II														X		
		DBA III																
	Vent Line-SRV Piping Penetration	NOC I																
		SBA II[1]		X		X	X		X	X	X	X					X	X
		IBA I																
		DBA III											X	X		X		

NOTE:

1. SSE loads and DBA pressurization and thrust loads are substituted for OBE loads and SBA II internal pressure loads when evaluating the SBA II load combination.

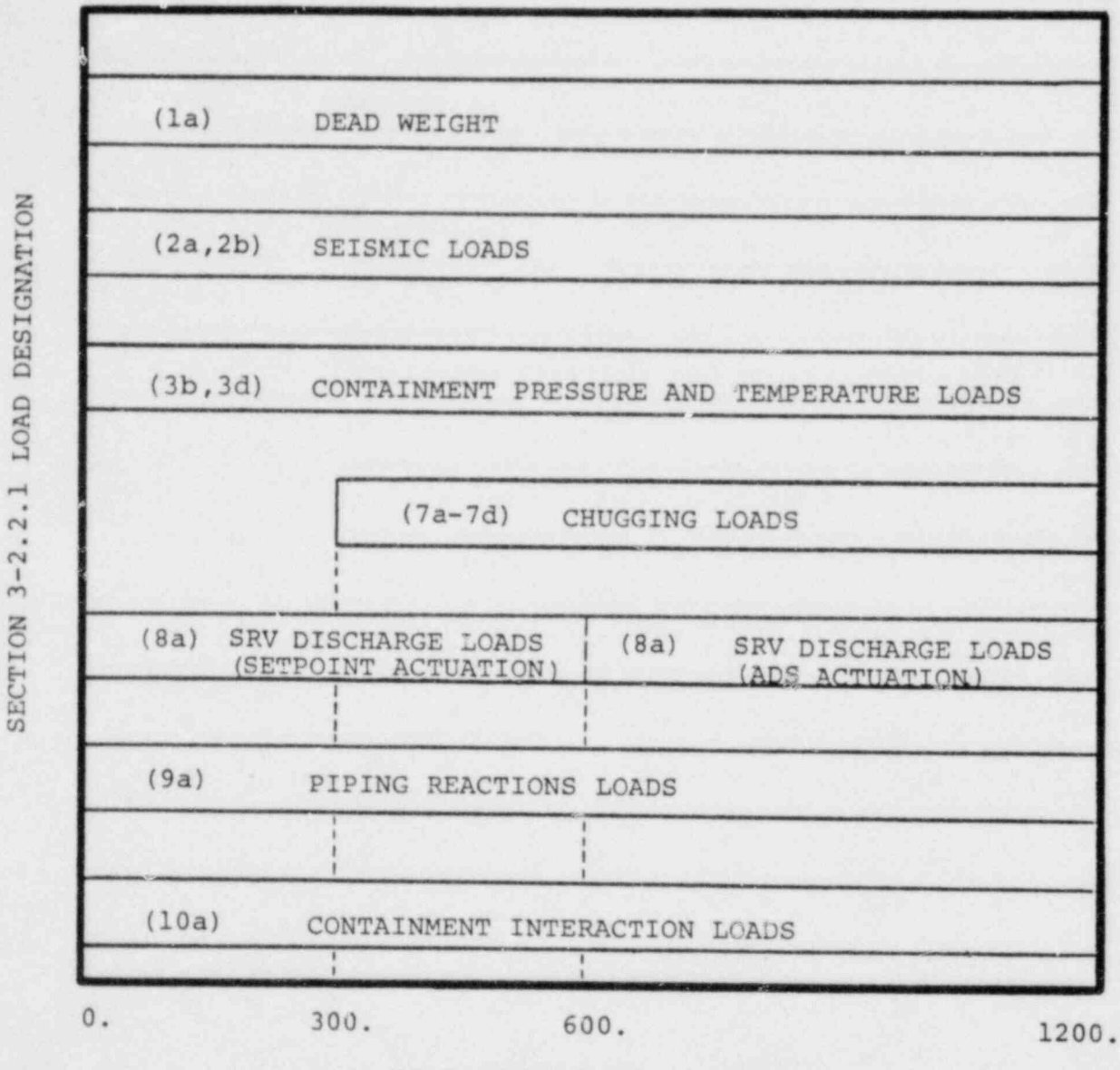

Figure 3-2.2-11

VENT SYSTEM SBA EVENT SEQUENCE

nutech ENGINEERS

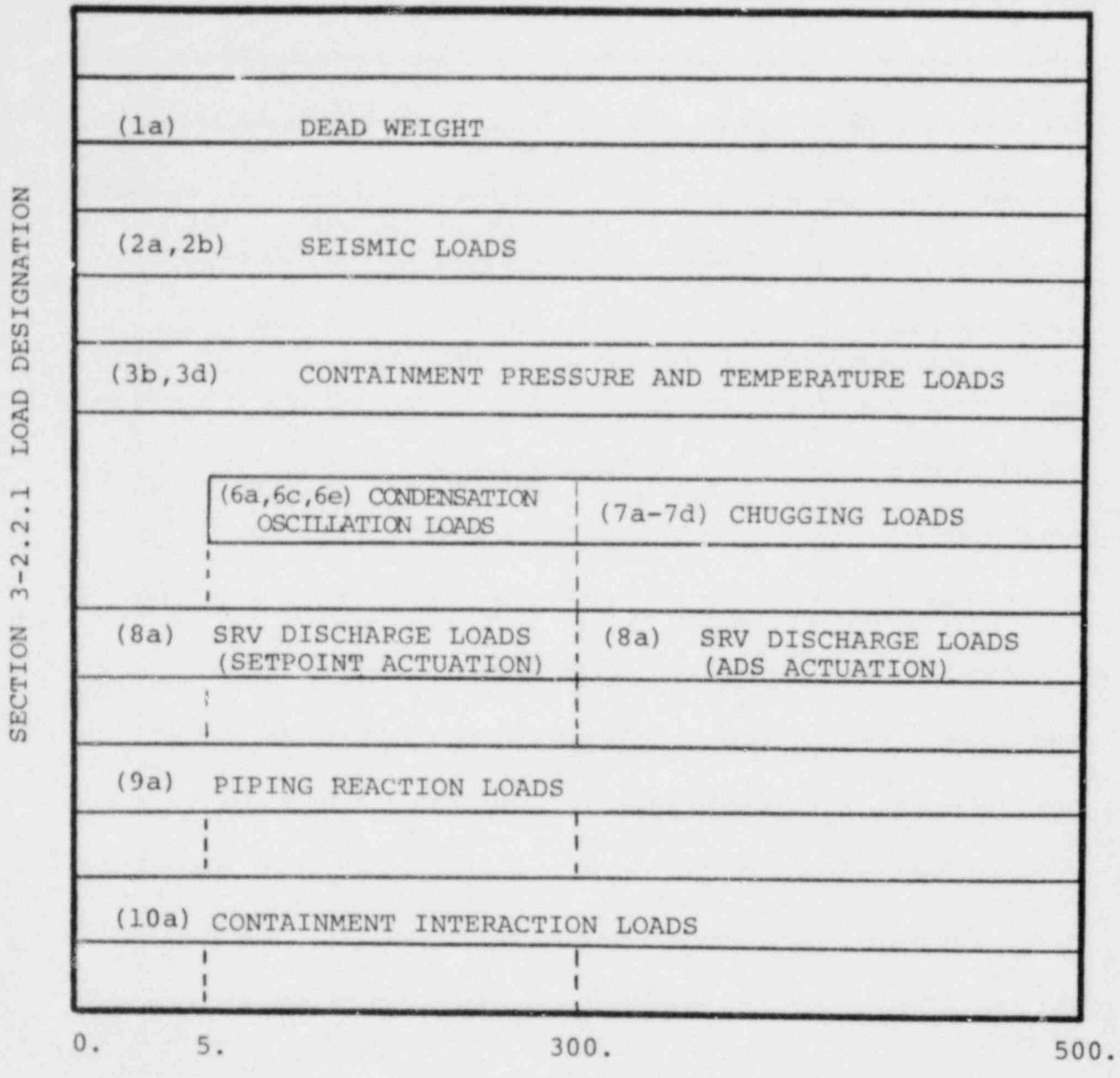

Figure 3-2.2-12

VENT SYSTEM IBA EVENT SEQUENCE

nutech ENGINEERS

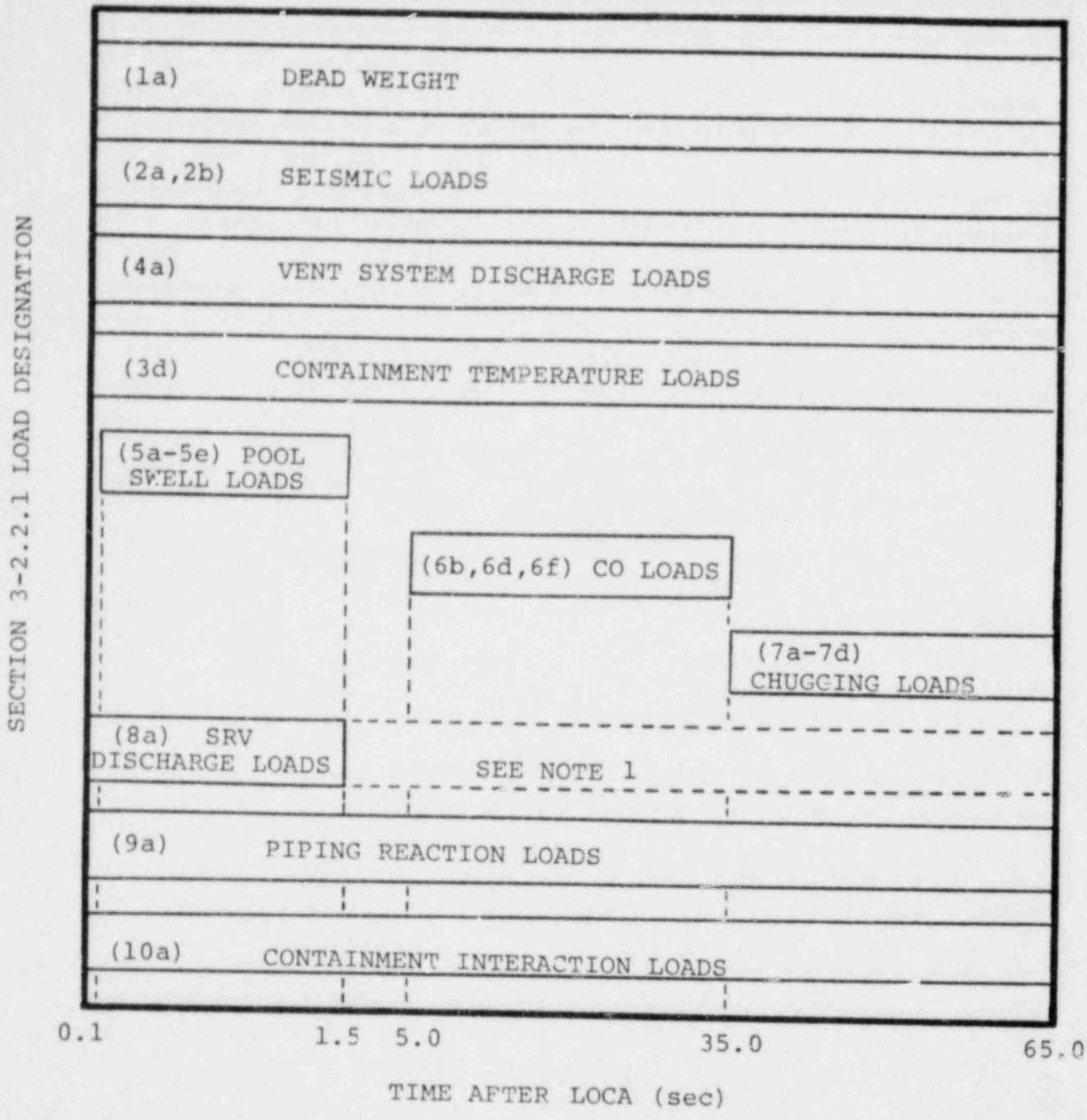

Note:

1. The SRV discharge loads which occur during this phase of the DBA event are negligible.

Figure 3-2.2-13

VENT SYSTEM DBA EVENT SEQUENCE

3-2.3 Analysis Acceptance Criteria

The acceptance criteria defined in NUREG-0661 on which the Fermi 2 vent system analysis is based are discussed in Section 1-3.2. In general, the acceptance criteria follows the rules contained in the ASME Code, Section III, Division 1 including the Summer 1977 Addenda for Class MC components and component supports (Reference 4). The corresponding service limit assignments, jurisdictional boundaries, allowable stresses, and fatigue requirements are consistent with those contained in the applicable subsections of the ASME Code and the Mark I Containment Program Plant Unique Analysis Application Guide (PUAAG) (Reference 5). The acceptance criteria used in the analysis of the vent system are summarized in the paragraphs which follow.

The items examined in the analysis of the vent system include the vent lines, vent header, downcomers, the support columns and associated support elements, the drywell shell near the vent line penetrations, the vent header deflectors, the downcomer-vent header intersection stiffener plates and bracing system, the vacuum breaker support system, the vent line-SRV piping penetration assembly, and the vent line bellows assembly.

The specific component parts associated with each of these items are identified in Figures 3-2.1-1 through 3-2.1-13.

The vent lines, vent header, downcomers, the support column ring plate away from the pin locations, the drywell shell, the downcomer-vent header intersection stiffener plates, the ring plates and stiffener plates attached to the vent line-vent header intersection, the vacuum breaker nozzle, and the vent line-SRV piping penetration assembly are evaluated in accordance with the requirements for Class MC components contained in Subsection NE of the ASME Code. Fillet welds and partial penetration welds joining these component parts or attaching other structures to these parts are also examined in accordance with the requirements for Class MC welds contained in Subsection NE of the ASME Code.

The support columns, the downcomer bracing members, the vacuum breaker support beam, and the associated connecting elements and welds are evaluated in accordance with the requirements for Class MC component supports contained in Subsection NF of the ASME Code. The vent header deflectors and associated component parts and welds are also evaluated in accordance with the require-

ments for Class MC component supports with allowable stresses corresponding to Service Level D.

As shown in Table 3-2.2-25, the NOC I, SBA II, IBA I, DBA I, and DBA II combinations all have Service Level B limits while the DBA III combination has Service Level C limits. Since these load combinations have somewhat different maximum temperatures, the allowable stresses for the two load combination groups with Service Level B and C limits are conservatively determined at the highest temperature for each load combination group.

The allowable stresses for all the major components of the vent system, such as the vent line, vent header and downcomers, are determined at the maximum DBA temperature of 292°F. The allowable stresses for the remaining vent system component parts away from the vent line-SRV piping penetration nozzle are determined at 173°F. The allowable stresses for the vent line-SRV piping nozzle and adjoining component parts are determined at 363°F. The allowable stresses for the load combinations with Service Level B and C limits are shown in Table 3-2.3-1.

The allowable displacements and associated number of cycles for the vent line bellows are shown in

Table 3-2.3-2. These values are taken from the FSAR, as permitted by NUREG-0661 in cases where the analysis technique used in the evaluation is the same as that contained in the plant's FSAR. The annular ring and the associated attachment weld to the vent line shown in Figure 3-2.1-8 are evaluated in accordance with the requirements for Class MC components as discussed above.

The acceptance criteria described in the preceding paragraphs result in conservative estimates of the existing margins of safety and ensure that the original vent system design margins are restored.

Table 3-2.3-1

ALLOWABLE STRESSES FOR VENT SYSTEM

COMPONENTS AND COMPONENT SUPPORTS

Items	Material	Material Properties (ksi) (1)	Stress Type	Allowable Stress (ksi)	
				Service Level B (2)	Service Level C (3)
COMPONENTS					
Drywell Shell	SA-516 Gr. 70	S_{mc} = 19.30 S_{m_1} = 22.68 S_y = 33.97	Local Primary Membrane	28.95	50.96
			Primary + (4) Secondary Stress Range	68.04	N/A
Vent Line	SA-516 Gr. 70	S_{mc} = 19.30 S_{m_1} = 22.68 S_y = 33.97	Primary Membrane	19.30	33.97
			Local Primary Membrane	28.95	50.96
			Primary + (4) Secondary Stress Range	68.04	N/A
Vent Header	SA-516 Gr. 70	S_{mc} = 19.30 S_{m_1} = 22.68 S_y = 33.97	Primary Membrane	19.30	33.97
			Local Primary Membrane	28.95	50.96
			Primary + (4) Secondary Stress Range	68.04	N/A
Downcomer	SA-516 Gr. 70	S_{mc} = 19.30 S_{m_1} = 22.68 S_y = 33.97	Primary Membrane	19.30	33.97
			Local Primary Membrane	28.95	50.96
			Primary + (4) Secondary Stress Range	68.04	N/A
Support Column Ring Plate	SA-516 Gr. 70	S_{mc} = 19.30 S_{m_1} = 22.68 S_y = 33.97	Primary Membrane	19.30	33.97
			Local Primary Membrane	28.95	50.96
			Primary + (4) Secondary Stress Range	68.04	N/A
SRV Piping Penetration Nozzle	SA-333 Gr. 6	S_{mc} = 16.50 S_{m_1} = 20.00 S_y = 30.25	Primary Membrane	16.50	30.25
			Local Primary Membrane	24.75	45.37
			Primary + (4) Secondary Stress Range	60.00	N/A

Table 3-2.3-1

(Continued)

ALLOWABLE STRESSES FOR VENT SYSTEM

COMPONENTS AND COMPONENT SUPPORTS

Item	Material	Material Properties (ksi)[1]	Stress Type	Allowable Stress (ksi)	
				Service Level B[2]	Service Level C[3]
COMPONENT SUPPORTS					
Columns[7]	SA-106 Gr. B	S_y = 32.74	Bending	19.64	26.19
			Tensile	19.64	26.19
			Combined	1.00	1.00
			Compressive	16.45	21.88
			Interaction	1.00	1.00
WELDS					
Column Ring Plate to Vent Header	SA-516 Gr. 70	S_{mc} = 19.30 S_y = 33.97	Primary	15.01	26.42
			Secondary	45.03	N/A
SRV Piping Penetration Sleeve to Nozzle	SA-333 Gr. 6	S_{mc} = 16.50 S_{m1} = 20.00 S_y = 30.25	Primary	12.38	22.69
			Secondary	45.00	N/A

Notes:

1. Material properties taken at maximum event temperatures.
2. Service Level B allowables are used when evaluating NOC I, SBA II, IBA I, DBA I, and DBA II load combination results.
3. Service Level C allowables are used when evaluating the DBA III Load combination results.
4. Thermal bending stresses are excluded when evaluating primary-plus-secondary stress ranges.
5. Evaluation of primary-plus-secondary stress intensity range and fatigue are not required for load combination DBA I.
6. The allowable stresses for local primary membrane stresses at penetrations are increased by 1.3 when evaluating load combinations DBA I and DBA II.
7. Stresses due to thermal loads may be excluded when evaluating component supports.

Table 3-2.3-2

ALLOWABLE DISPLACEMENTS AND CYCLES

FOR VENT LINE BELLOWS

Type		Allowable Value
Axial	Compression	0.875 in.
	Extension	0.375 in.
Lateral	Meridional	±0.625 in.
	Longitudinal	±0.625 in.
Number of Cycles of Maximum Displacements		500

3-2.4 Method of Analysis

The governing loads for which the Fermi 2 vent system is evaluated are presented in Section 3-2.2.1. The methodology used to evaluate the vent system for the overall effects of all loads, except those which exhibit asymmetric characteristics, is discussed in Section 3-2.4.1. The effects of asymmetric loads on the vent system are evaluated using the methodology discussed in Section 3-2.4-2. The methodology used to examine the local effects at the penetrations and intersections of the vent system major components is discussed in Section 3-2.4.3.

The methodology used to formulate results for the controlling load combinations, examine fatigue effects, and evaluate the analysis results for comparison with the applicable acceptance limits, is discussed in Section 3-2.4.4.

3-2.4.1 Analysis for Major Loads

The repetitive nature of the vent system geometry is such that the vent system can be divided into 16 identical segments which extend from midbay of the vent line bay to midbay of the non-vent line bay, as shown in Figure 3-2.1-6. The governing loads which act on the vent system, except for seismic loads and a few chugging load cases, exhibit symmetric and/or anti-symmetric characteristics with respect to a 1/16th segment of the vent system. The analysis of the vent system for the majority of the governing loads is therefore performed for a typical 1/16th segment.

A beam model of a 1/16th segment of the vent system, as shown in Figure 3-2.4-1, is used to obtain the response of the vent system to all loads except those which result in asymmetric effects on the vent system. The model includes the vent line, vent header, downcomers, and the support columns. The model also includes the vent header deflectors, the downcomer bracing system, and the vacuum breaker and vacuum breaker support system. The portion of the SRV piping and its associated supports on the vent system, which extends from the vent line-SRV piping penetration to the ramshead, is also

included to account for the interaction effects of these two structures.

The local stiffness effects at the penetrations and intersections of the major vent system components, shown in Figures 3-2.1-7 through 3-2.1-12, are included using stiffness matrix elements of these penetrations and intersections. A matrix element for the vent line-drywell penetration, which connects the upper end of the vent line to the spherical transition segment, is developed using the finite difference model of the penetration shown in Figure 3-2.4-9. The finite element model of the vent line-SRV piping penetration shown in Figure 3-2.4-10, is used to develop a matrix element which connects the beams on the centerline of the vent line to the SRV piping penetration nozzle. A matrix element which connects the lower end of the vent line to the beams on the centerline of the vent header is developed using the finite element model of the vent line-vent header intersection shown in Figure 3-2.4-11.

Finite element models of each downcomer-vent header intersection, similar to the one shown in Figure 3-2.4-12, are used to develop matrix elements which connect the beams on the centerline of the vent header

to the upper ends of the downcomers at the downcomer ring locations. These elements also connect the attachment points of the vent header deflector to the downcomer crotch plates. The length of the vent header segment in the analytical models used for downcomer-vent header intersection stiffness determination is increased to ensure that vent header ovaling effects are properly accounted for. Use of this modeling approach has been verified using results from FSTF tests. Additional information on the analytical models used to evaluate the penetrations and intersections of major vent system components is contained in Section 3-2.4.3.

The local stiffness effects at the attachments of the downcomer bracing, vent header deflectors, vacuum breaker supports, vent system support columns, and SRV piping to support rings and pad plates located on the major components of the vent system are also included. Beams which account for the local stiffness of the support rings and pad plates are used to connect the associated component parts to beams which model the vent line, vent header, and downcomers.

The 1/16th beam model contains 231 nodes, 238 beam elements, and 6 matrix elements. The node spacing used

in the analytical model is refined to ensure adequate distribution of mass and determination of component part frequencies and mode shapes, and to facilitate accurate application of loadings. The stiffness and mass properties used in the model are based on the nominal dimensions and densities of the materials used to construct the vent system. Small displacement linear-elastic behavior is assumed throughout.

The boundary conditions used in the 1/16th beam model are both physical and mathematical in nature. The physical boundary conditions include the elastic restraints provided at the attachments of the support columns and the SRV piping ramshead support to the suppression chamber ring beam and pedestal. The associated stiffnesses are developed using the analytical model of the suppression chamber described in Volume 2 of this report. The vent system columns are assumed to be pinned in all directions at their upper and lower ends. Additional physical boundary conditions include the elastic restraints provided at the attachment of the vent line to the drywell. The associated vent line-drywell penetration stiffnesses are included as a stiffness matrix element, the development of which is discussed in the preceding paragraphs. The mathematical boundary

conditions consist of either symmetry, anti-symmetry, or a combination of both at the midcylinder planes, depending on the characteristics of the load being evaluated.

Additional mass is lumped along the length of the submerged portions of the downcomers, support columns, and SRV piping to account for the effective mass of water which acts with these components during dynamic loadings. The total mass of water added is equal to the mass of water displaced by each of these components. For all but the pool swell and condensation oscillation dynamic loadings, the mass of water inside the submerged portion of the downcomers is included. The downcomers are assumed to contain air and/or steam during pool swell and condensation oscillation, the mass of which is neglected. The mass of water inside the submerged portion of the SRV piping is also included for all dynamic loadings. An additional mass of 1125 lbs to account for the weight of the drywell/wetwell vacuum breaker is lumped at the center of gravity of the vacuum breaker.

A frequency analysis is performed using the 1/16th beam model of the vent system for the case with water inside the downcomers and the case with no water inside the downcomers. All structural modes in the range of 0 to

50 hertz and 0 to 200 hertz, respectively, are extracted for these cases. The resulting frequencies and mass participation factors are shown in Tables 3-2.4-1 and 3-2.4-2.

A dynamic analysis is performed for the pool swell loads and condensation oscillation loads specified in Section 3-2.2-1, using the 1/16th beam model of the vent system. The analysis consists of a transient analysis for pool swell loads, and a harmonic analysis for condensation oscillation loads. The modal superposition technique, including modes to 200 hertz with 2% damping, is utilized in both the transient and harmonic analyses. The pool swell and condensation oscillation load frequencies are enveloped by including vent system frequencies to 200 hertz.

The remaining vent system load cases specified in Section 3-2.2.1 involve either static loads or dynamic loads, which are evaluated using an equivalent static approach. For the latter, conservative dynamic amplification factors are developed and applied to the maximum spatial distributions of the individual dynamic loadings.

The effects of asymmetric loads are evaluated by applying loads generated using the 180° beam model discussed in Section 3-2.4.2 to the 1/16th beam model. Displacements taken from the 180° beam model results are imposed at the midcylinder boundary planes of the 1/16th beam model. Inertia forces due to horizontal seismic loads and concentrated forces due to asymmetric chugging loads which are also taken from the 180° beam model results, are applied to the portion of the 1/16th beam model which lies between the midcylinder boundary planes. Additional information related to the vent system analysis for asymmetric loads is provided in Section 3-2.4.2.

The 1/16th beam model is also used to generate loads for the evaluation of stresses in the major vent system component penetrations and intersections. Beam end loads, distributed loads, reaction loads, and inertia loads are developed and applied to the analytical models of the vent system penetrations and intersections shown in Figures 3-2.4-9 through 3-2.4-12. Additional information related to the vent system penetrations and intersection stress evaluation is provided in Section 3-2.4.3.

The specific treatment of each load in the load categories identified in Section 3-2.2.1 is discussed in the paragraphs which follow.

1. Dead Weight Loads

   a. Dead Weight of Steel: A static analysis is performed for a unit vertical acceleration applied to the weight of vent system steel.

2. Seismic Loads

   a. OBE Loads: A static analysis is performed for a 0.067g vertical seismic acceleration applied to the weight of steel included in the 1/16th beam model. An additional static analysis is performed for the boundary displacements and associated inertia loads generated for a 0.23g seismic acceleration applied in each horizontal direction using the 180° beam model. The results of the three earthquake directions are combined using SRSS.

   b. SSE Loads: The procedure used to evaluate the 0.133g vertical and 0.46g horizontal SSE seismic accelerations is the same as that discussed for OBE seismic loads in load case 2a.

3. Containment Pressure and Temperature Loads

a. Normal Operating Internal Pressure Loads: A static analysis is performed for a 2.0 psi internal pressure applied as concentrated forces to the unreacted areas of the vent system.

b. LOCA Internal Pressure Loads: A static analysis is performed for the SBA and IBA net internal pressures applied as concentrated forces to the unreacted areas of the major components of the vent system. These pressures are shown in Figures 3-2.2-1 through 3-2.2-3. The effects of DBA internal pressure loads are included in the pressurization and thrust loads discussed in load case 4a.

Concentrated forces are also applied at the vent line-drywell penetration location using the SBA, IBA, and DBA drywell internal pressures. These forces account for the pressures acting on the vent line-drywell penetration unreacted area and for the movement of the drywell due to internal pressure. The move-

ment of the suppression chamber due to internal pressure, although small in magnitude, is also applied.

c. Normal Operating Temperature Loads: A static analysis is performed for the case with the containment at an ambient temperature of 70°F and a 363°F temperature uniformly applied to the wetwell SRV piping. The reaction loads at the vent line-SRV piping penetration are also applied. The methodology used to evaluate local thermal effects in the vent line-SRV piping penetration is discussed in Section 3-2.4.3.

An additional static analysis is performed for the maximum normal operating temperature listed in Table 3-2.2-2. This temperature is uniformly applied to the portion of the vent system inside the suppression chamber. Corresponding temperatures of 70°F for the drywell and vent system components outside the suppression chamber, 173°F for the suppression chamber, and 363°F for the SRV piping are also applied in this analysis.

d. LOCA Temperature Loads: A static analysis is performed for the SBA, IBA, and DBA temperatures, which are uniformly applied to the major components and external components of the vent system. These temperatures are shown in Figures 3-2.2-4 through 3-2.2-6. A temperature of 363°F is also uniformly applied to the SRV piping for those controlling load combinations which include SRV discharge loads.

Concentrated forces are applied at the vent line-drywell penetration and at the support column and SRV piping attachment points to the suppression chamber to account for the thermal expansion of the drywell and suppression chamber during the SBA, IBA, and DBA events. The greater of the temperatures specified in Figure 3-2.2-4 and Table 3-2.2-2 is used in the analysis for SBA temperatures.

4. Vent System Discharge Loads

a. DBA Pressurization and Thrust Loads: A static analysis is performed for the DBA pressurization and thrust loads shown in Table 3-2.2-3.

5. Pool Swell Loads

a. Vent System Impact and Drag Loads:

A dynamic analysis is performed for the vent line, downcomer, and vent header deflector pool swell impact loads shown in Table 3-2.2-4 and in Figures 3-2.2-7 and 3-2.2-8.

b. Impact and Drag Loads on Other Structures: A dynamic analysis is performed for pool swell impact loads on the downcomer bracing members and ring plates, and on the vacuum breaker and vacuum breaker supports. These loads are shown in Table 3-2.2-5. The pool swell impact loads acting on the SRV piping and support located beneath the vent line are also applied.

c. Froth Impingement and Fallback Loads: A dynamic analysis is performed for froth impingement and fallback loads on the downcomer bracing members and ring plates, and on the vacuum breaker and vacuum breaker supports. These loads are shown in Table 3-2.2-6. The froth impingement loads acting on the SRV

piping and the support located beneath the vent line are also applied.

d. Pool Fallback Loads: A dynamic analysis is performed for pool fallback loads on the downcomer bracing members and ring plates. These loads are shown in Table 3-2.2-7. The pool fallback loads acting on the SRV piping and the support located beneath the vent line are also applied.

e. LOCA Air Clearing Submerged Structure Loads: An equivalent static analysis is performed for LOCA air clearing submerged structure loads on the downcomers and support columns. These loads are shown in Tables 3-2.2-8 and 3-2.2-9. The values of the loads include dynamic amplification factors which are computed using first principles and the dominant frequencies of the downcomer and the support columns. The dominant frequencies are derived from harmonic analyses of these components. The results of these harmonic analyses are shown in Figures 3-2.4-2 and 3-2.4-3. The LOCA air clearing submerged structure loads acting on the

submerged portion of the SRV piping are also applied.

6. Condensation Oscillation Loads

   a. IBA Condensation Oscillation Downcomer Loads: A dynamic analysis is performed for the IBA condensation oscillation downcomer loads shown in Table 3-2.2-10 and Figure 3-2.2-9. The dominant downcomer frequency is determined from the harmonic results shown in Figure 3-2.4-4. It is apparent from this figure that the dominant downcomer frequency occurs in the frequency range of the second condensation oscillation downcomer load harmonic. The first and third condensation oscillation downcomer load harmonics are therefore applied at frequencies equal to 0.5 and 1.5 times the value of the dominant downcomer frequency.

   b. DBA Condensation Oscillation Loads: The procedure used to evaluate the DBA condensation oscillation downcomer loads shown in Table 3-2.2-11 is the same as that discussed for IBA condensation oscillation downcomer loads in load case 6a.

c. IBA Condensation Oscillation Vent System Pressures: A dynamic analysis is performed for IBA condensation oscillation vent system pressures on the vent line and vent header. These loads are shown in Table 3-2.2-12. The dominant vent line and vent header frequencies are determined from the harmonic analysis results shown in Figure 3-2.4-5. An additional static analysis is performed for a 1.5 psi internal pressure applied as concentrated forces to the unreacted areas of the vent system.

d. DBA Condensation Oscillation Vent System Pressure Loads: The procedure used to evaluate the DBA condensation oscillation vent system pressure loads shown in Table 3-2.2-12 is the same as that discussed for IBA condensation oscillation vent system pressure loads in load case 6c.

e. IBA Condensation Oscillation Submerged Structure Loads: As previously discussed, pre-chug loads described in load case 7c are specified in lieu of IBA condensaton oscillation loads.

f. DBA Condensation Oscillation Submerged Structure Loads: An equivalent static analysis is performed for the DBA condensation oscillation submerged structure loads on the support columns. These loads are shown in Table 3-2.2-13. The loads include dynamic amplification factors which are computed using the methodology described for LOCA air clearing submerged structure loads in load case 5e. The DBA condensation oscillation submerged structure loads acting on the submerged portion of the SRV piping are also applied.

7. Chugging Loads

a. Chugging Downcomer Lateral Loads: A harmonic analysis of the downcomers is performed to determine the dominant downcomer frequency for use in calculating the maximum chugging load magnitude. The harmonic analysis results are shown in Figure 3-2.4-6. The resulting chugging load magnitudes are shown in Table 3-2.2-14. A static analysis using the 1/16th beam model is performed for chugging downcomer lateral load cases 8 through 22. These load

cases are shown in Tables 3-2.2-16 and 3-2.2-17. An additional static analysis using the 180° beam model is performed for boundary displacements and associated concentrated forces generated for load cases 1 through 7.

A static analysis is also performed for the maximum chugging load shown in Table 3-2.2-18, applied to a single downcomer in the in-plane and out-of-plane directions. The results of this analysis are used in evaluating fatigue.

b. Chugging Vent System Pressures: An equivalent static analysis is performed for the chugging vent system pressures applied to the unreacted areas of the vent system. These loads are shown in Table 3-2.2-19. The dominant vent line and vent header frequencies are determined from the harmonic analysis results shown in Figure 3-2.4-7.

c. Pre-Chug Submerged Structure Loads: An equivalent static analysis is performed for the pre-chug submerged structure loads on the support columns. These loads are shown in

Table 3-2.2-20. The loads include dynamic amplification factors which are computed using the methodology described for submerged structure LOCA air clearing loads in load case 5e. The pre-chug submerged structure loads acting on the submerged portion of the SRV piping are also applied.

d. Post-Chug Submerged Structure Loads: The procedure used to evaluate the post-chug submerged structure loads on the support columns is the same as that discussed for pre-chug submerged structure loads in load case 6c. These loads are shown in Table 3-2.2-21.

8. Safety Relief Valve Discharge Loads

a. SRV Discharge Air Clearing Submerged Structure Loads: An equivalent static analysis is performed for SRV discharge drag loads on the downcomers and support columns. These loads are shown in Tables 3-2.2-22 and 3-2.2-23. The loads include a dynamic load factor of 3.0 as discussed in Section 1-4.2.4. A dynamic load factor of 2.0 is used for the downcomer loads applied in the out-of-plane direction,

since the out-of-plane downcomer frequency is well above the maximum SRV discharge load frequency, as shown in Figure 3-2.4-2. The SRV discharge submerged structure loads acting on the submerged portion of the SRV piping are also applied.

9. Piping Reaction Loads

a. SRV Piping Reaction Loads: As previously discussed, the wetwell SRV piping is included in the 1/16th beam model of the vent system. Loads in categories 1 through 8 which act on the vent system and the wetwell SRV piping are applied to both structures and the interaction effects are evaluated.

Additional equivalent static loads caused by SRV discharge line clearing pressurization and by thrust loads acting on the wetwell SRV piping are also applied. The conditions which cause the maximum reaction loads on the vent line-SRV piping penetration and on the supports located under the vent line and vent header are evaluated. Reaction loads from the SRV piping analysis are applied at the vent

line-SRV piping penetration location to account for loads acting on the drywell portion of the SRV piping systems.

10. Containment Interaction Loads

    a. Containment Structure Motions: The motions of the drywell and the suppression chamber due to internal pressure and thermal expansion are applied to the 1/16th beam model. The motions caused by loads in other load categories acting on the drywell and suppression chamber have been evaluated and found to have a negligible effect on the vent system.

The methodology described in the preceding paragraphs results in a conservative evaluation of the vent system response and associated stresses for the governing loads.

Table 3-2.4-1

VENT SYSTEM FREQUENCY ANALYSIS RESULTS WITH WATER INSIDE DOWNCOMERS

Mode Number	Frequency (Hz)	Mass Participation Factor(lb)		
		$X^{(1)}$	$Y^{(1)}$	$Z^{(1)}$
1	**12.4**	**15998.20**	**1319.45**	**5.47**
2	17.1	666.32	2620.29	81.65
3	17.2	7.68	1624.82	1.11
4	18.7	7480.85	686.80	3207.43
5	21.3	1178.74	204.38	1616.30
6	22.8	338.87	99.46	147.26
7	23.8	1967.28	6356.07	227.15
8	25.0	266.33	8.94	1398.14
9	25.1	1447.71	486.04	1619.28
10	25.3	54.55	81.31	179.90
11	25.4	13.79	1223.46	0.00
12	25.9	300.88	3.65	228.48
13	28.6	22.70	26.33	5492.87
14	29.0	211.40	0.00	233.20
15	30.1	25.36	48.98	0.04
16	30.9	2010.05	35.16	196.99
17	31.1	227.26	2.49	0.98
18	31.9	2.41	102.77	74.50
19	33.7	943.63	67.63	2156.92
20	35.3	937.13	59.13	83.81
21	36.4	1117.20	96.69	2.08
22	37.1	1192.58	127.77	7292.97
23	39.0	27.94	811.74	2081.15
24	40.4	0.28	0.48	0.01
25	40.4	1.90	43.64	32.90
26	41.8	117.34	1303.53	3.30
27	44.6	3.19	13.73	0.75
28	47.2	2.34	57.37	34.12
29	49.6	93.97	224.74	58.26

Note:

1. See Figure 3-2.4-1 for coordinate system directions.

Table 3-2.4-2

VENT SYSTEM FREQUENCY ANALYSIS

RESULTS WITHOUT WATER INSIDE DOWNCOMER

Mode Number	Frequency (Hz)	Mass Participation Factor(lb)		
		$X^{(1)}$	$Y^{(1)}$	$Z^{(1)}$
1	**14.2**	**15512.29**	**1018.50**	**25.59**
2	17.2	461.35	2442.62	37.69
3	17.2	1.20	1436.35	0.00
4	20.0	6752.19	273.72	5113.41
5	22.9	565.20	1377.60	1230.36
6	24.7	3110.03	1906.31	842.33
7	25.3	0.05	3.68	12.74
8	25.4	2.38	1470.71	4.18
9	26.1	130.76	682.22	851.91
10	27.7	944.40	792.54	23.03
11	28.6	85.50	541.42	7336.01
12	30.2	289.04	0.29	713.87
13	31.2	2570.99	94.92	245.80
14	31.6	794.80	22.57	267.67
15	33.5	120.01	24.99	1190.92
16	35.7	375.41	199.21	572.79
17	36.6	27.64	35.40	235.69
18	37.2	224.90	16.75	442.08
19	37.6	5.45	61.49	2638.28
20	38.8	63.95	245.71	190.10
21	39.7	576.95	154.23	1257.98
22	39.9	984.07	252.59	2171.34
23	40.4	11.34	127.64	0.03

Table 3-2.4-2
(Continued)

VENT SYSTEM FREQUENCY ANALYSIS

RESULTS WITHOUT WATER INSIDE DOWNCOMER

Mode Number	Frequency (Hz)	Mass Participation Factor(lb)		
		$X^{(1)}$	$Y^{(1)}$	$Z^{(1)}$
24	40.4	1.33	34.37	0.35
25	42.3	182.43	1638.55	885.73
26	46.6	18.41	79.96	112.70
27	48.4	0.13	143.11	0.79
28	50.9	20.26	283.94	17.70
29	51.1	66.40	118.87	27.00
30	56.7	0.19	5.78	25.15
31	65.0	24.14	238.26	18.43
32	68.0	17.03	601.50	40.39
33	73.2	402.38	16.66	27.94
34	75.3	11.42	3.89	96.00
35	77.7	1.06	25.72	108.57
36	79.1	151.13	1.62	2.45
37	83.1	103.98	9.92	10.12
38	85.4	101.03	37.33	26.42
39	91.3	456.04	54.62	24.27
40	95.5	99.52	2.36	10.08
41	97.6	12.96	0.01	28.30
42	100.3	0.88	0.11	3.06
43	105.4	443.98	30.80	497.02
44	112.8	277.22	0.80	122.76
45	113.6	9.04	248.74	0.18
46	113.6	0.38	4.60	0.14

Table 3-2.4-2
(Concluded)

VENT SYSTEM FREQUENCY ANALYSIS

RESULTS WITHOUT WATER INSIDE DOWNCOMER

Mode Number	Frequency (Hz)	Mass Participation Factor(lb)		
		$X^{(1)}$	$Y^{(1)}$	$Z^{(1)}$
47	113.9	1.87	0.00	26.12
48	116.8	0.02	0.04	286.20
49	118.1	2.08	0.16	67.69
50	118.7	35.42	0.00	242.71
51	124.5	0.76	16.08	49.76
52	131.1	0.76	15.16	1.11
53	132.6	4.38	22.35	6.02
54	142.7	42.64	7.09	0.67
55	150.9	0.79	317.14	76.20
56	154.1	7.81	184.64	30.55
57	157.2	11.43	12.88	262.73
58	159.6	18.38	56.53	2.10
59	165.6	5.82	115.45	60.61
60	167.6	2.72	289.77	16.30
61	169.4	12.28	45.80	0.48
62	182.7	120.61	588.81	335.89
63	185.4	2.22	2082.12	8.54
64	186.4	245.26	633.83	211.61
65	193.9	74.29	14.88	101.10
66	196.6	4.67	1.25	20.52
67	197.9	5.05	2.59	17.03
68	199.1	19.28	100.04	42.02

Note:

1. See Figure 3-2.4-1 for coordinate directions.

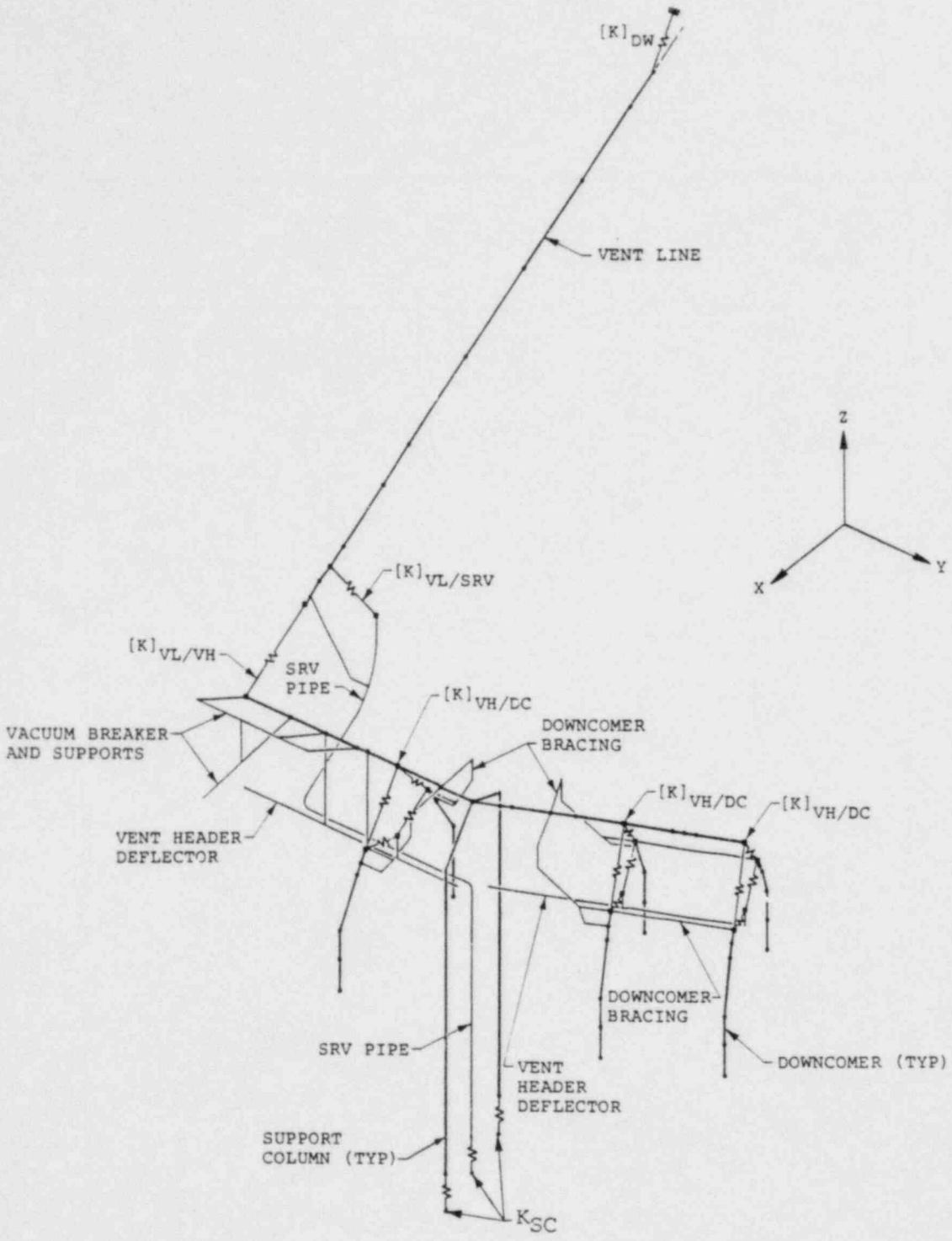

Figure 3-2.4-1

VENT SYSTEM 1/16th SEGMENT BEAM MODEL - ISOMETRIC VIEW

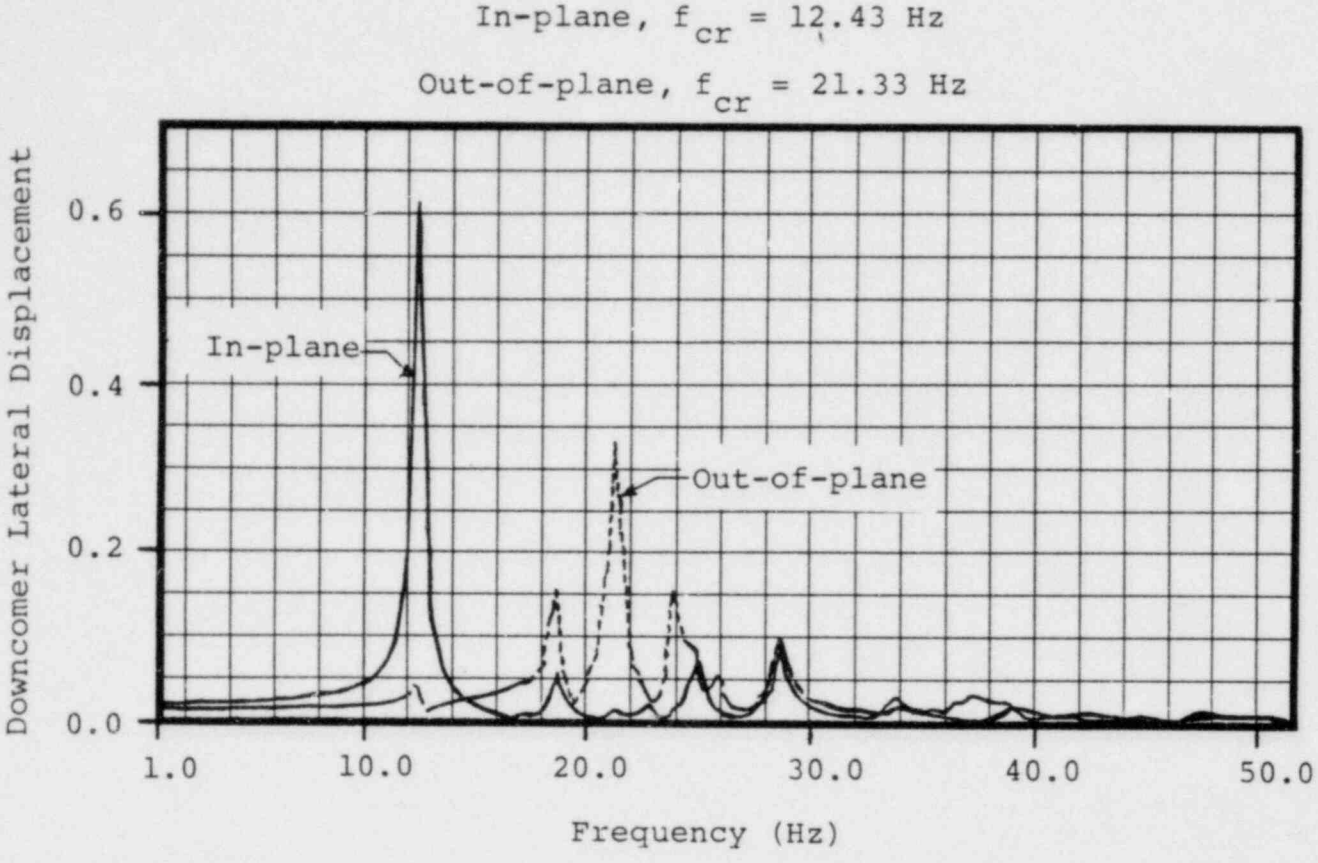

Notes:

1. Results shown are obtained by applying unit drag pressures to submerged portion of downcomers in the in-plane and out-of-plane directions.
2. Frequencies are determined with water inside submerged portion of downcomers.
3. Results shown are typical representative of all downcomers.

Figure 3-2.4-2

HARMONIC ANALYSIS RESULTS FOR DOWNCOMER SUBMERGED STRUCTURE

LOAD FREQUENCY DETERMINATION

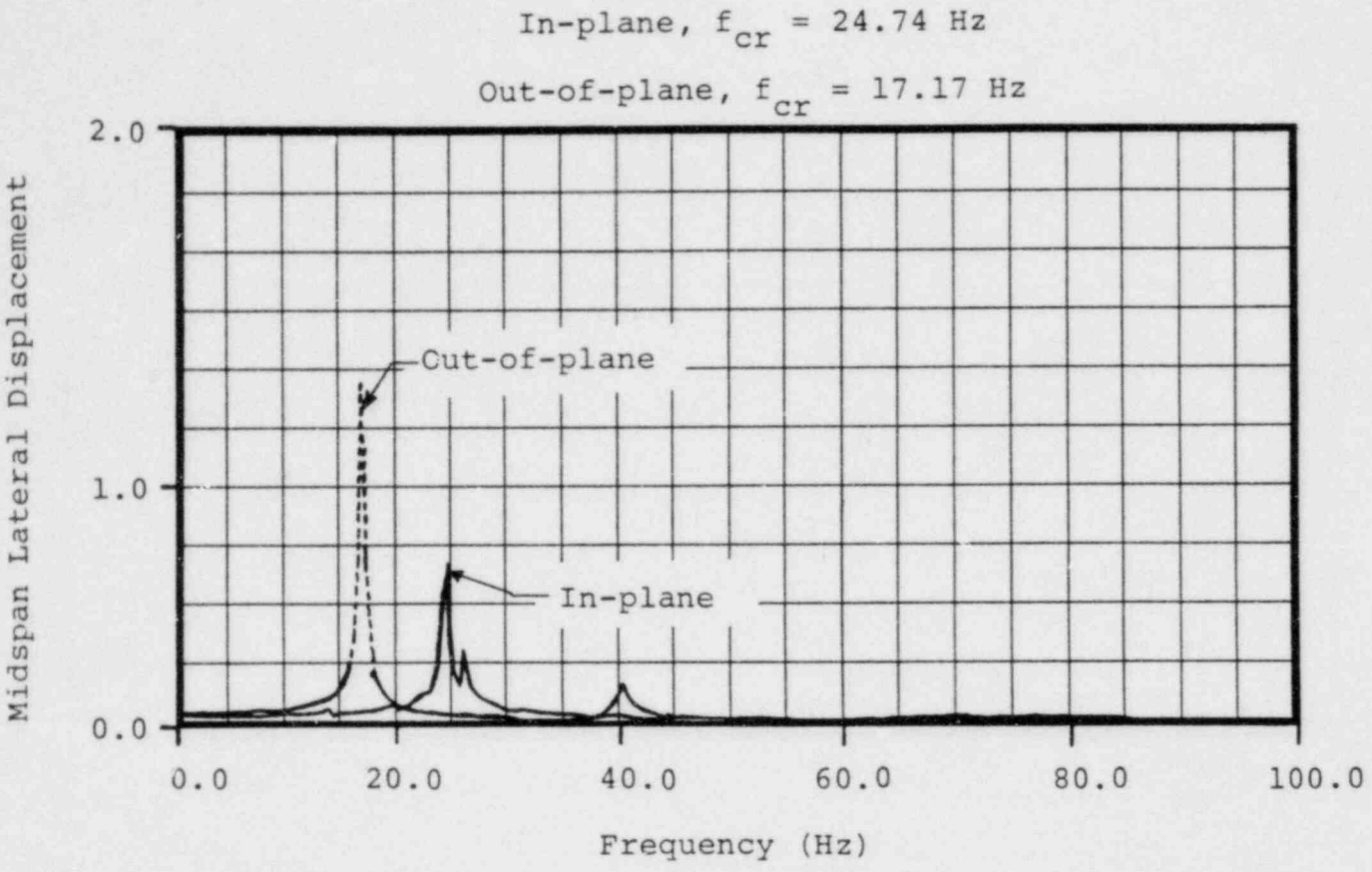

Notes:

1. Results shown are obtained by applying unit drag pressures to submerged portion of columns in the in-plane and out-of-plane directions relative to the mitered joint.
2. Results shown are typical for inside and outside columns.

Figure 3-2.4-3

HARMONIC ANALYSIS RESULTS FOR SUPPORT COLUMN

SUBMERGED STRUCTURE LOAD FREQUENCY DETERMINATION

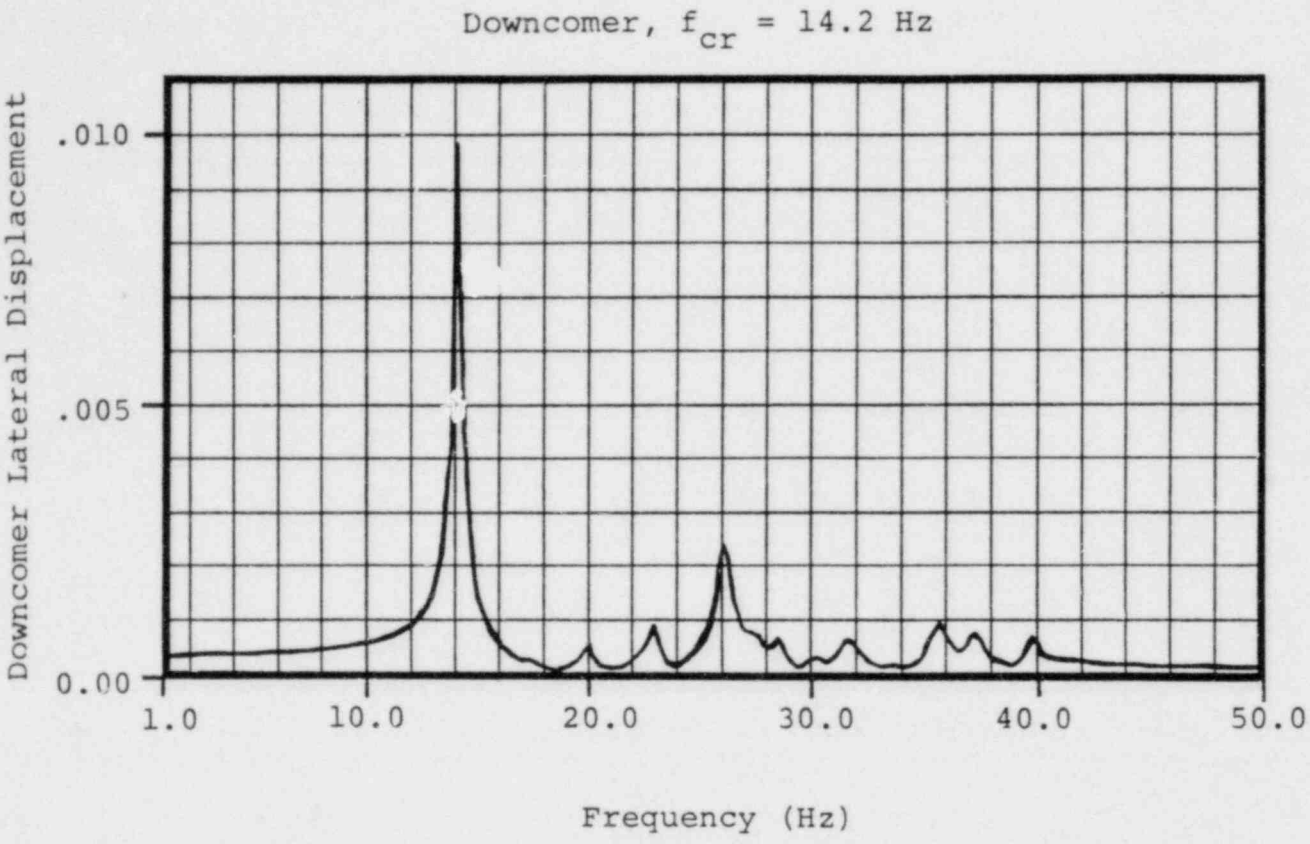

Notes:

1. Results shown are obtained by applying unit internal pressures to one downcomer in a downcomer pair.
2. Frequencies are determined without water inside submerged portion of the downcomers.
3. Results shown are typical for all downcomers.

Figure 3-2.4-4

HARMONIC ANALYSIS RESULTS FOR CONDENSATION OSCILLATION

DOWNCOMER LOAD FREQUENCY DETERMINATION

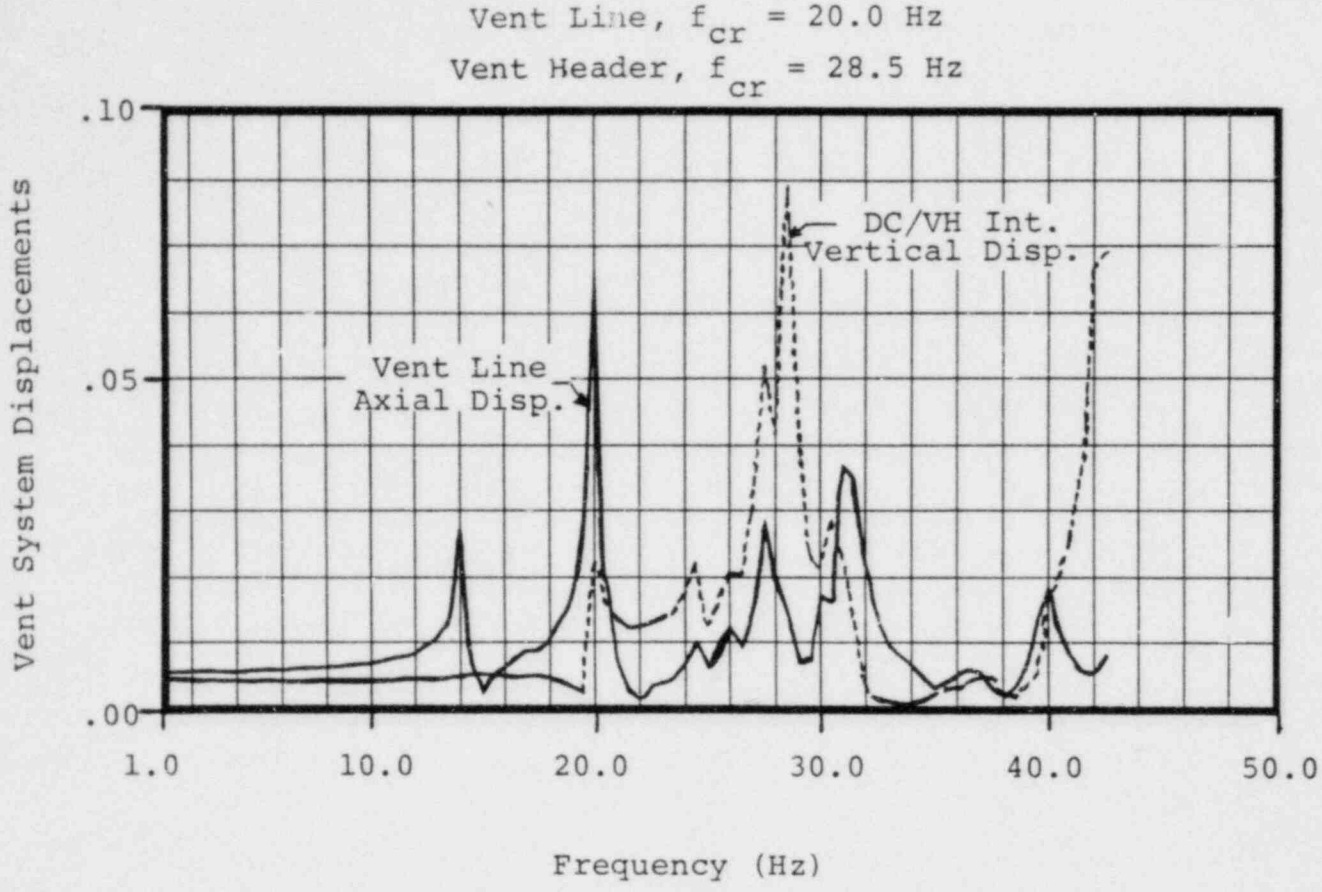

Note:

1. Results shown are obtained by applying 2.5 psi internal pressures to unreacted areas of vent system.

Figure 3-2.4-5

HARMONIC ANALYSIS RESULTS FOR CONDENSATION OSCILLATION

VENT SYSTEM PRESSURE LOAD FREQUENCY DETERMINATION

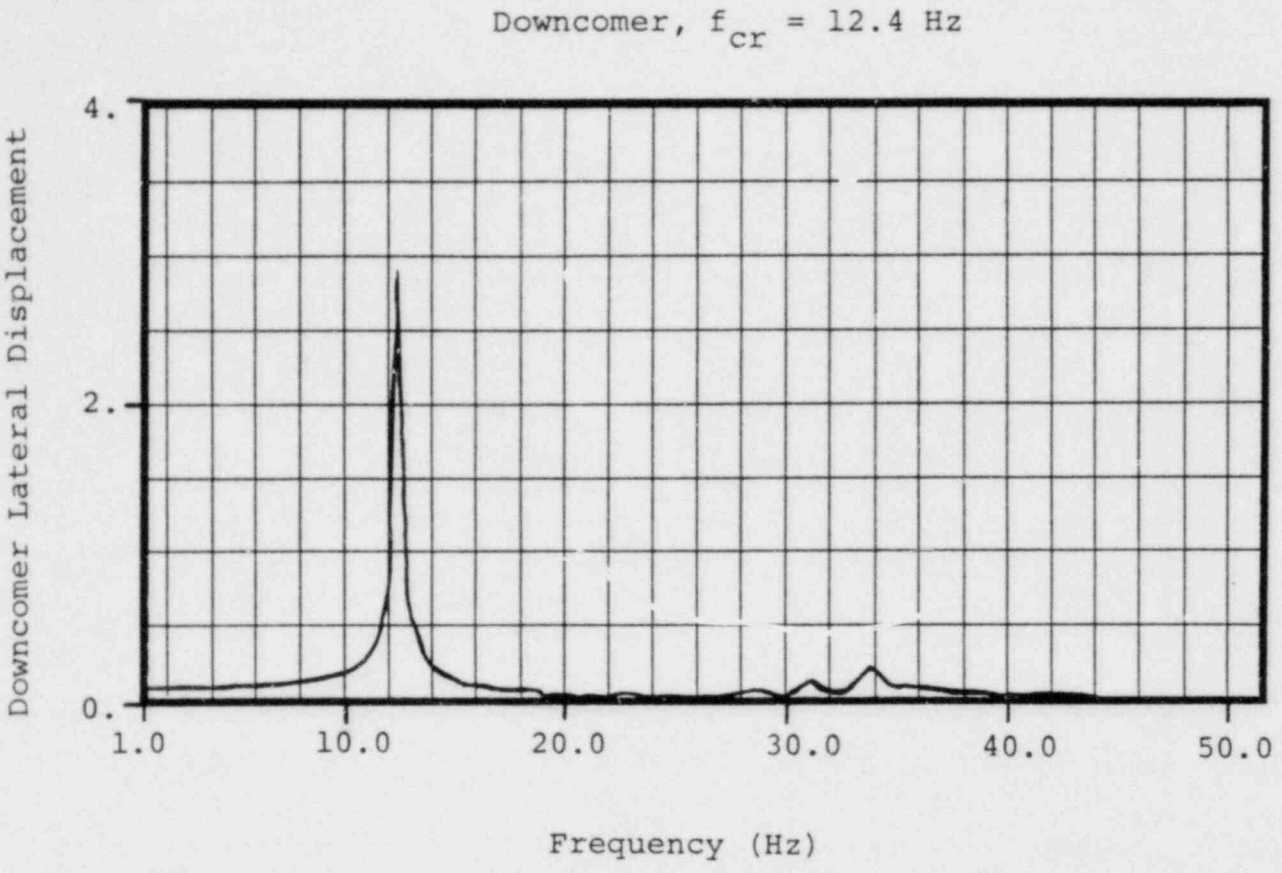

Notes:

1. Results shown are obtained by applying unit forces to downcomer ends in the plane of the downcomers in the same direction.

2. Frequencies are determined with water inside submerged portion of the downcomer.

3. Results shown are typical for all downcomers.

Figure 3-2.4-6

HARMONIC ANALYSIS RESULTS FOR CHUGGING DOWNCOMER LATERAL LOAD FREQUENCY DETERMINATION

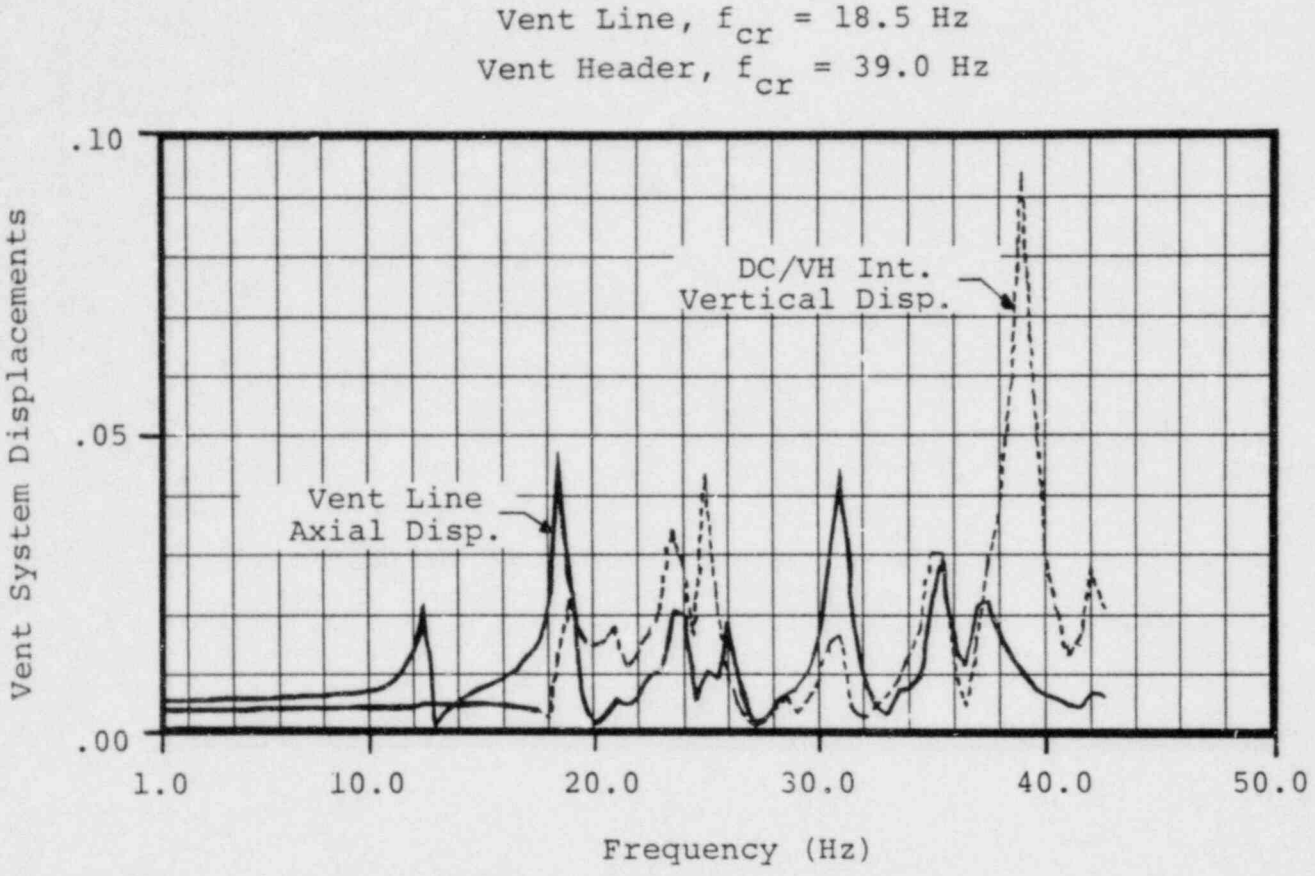

Note:

1. Results shown are obtained by applying 2.5 and 3.0 psi internal pressures to unreacted areas of vent line and vent header, respectively.

Figure 3-2.4-7

HARMONIC ANALYSIS RESULTS FOR CHUGGING VENT SYSTEM

PRESSURE LOAD FREQUENCY DETERMINATION

3-2.4.2 Analysis for Asymmetric Loads

The asymmetric loads which act on the vent system are evaluated by decomposing each of the asymmetric loadings into symmetric and/or asymmetric components with respect to a 180° segment of the vent system. The analysis of the vent system for asymmetric loads is performed for a typical 180° segment of the vent system cut along the plane of a principal azimuth.

A beam model of a 180° segment of the vent system, shown in Figure 3-2.4-8, is used to obtain the response of the vent system to asymmetric loads. The model includes the vent line, vent header, downcomers, and support columns.

Many of the modeling techniques used in the 180° beam model, such as those used for local mass and stiffness determination, are the same as those utilized in the 1/16th beam model of the vent system discussed in Section 3-2.4.1. The local stiffness effects at the vent line-drywell penetrations and vent line-vent header intersections are included using stiffness matrix elements for these penetrations and intersections. The local stiffness effects at the attachments of the support columns to the support ring on the vent header

are included using beams which account for the local stiffness of the support ring.

The 180° beam model contains 251 nodes, 258 beams, and 16 matrix elements. The model is less refined than the 1/16th beam model of the vent system, and is used to characterize the overall response of the vent system to asymmetric loadings. It includes those component parts and local stiffnesses which have an effect on the overall response of the vent system. The stiffness and mass properties used in the model are based on the nominal dimensions and densities of the materials used to construct the vent system. Small displacement linear-elastic behavior is assumed throughout.

The boundary conditions used in the 180° beam model are both physical and mathematical in nature. The physical boundary conditions used in the model are similar to those used in the 1/16th beam model of the vent system. The mathematical boundary conditions used in the model consist of either symmetry, anti-symmetry, or a combination of both at the 0° and 180° planes. The specific boundary condition used depends on the characteristics of the load being evaluated.

Additional mass is lumped along the length of the submerged portion of the downcomers and support columns in a manner similar to that used in the 1/16th beam model. The mass of water inside the submerged portion of the downcomers is also included. An additional mass of 1125 lbs is lumped at the center of gravity of the drywell/wetwell vacuum breaker to account for its weight. The masses of other vent system component parts are also lumped at the appropriate locations in the model.

The asymmetric loads which act on the vent system include horizontal seismic loads and asymmetric chugging loads as specified in Section 3-2.2.1. An equivalent static analysis is performed for each of the loads using the 180° beam model.

The 180° beam model analysis results are used to generate loads for use in the 1/16th beam model analysis. This allows evaluation of the effects of asymmetric loads on the component parts of the vent system not included in the 180° beam model. Beam stresses in the vent line and vent header are examined for each asymmetric loading to determine which 1/16th segment or segments of the 180° beam model produce the maximum

response. The displacements at the midcylinder planes of the controlling 1/16th segments are imposed on the corresponding midcylinder boundary planes of the 1/16th beam model. The inertia forces and concentrated forces acting on the 180° beam model between the midcylinder boundary planes are also applied to the 1/16th beam model at the appropriate node locations.

The magnitudes and characteristics of governing asymmetric loads on the vent system are presented and discussed in Section 3-2.2.1. The overall effects of asymmetric loads on the vent system are evaluated using the 180° beam model and the general analysis techniques discussed in the preceding paragraphs. The specific treatment of each load which results in asymmetric loads on the vent system is discussed in the paragraphs which follow.

2. Seismic Loads

   a. OBE Loads: A static analysis is performed for a 0.23g horizontal seismic acceleration applied to the weight of steel and water included in the 180° beam model. Seismic loads are applied in the direction of both principal azimuths.

b. SSE Loads: The procedure used to evaluate 0.46g horizontal SSE accelerations is the same as that discussed for OBE loads in load case 2a.

7. Chugging Loads

a. Chugging Downcomer Lateral Loads: A static analysis is performed for chugging downcomer lateral load cases 1 through 7, shown in Table 3-2.2-16.

Use of the methodology described in the preceding paragraphs results in a conservative evaluation of vent system response to the asymmetric loads defined in NUREG-0661.

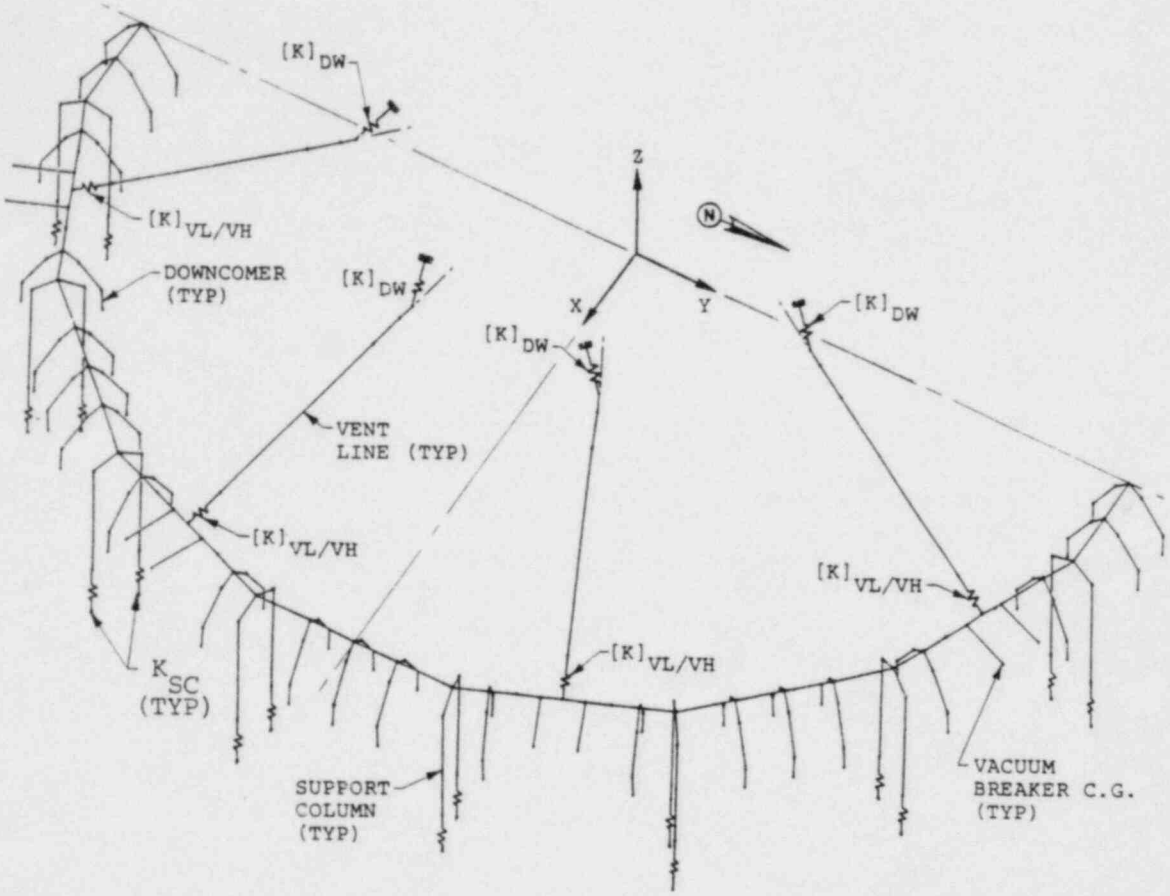

Figure 3-2.4-8

VENT SYSTEM 180° BEAM MODEL-ISOMETRIC VIEW

3-2.4.3 Analysis for Local Effects

The penetrations and intersections of the major components of the vent system are evaluated using refined analytical models of each penetration and intersection. These include the vent line-drywell penetration, the vent line-SRV piping penetration, the vent line-vent header intersection, and the downcomer-vent header intersections. The analytical models used to evaluate these penetrations and intersections are shown in Figures 3-2.4-9 through 3-2.4-12. An additional analytical model of the vent line-SRV piping penetration, shown in Figure 3-2.4-13 is used to evaluate local thermal effects in the penetration.

Each of the penetration and intersection analytical models includes mesh refinement near discontinuities to facilitate evaluation of local stresses. The stiffness properties used in the model are based on the nominal dimensions of the materials used to construct the penetrations and intersections. Small displacement linear-elastic theory is assumed throughout.

The analytical models are used to generate local stiffnesses of the penetrations and intersections for use in

the 1/16th beam model and the 180° beam model as discussed in Sections 3-2.4.1 and 3-2.4.2. Local stiffnesses are developed which represent the stiffness of the entire penetration or intersection in terms of a few local degrees of freedom on the penetration or intersection. This is accomplished either by applying unit forces or displacements to the selected local degrees of freedom, or by performing a matrix condensation to reduce the total stiffness of the penetration or intersection to those of the selected local degrees of freedom. The results are used to formulate stiffness matrix elements which are added to the 1/16th beam model and the 180° beam model at the corresponding penetration or intersection locations.

In general, the shell segment lengths of the penetration and intersection analytical models used for stiffness calculations are extended to account for the ovaling stiffness of the respective shell segment. For example, the segments of the vent line, vent header, and downcomers at each of the penetrations and intersections are extended at least to the location of the first circumferential stiffener ring which inhibits shell ovaling.

The analytical models are also used to evaluate stresses in the penetrations and intersections. Stresses are computed by idealizing the penetrations and intersections as free bodies in equilibrium under a set of statically applied loads. The applied loads, which are extracted from the 1/16th beam model results, consist of loads acting on the penetration and intersection model boundaries and of loads acting on the interior of penetration and intersection models. The loads acting on the penetration and intersection model boundaries are the beam end loads taken from the 1/16th beam model analysis at nodes coincident with the penetration or intersection model boundary locations.

The loads which act on the interior of the penetration or intersection models consist of reaction loads and distributed loads taken from the 1/16th beam model results. The reaction loads include the forces and moments applied to the appropriate penetration or intersection at the attachment points of the SRV piping, downcomer bracing, and vent header deflectors. The distributed loads include the pressures and acceleration loads applied to penetration and intersection models to account for internal pressure loads, thrust loads, pool swell loads, and inertia loads. By the application of

boundary loads, reaction loads, and distributed loads to the penetration and intersection models, equilibrium of the penetrations and intersections is achieved for each of the governing vent system loadings.

Loads which act on the shell segment boundaries are applied to the penetration and intersection models through a system of radial beams. The radial beams extend from the middle surface of each of the shell segments to a node located on the centerline of the corresponding shell segment. The beams have large bending stiffnesses, zero axial stiffness and are pinned in all directions at the shell segment middle surface. Boundary loads applied to the centerline nodes cause only axial and shear loads to be transferred to the shell segment middle surface with no local bending effects. Use of this boundary condition minimizes end effects on penetration and intersection stresses in the local areas of interest. The system of radial beams constrains the boundary planes to remain plane during loading, which is consistent with the assumption made in small deflection beam theory.

The methodology used to evaluate the overall effects of the governing loads acting on the vent system using the

1/16th beam model is discussed in Section 3-2.4.1. The general methodology used to evaluate local vent system penetration and intersection stresses is discussed in the preceding paragraphs. A description of each vent system penetration and intersection analytical model and its use is provided in the paragraphs which follow.

- Vent Line-Drywell Penetration Axisymmetric Finite Difference Model: The vent line-drywell penetration model shown in Figure 3-2.4-9 includes a segment of the drywell shell, the jet deflector, the cylindrical penetration nozzle, the annular pad plate, and the spherical transition piece. The analytical model contains 9 segments with 175 mesh points. The reaction loads applied to the model include those computed at the upper end of the vent line. The distributed loads applied to the model include internal pressure loads.

- Vent Line-SRV Piping Penetration Finite Element Model: The vent line-SRV piping penetration model shown in Figure 3-2.4-10 includes a segment of the vent line, the penetration insert plate, the penetration nozzles, the penetration sleeves, the ring plates on the vent lines, and the associated pene-

tration stiffener plates. The model contains 1539 nodes, 186 beam elements, and 2222 plate bending and stretching elements. Boundary loads are applied at each end of the vent line shell segment. The reaction loads applied to the analytical model include the drywell and wetwell SRV piping reaction loads. The distributed loads applied to the analytical model include internal pressure loads and inertia forces from dynamic loadings.

- Vent Line-Vent Header Intersection Finite Element Model. The vent line-vent header intersection finite element model shown in Figure 3-2.4-11 includes a segment of the vent line, a segment of the vent header with conical transitions, the vacuum breaker nozzles, the intersection ring plates and stiffener plates, the SRV piping supports located under the vent line, and the vacuum breaker support system. The model contains 1486 nodes, 160 beam elements, and 2296 plate bending and stretching elements. Boundary loads are applied at the end of the vent line shell segment, at each end of the vent header shell segment, and at the end of each vacuum breaker nozzle. The reaction loads applied to the analytical model include vent header

deflector reaction loads and SRV piping reaction loads. The distributed loads applied to the analytical model include internal pressure loads and thrust loads, pool swell loads on the vent line and vacuum breaker supports, and inertia forces from dynamic loadings.

- Downcomer-Vent Header Intersection Finite Element Model: The downcomer vent header intersection finite element model shown in Figure 3-2.4-12 includes a segment of the vent header, a segment of each downcomer, the crotch plate, the downcomer rings, and the outer stiffener plates. The analytical model contains 924 nodes, 92 beam elements, and 1192 plate bending and stretching elements. Boundary loads are applied at the ends of the vent header segment and at the ends of the downcomer segment. The reaction loads applied to the analytical model include the vent header deflector reaction loads and the downcomer bracing system reaction loads. The distributed loads applied to the model include internal pressure loads and thrust loads, pool swell loads on the downcomers and downcomer ring plates, and inertia forces from dynamic loadings.

e. Vent Line-SRV Penetration Axisymmetric Finite Element Model: The vent line penetration model shown in Figure 3-2.4-13 includes a piece of the vent line, the penetration insert plate, a segment of the SRV penetration nozzle, the penetration sleeves, and the upper and lower nozzle-to-sleeve welds. The analytical model contains 306 nodes and 250 axisymmetric shell elements.

The analytical model is used to perform a transient thermal analysis of the penetration for a sustained SRV actuation. The penetration is initially assumed to be at 70°F, and is then subjected to an instantaneous temperature increase of 293°F at the inside surface of the penetration nozzle. Conservative values of heat transfer coefficients are used and transient temperatures in each of the analytical model components are calculated. Stresses in the penetration nozzle, penetration sleeve, upper and lower nozzle-to-sleeve welds, and in the insert plate in the vicinity of the nozzle are calculated at several times during the transient. The maximum stresses for the times with the highest thermal gradients are combined with

those from the analytical model of the penetration shown in Figure 3-2.4-10 for use in evaluating fatigue effects in the vent line-SRV piping penetration.

Use of the methodology described in the preceding paragraphs results in a conservative evaluation of vent system local stresses due to the loads defined in NUREG-0661.

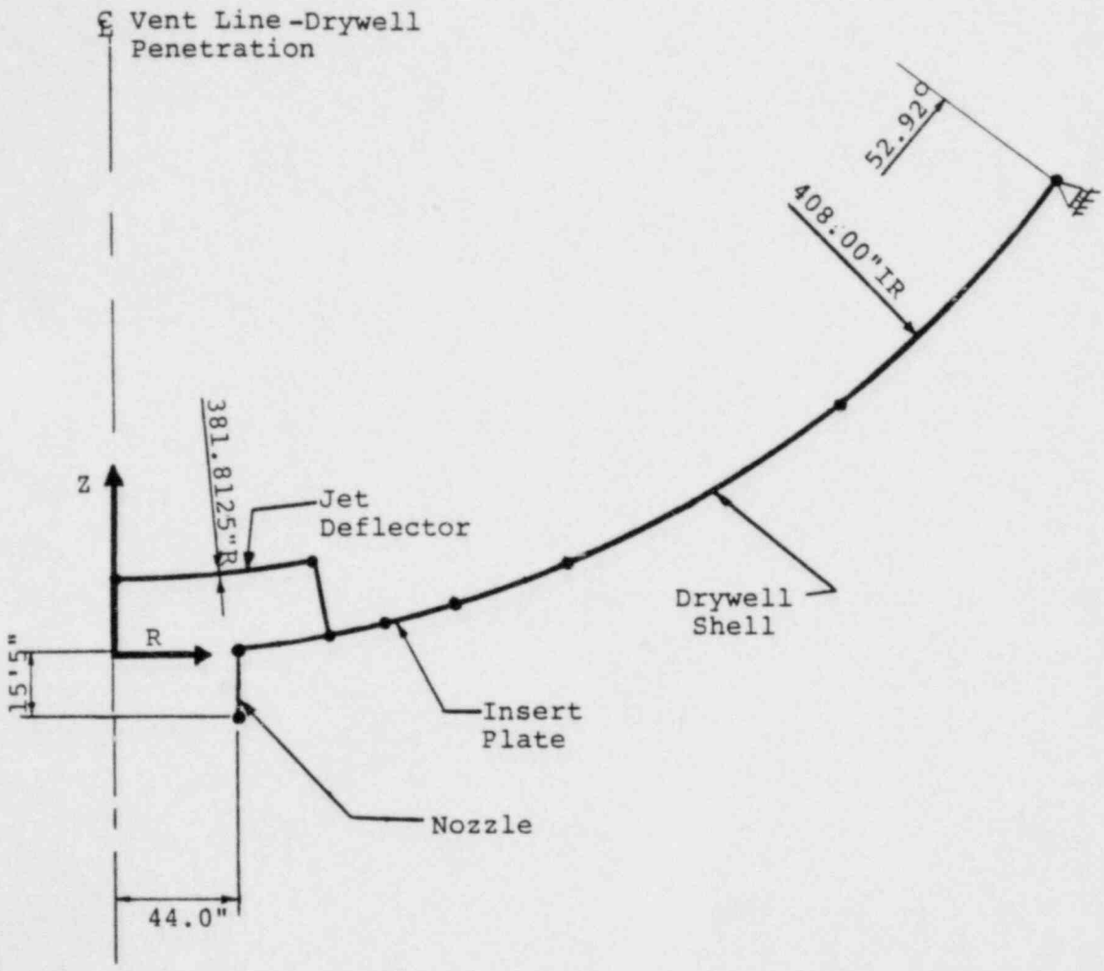

Figure 3-2.4-9

VENT LINE DRYWELL PENETRATION AXISYMMETRIC

FINITE DIFFERENCE MODEL - VIEW OF TYPICAL MERIDIAN

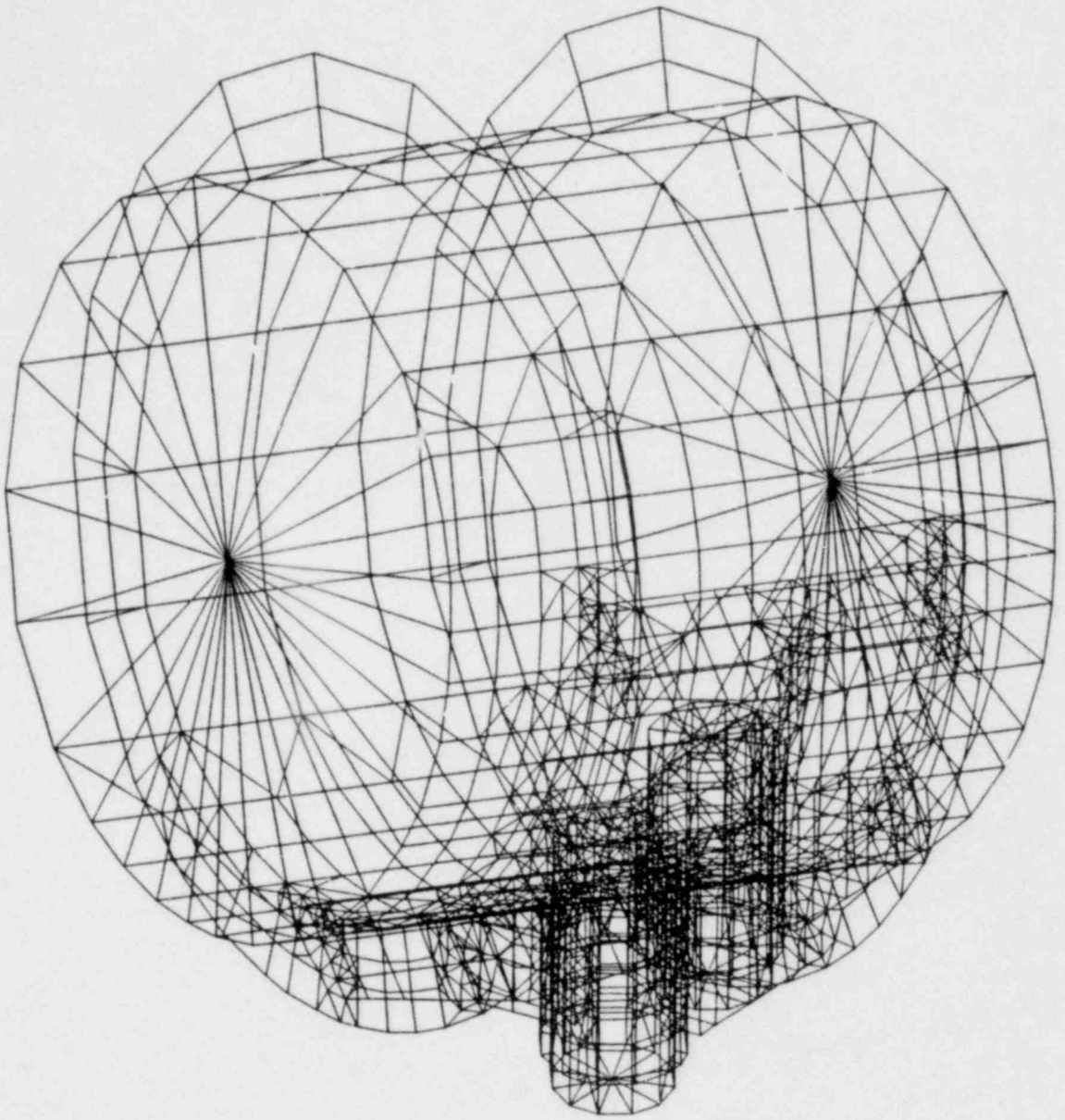

Figure 3-2.4-10

SRV PIPING-VENT LINE PENETRATION FINITE ELEMENT

MODEL-ISOMETRIC VIEW

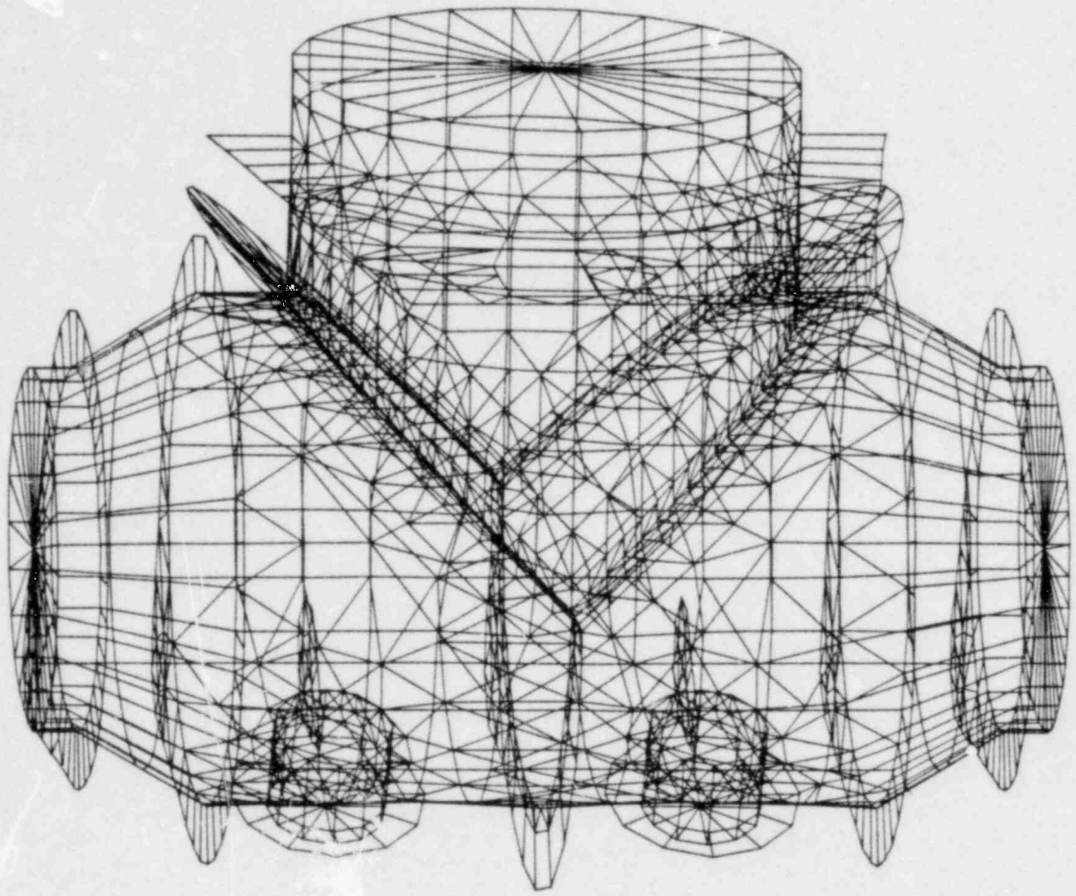

Figure 3-2.4-11

VENT LINE-VENT HEADER INTERSECTION FINITE ELEMENT MODEL-ISOMETRIC VIEW

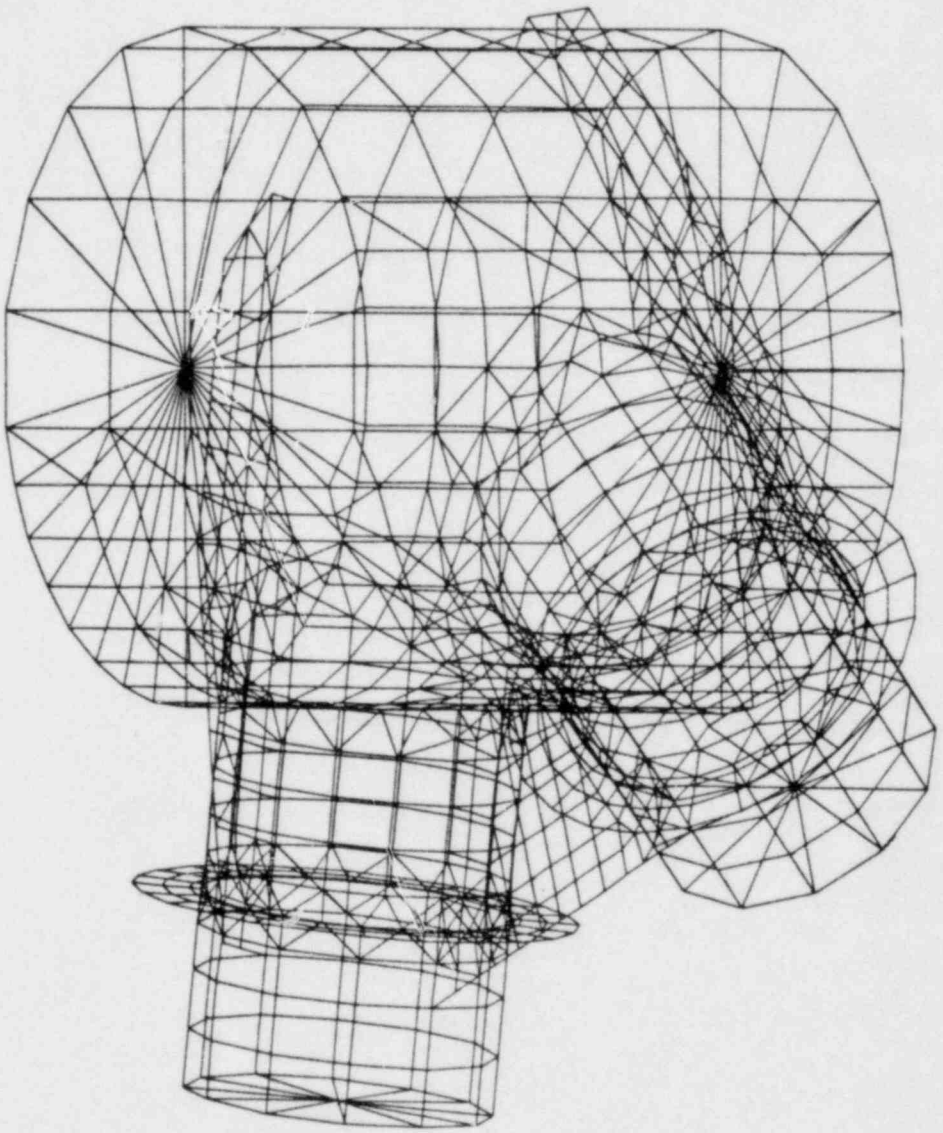

Figure 3-2.4-12

DOWNCOMER-VENT HEADER INTERSECTION

FINITE ELEMENT MODEL-ISOMETRIC VIEW

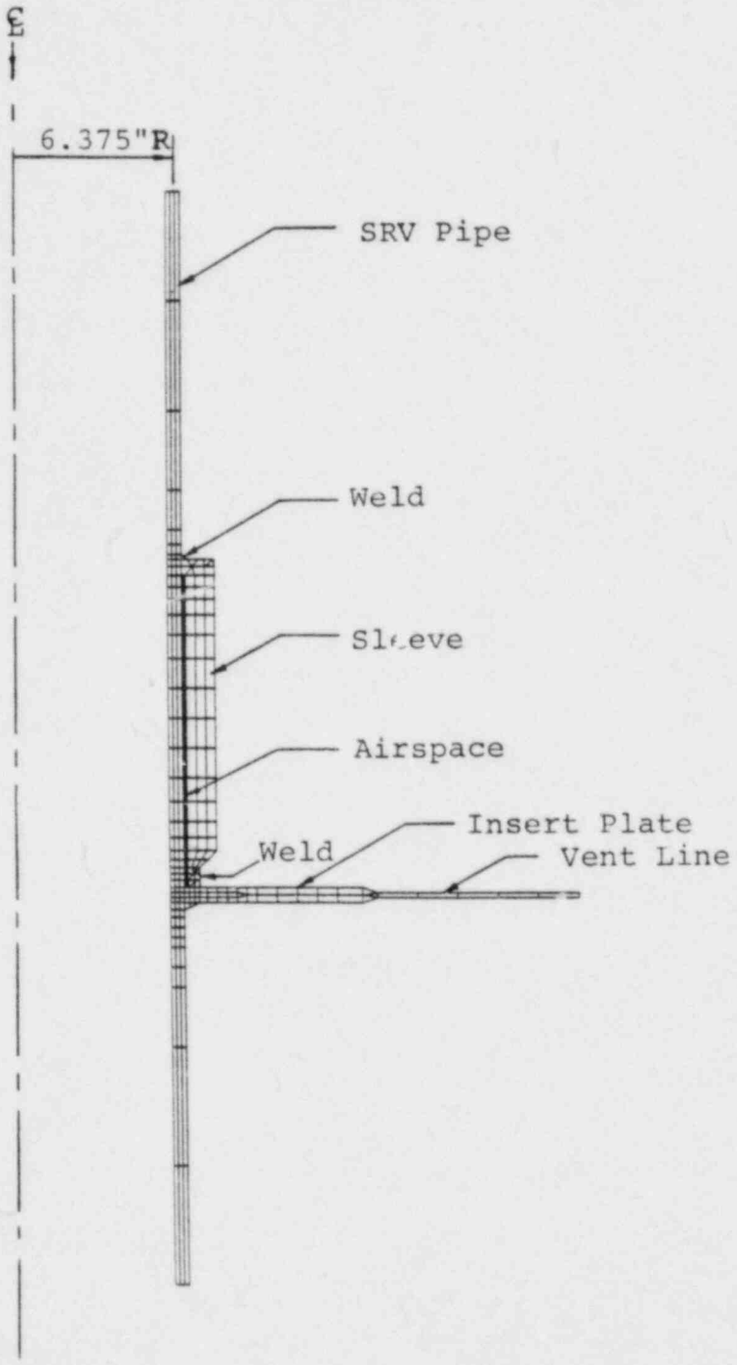

Figure 3-2.4-13

SRV PIPING-VENT LINE PENETRATION AXISYMMETRIC FINITE ELEMENT MODEL FOR LOCAL THERMAL ANALYSIS-VIEW OF TYPICAL MERIDIAN

3-2.4.4 Methods for Evaluating Analysis Results

The methodology discussed in Sections 3-2.4.1 and 3-2.4.2 is used to determine element forces and component stresses in the vent system component parts. The methodology used to evaluate the analysis results, determine the controlling stresses in the vent system components parts and examine fatigue effects is discussed in the paragraphs which follow.

To evaluate analysis results for the vent system Class MC components, membrane and extreme fiber stress intensities are computed. The values of the membrane stress intensities away from discontinuities are computed using 1/16th beam model results. These stresses are compared with the primary membrane stress allowables contained in Table 3-2.3-1. The values of membrane stress intensities near discontinuities are computed using results from the penetration and intersection analytical models. These stresses are compared with local primary membrane stress allowables contained in Table 3-2.3-1. Primary stresses in vent system Class MC component welds are computed using maximum principal stresses or the resultant forces acting on the weld

throat. The results are compared to primary weld stress allowables contained in Table 3-2.3-1.

Many of the loads contained in each of the controlling load combinations are dynamic loads which result in stresses which cycle with time and are partially or fully reversible. The maximum stress intensity ranges for all vent system Class MC components are calculated using the maximum values of the extreme fiber stress differences which occur near discontinuities in the penetration and intersection analytical models. These stresses are compared to the secondary stress range allowables contained in Table 3-2.3-1. A similar procedure is used to compute the stress range for the vent system Class MC component welds. The results are compared to the secondary weld stress allowables contained in Table 3-2.3-1.

To evaluate the vent system Class MC component supports, beam end loads obtained from the 1/16th beam model results are used to compute stresses. The results are compared with the corresponding allowable stresses contained in Table 3-2.3-1. Stresses in vent system Class MC component support welds are obtained using the 1/16th beam model results to compute the maximum

resultant force acting on the associated weld throat. The results are compared to weld stress limits discussed in Section 3-2.3.

The controlling vent system load combinations are defined in Section 3-2.2.2. During load combination formulation, the maximum stress components in a particular vent system part at a given location are combined for the individual loads contained in each combination. The stress components for dynamic loadings are combined so as to obtain the maximum stress intensity.

The maximum differential displacements of the vent line bellows are determined using results from the 1/16 beam model of the vent system and the analytical model of the suppression chamber discussed in Volume 2 of this report. The displacements of the attachment points of the bellows to the suppression chamber and to the vent line are determined for each load case. The differential displacement is computed from these values. The results for each load are combined to determine the total differential displacements for the controlling load combinations. These results are compared to the allowable bellows displacements in Table 3-2.3-2.

To evaluate fatigue effects in the vent system Class MC components and associated welds, extreme fiber alternating stress intensity histograms for each load in each event or combination of events are determined. Fatigue effects for chugging downcomer lateral loads are evaluated using the stress reversal histrograms shown in Table 3-2.2-18. Stress intensity histograms are developed for the vent system major components and welds with the highest stress intensity ranges. Fatigue strength reduction factors of 2.0 for major component stresses and 4.0 for component weld stresses are conservatively used to account for peak stresses at all locations except at the SRV piping-vent line penetration where the welds are modeled explicitly to obtain peak stresses. For each combination of events, a load combination stress intensity histogram is formulated and the corresponding fatigue usage factors are determined using the curve shown in Figure 3-2.4-14. The usage factors for each event are then summed to obtain the total fatigue usage.

Use of the methodology described above results in a conservative evaluation of the vent system design margins.

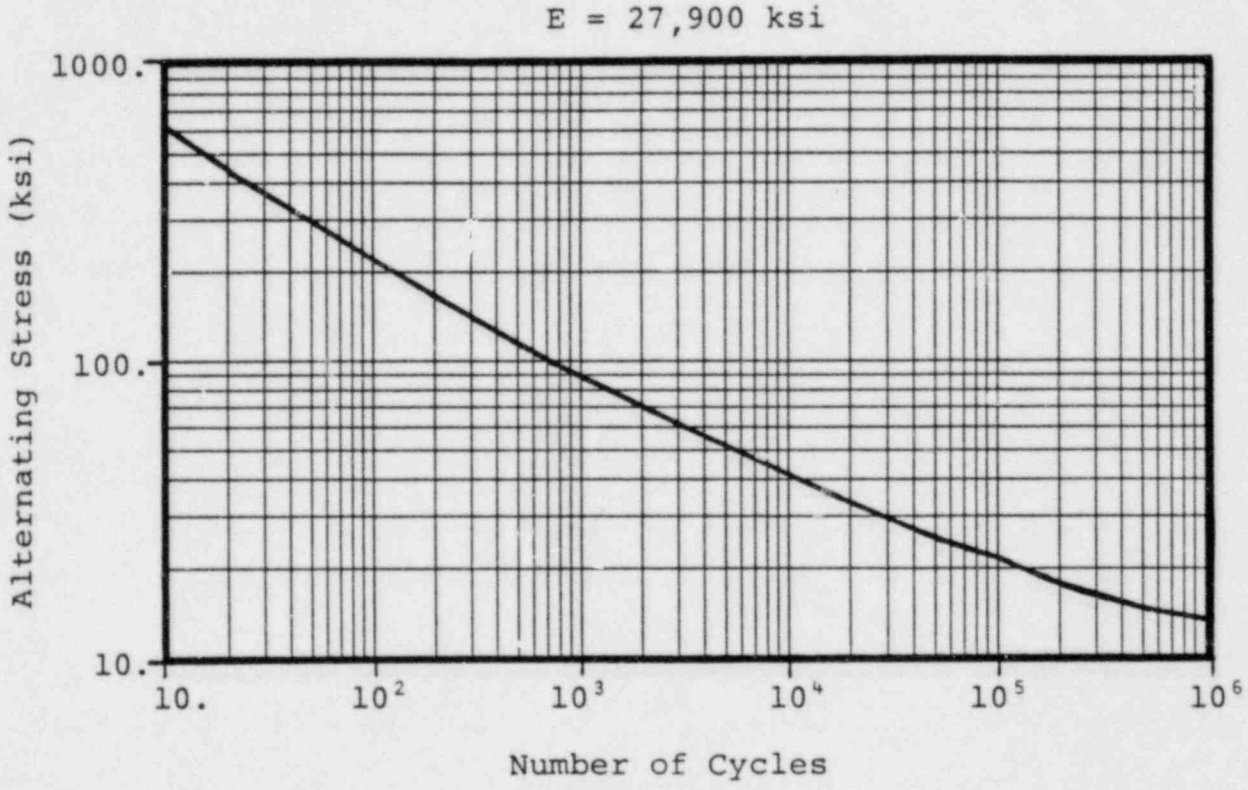

Figure 3-2.4-14

ALLOWABLE NUMBER OF STRESS CYCLES FOR VENT SYSTEM

FATIGUE EVALUATION

3-2.5 Analysis Results

The geometry, loads and load combinations, acceptance criteria, and analysis methods used in the evaluation of the Fermi 2 vent system are presented and discussed in the preceding sections. The results and conclusions derived from the evaluation of the vent system are presented in the paragraphs and sections which follow.

The maximum primary membrame stresses for the major components of the vent system are shown in Table 3-2.5-1 for each of the governing loads. The corresponding reaction loads for the vent system support columns and vent line-drywell penetration are shown in Tables 3-2.5-2 and 3-2.5-3. The maximum differential displacements of the vent line bellows for the governing load cases are shown in Table 3-2.5-4. The transient response of the vent system support columns and the drywell/wetwell vacuum breaker for pool swell loads are shown in Figures 3-2.5-1 through 3-2.5-3.

The maximum stresses and associated design margins for the major vent system components, component supports, and welds for the SBA II, IBA I, DBA I, DBA II, and DBA III load combinations are shown in Table 3-2.5-5. The

maximum stresses and associated design margins for the components and welds of the vent line-SRV piping penetration for the NOC I, SBA II, IBA I, and DBA III load combinations are shown in Table 3-2.5-6. The maximum differential displacements and design margins for the vent line bellows for the SBA II, IBA I, DBA II, and DBA III load combinations are shown in Table 3-2.5-7. The fatigue usage factors for the controlling vent system component and weld for the Normal Operating plus SBA events, and the Normal Operating plus IBA events are shown in Table 3-2.5-8.

The vent system evaluation results presented in the preceding paragraphs are discussed in Section 3-2.5.1.

Table 3-2.5-1

MAJOR VENT SYSTEM COMPONENT MAXIMUM MEMBRANE STRESSES

FOR GOVERNING LOADS

Section 3-2.2.1 Load Designation		Primary Membrane Stress (ksi)		
Load Type	Load Case Number	Vent Line	Vent Header	Downcomer
Dead Weight	1a	0.40	0.96	0.04
Seismic	2a	0.92	1.93	0.88
	2b	1.84	3.86	1.75
Pressure and Temperature	3b	5.92	11.95	4.81
	3d	N/A	N/A	N/A
Vent System Discharge	4a	6.48	9.79	4.63
Pool Swell	5a-5d	2.12	3.41	1.05
	5e	0.02	0.32	0.74
Condensation Oscillation	6a+6d	1.12	2.04	0.88
	6b+6d	3.24	10.83	5.04
	6f	0.05	0.23	-
Chugging	7a	3.93	2.98	5.29
	7b	0.79	0.95	1.28
	7c(6e)	-	-	-
	7d	0.10	0.36	0.01
SRV Discharge	8a	0.69	0.66	1.45
Piping Reactions	9a	6.68	1.15	0.01

Note:

1. Values shown are maximums irrespective of time and location for individual load types and may not be added to obtain load combination results.

Table 3-2.5-2

MAXIMUM COLUMN REACTIONS FOR GOVERNING VENT SYSTEM LOADS

Section 3-2.2.1 Load Designation				Column Reaction Load (kips)		
Load Type		Load Case Number	Direction	Inside	Outside	Total (1)
Dead Weight		1a	Compression	14.59	11.46	26.05
Seismic	OBE	2a	Tension	1.72	6.24	7.96
			Compression	1.72	6.24	7.96
	SSE	2b	Tension	3.44	12.48	15.92
			Compression	3.44	12.48	15.92
Internal Pressure		3b	Tension	25.94	20.64	46.58
Temperature		3d	Compression	43.68	-18.79	24.89
Vent System Discharge		4a	Tension	34.49	24.80	59.29
Pool Swell		5a-5d	Tension	47.97	29.08	77.05
			Compression	15.20	9.85	25.05
Condensation Oscillation	IBA	6a+6c	Tension	6.53	7.66	14.19
			Compression	6.53	7.66	14.19
	DBA	6b+6d	Tension	36.04	50.42	86.46
			Compression	36.04	50.42	86.46
Chugging		7a+7b	Tension	16.30	20.96	37.26
			Compression	16.30	20.96	37.26
Piping Reactions		9a	Tension	0.15	6.70	6.85
			Compression	0.15	6.70	6.85

Note:

1. For dynamic loads reactions are added in time.

Table 3-2.5-3

MAXIMUM VENT LINE-DRYWELL PENETRATION REACTIONS FOR GOVERNING VENT SYSTEM LOADS

Section 3-2.2.1 Load Designation			Penetration Reaction Load					
Load Type		Load Case Number	Force (kips)			Moments (in-kip)		
			Radial	Merid.	Circum.	Radial	Merid.	Circum.
Dead Weight		1a	3.30	-2.70	0.00	0.00	0.00	221.70
Seismic	OBE	2a	17.70	0.80	1.30	8.60	122.90	148.10
	SSE	2b	35.40	1.50	2.70	17.30	445.70	296.10
Internal Pressure		3b	-19.70	0.80	0.00	0.00	0.00	-173.20
Temperature		3d	-130.60	1.70	0.00	0.00	0.00	-3704.10
Vent System Discharge		4a	46.60	1.70	0.00	0.00	0.00	-302.70
Pool Swell		5a-5d	18.80	-2.30	0.00	0.00	0.00	135.00
Condensation Oscillation	IBA	6a+6c	9.70	0.33	0.00	0.00	0.00	33.00
	DBA	6b+6d	31.80	3.33	0.00	0.00	0.00	129.80
Chugging		7a+7b	14.70	-1.10	4.00	156.40	482.40	12.70
Piping Reactions		9a	-31.40	12.30	0.00	0.00	0.00	-654.60

Table 3-2.5-4

MAXIMUM VENT LINE BELLOWS DISPLACEMENTS FOR

GOVERNING VENT SYSTEM LOADS

Section 3-2.2.1 Load Designation			Differential Bellows Displacements (in)			
			Axial		Lateral	
Load Type		Load Case Number	Compression	Extension	Meridional	Longitudinal
Dead Weight		1a	.001	-	.004	.000
Seismic	OBE	2a	.011	.011	.007	.010
	SSE	2b	.022	.022	.014	.020
Internal Pressure		3b	.132	-	.047	.000
Temperature		3d	.510	-	.175	.000
Vent System Discharge		4a	.060	-	.041	.000
Pool Swell		5a-5d	.048	.048	.077	.000
Condensation Oscillation	IBA	6a+6c	.006	.003	.005	.000
	DBA	6b+6d	.031	.028	.110	.000
Chugging		7a+7b	.012	.012	.032	.131
Piping Reactions		9a	.020	.020	.035	.000

Note:

1. The values shown are maximums irrespective of time for individual load types and may not be added to obtain load combination results.

Table 3-2.5-5

MAXIMUM VENT SYSTEM STRESSES FOR CONTROLLING LOAD COMBINATIONS

Item	Stress Type	Load Combination Stresses (ksi)									
		SBA II (1)		IBA I (1)		DBA I (1)		DBA II (1)		DBA III (1)	
		Calc. Stress	Calc./Allow. (2)	Calc. Stress	Calc./Allow. (2)	Calc. Stress	Calc./Allow. (2)	Calc. Stress	Calc./Allow. (2)	Calc. Stress	Calc./Allow. (2)
COMPONENTS											
Drywell Shell	Local Primary Membrane	7.44	0.26	4.77	0.16	7.16	0.25	7.82	0.27	8.23	0.16
	Prim. + Sec. Stress Range	27.25	0.40	20.41	0.30	N/A	N/A	16.44	0.24	N/A	N/A
Vent Line	Primary Membrane	15.31	0.79	11.08	0.57	16.92	0.88	17.52	0.91	18.53	0.55
	Local Primary Membrane	14.71	0.51	11.36	0.39	13.20	0.46	28.32	0.98	18.18	0.36
	Prim. + Sec. Stress Range	48.58	0.71	34.71	0.51	N/A	N/A	65.51	0.96	N/A	N/A
Vent Header	Primary Membrane	12.20	0.63	10.62	0.55	17.63	0.91	18.58	0.96	19.70	0.58
	Local Primary Membrane	24.29	0.84	12.88	0.44	23.90	0.83	24.90	0.86	28.16	0.55
	Prim. + Sec. Stress Range	61.28	0.90	44.64	0.66	N/A	N/A	61.73	0.91	N/A	N/A
Downcomer	Primary Membrane	9.24	0.48	3.32	0.17	7.53	0.39	9.25	0.48	9.85	0.29
	Local Primary Membrane	13.14	0.45	9.43	0.33	18.68	0.65	21.44	0.74	19.59	0.38
	Prim. + Sec. Stress Range	36.06	0.53	21.39	0.31	N/A	N/A	53.61	0.79	N/A	N/A
Support Column Ring Plate	Primary Membrane	7.91	0.41	4.72	0.24	5.46	0.28	7.13	0.37	6.20	0.18
	Local Primary Membrane	14.81	0.51	11.15	0.39	25.42	0.88	20.25	0.70	28.23	0.55
	Prim. + Sec. Stress Range	45.14	0.66	31.26	0.46	N/A	N/A	33.35	0.49	N/A	N/A
COMPONENT SUPPORTS											
Support Columns	Bending	5.43	0.28	5.67	0.29	1.50	0.08	7.51	0.38	2.52	0.10
	Tensile	0.52	0.03	0.14	0.01	1.48	0.08	1.42	0.07	1.52	0.06
	Combined	0.31	0.31	0.30	0.30	0.16	0.16	0.45	0.45	0.16	0.16
	Compressive	0.78	0.05	0.51	0.03	0.14	0.01	0.49	0.03	0.24	0.01
	Interaction	0.41	0.41	0.46	0.46	0.16	0.16	0.54	0.54	0.16	0.16
WELDS											
Column Ring Plate to VH	Primary	1.42	0.09	1.07	0.07	2.45	0.16	1.93	0.13	2.69	0.10
	Secondary	4.32	0.10	2.99	0.07	N/A	N/A	3.18	0.07	N/A	N/A

Table 3-2.5-6

MAXIMUM VENT LINE-SRV PIPING PENETRATION STRESSES

FOR CONTROLLING LOAD COMBINATIONS

Item	Stress Type	NOC I (1)		SBA II (1)		IBA I (1)		DBA III (1)	
		Calc. (ksi)	Calc. (2) / Allow	Calc. (ksi)	Calc. (2) / Allow	Calc. (ksi)	Calc. (2) / Allow	Calc. (ksi)	Calc. (2) / Allow
C O M P O N E N T									
Penetration Nozzle	Primary Membrane	5.96	0.36	8.93	0.54	8.03	0.49	8.83	0.29
	Local Primary Membrane	12.51	0.51	14.24	0.58	14.11	0.57	15.99	0.35
	Primary + Secondary Stress Range	45.93	0.77	46.10	0.77	45.93	0.77	N/A	-
W E L D S									
Nozzle to Sleeve (Upper)	Primary	3.77	0.30	4.44	0.36	3.67	0.30	4.49	0.20
	Secondary	33.97	0.75	35.30	0.78	33.98	0.76	N/A	-
Nozzle to Sleeve (Lower)	Primary	5.70	0.46	7.82	0.63	5.78	0.47	6.45	0.28
	Secondary	40.59	0.90	44.06	0.98	39.92	0.89	N/A	-

Notes:

1. Reference Table 3-2.2-25 for load combination designations.
2. Reference Table 3-2.3-1 for allowable stresses.

Table 3-2.5-7

MAXIMUM VENT LINE BELLOWS DIFFERENTIAL DISPLACEMENTS

FOR CONTROLLING LOAD COMBINATIONS

Displacement Component		SBA II		IBA I		DBA II		DBA III	
		Calc. (in)	Calc. / Allow.	Calc. (in)	Calc. / Allow.	Calc. (in)	Calc. / Allow.	Calc. (in)	Calc. / Allow.
Axial	Compression	.502	.57	.579	.66	.629	.72	.602	.69
	Tension	-	-	-	-	-	-	-	-
Lateral	Meridional	.185	.30	.265	.42	.288	.46	.271	.43
	Longitudinal	.173	.28	.032	.05	.010	.02	.042	.07

Note:

1. The DBA III bellows displacements envelop those of DBA I since DBA III contains SRV discharge loads in addition to the other loads in DBA I as shown in Table 3-2.2-25.

Table 3-2.5-8

MAXIMUM FATIGUE USAGE FACTORS FOR VENT SYSTEM COMPONENTS AND WELDS

Event Sequence	Load Case Cycles				Condensation Oscillation (sec.)	(4) Chugging (sec.)	Event Usage Factor	
	Seismic	Pressure	Temperature	SRV (3) Discharge			(5) Vent Header	(6) Weld
NOC W/SRV Discharge	0	(2) 150	(2) 150	2804	N/A	N/A	.00	.36
SBA 0. to 600. sec	0	0	0	50	N/A	300.	.19	.00
SBA 600. to 1200 sec	1000 (2)	1	1	2	N/A	600.	.36	.01
IBA 0. to 300. sec	0	0	0	25	300.	N/A	.00	.00
IBA 300. to 500. sec	1000 (2)	1	1	2	N/A	200.	.51	.00
Maximum Cumulative Usage Factors					NOC + SBA		.55	.37
					NOC + IBA		.51	.36

Notes:

1. See Table 3-2.2-25 and Figures 3-2.2-11 and 3-2.2-12 for load cycles and event sequencing information.
2. Entire number of load cycles conservatively assumed to occur during time of maximum event usage.
3. Total number of SRV actuations shown are conservatively assumed to occur in same suppression chamber bay.
4. Each chug-cycle has a duration of 1.4 sec. See Figure 3-2.2-18 for chugging downcomer load histogram. The maximum fatigue usage factor for chugging downcomer loads at the downcomer-vent header intersection is 0.24.
5. The maximum cumulative usage for a vent system component occurs in the vent header at the downcomer-vent header intersection.
6. The maximum cumulative usage for a vent system component weld occurs at the SRV piping-vent line penetration.

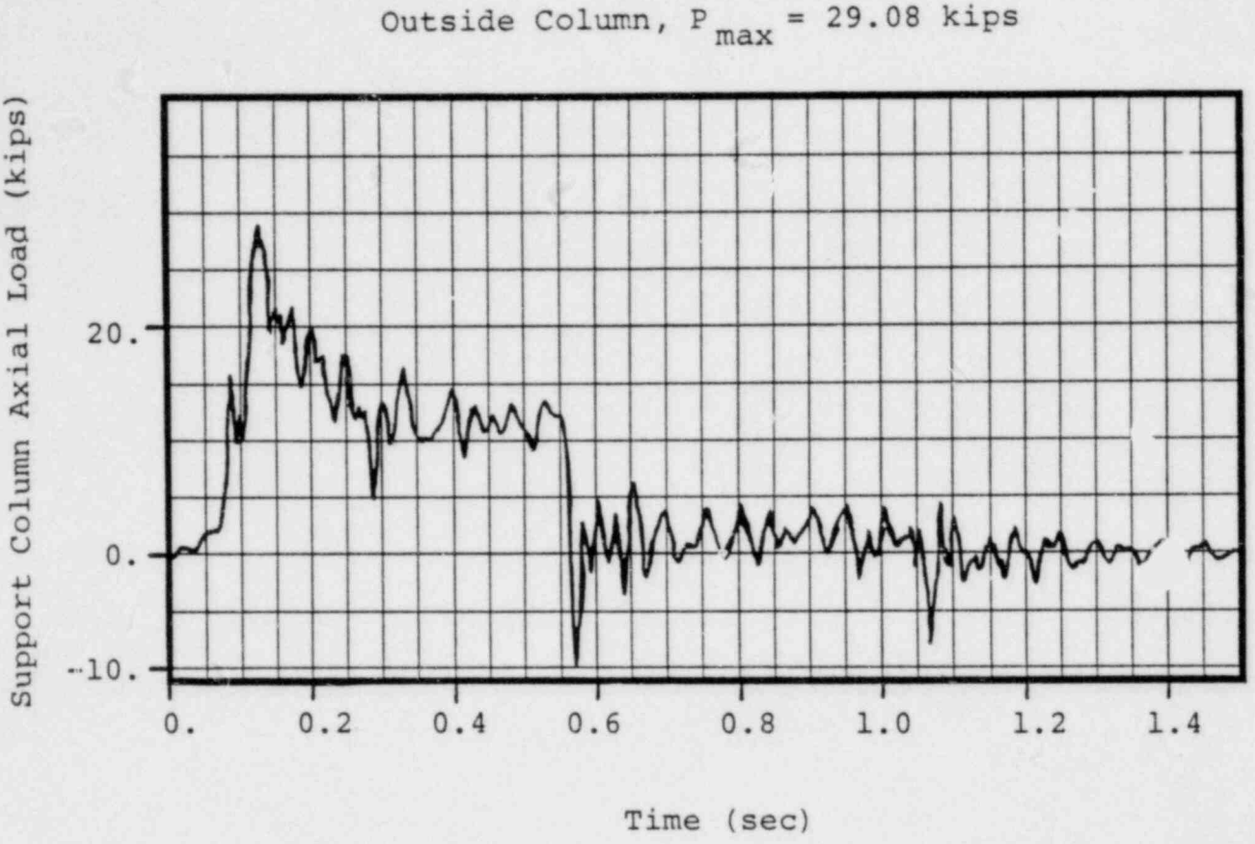

Figure 3-2.5-1

VENT SYSTEM SUPPORT COLUMN RESPONSE DUE TO POOL SWELL IMPACT LOADS-OUTSIDE COLUMN

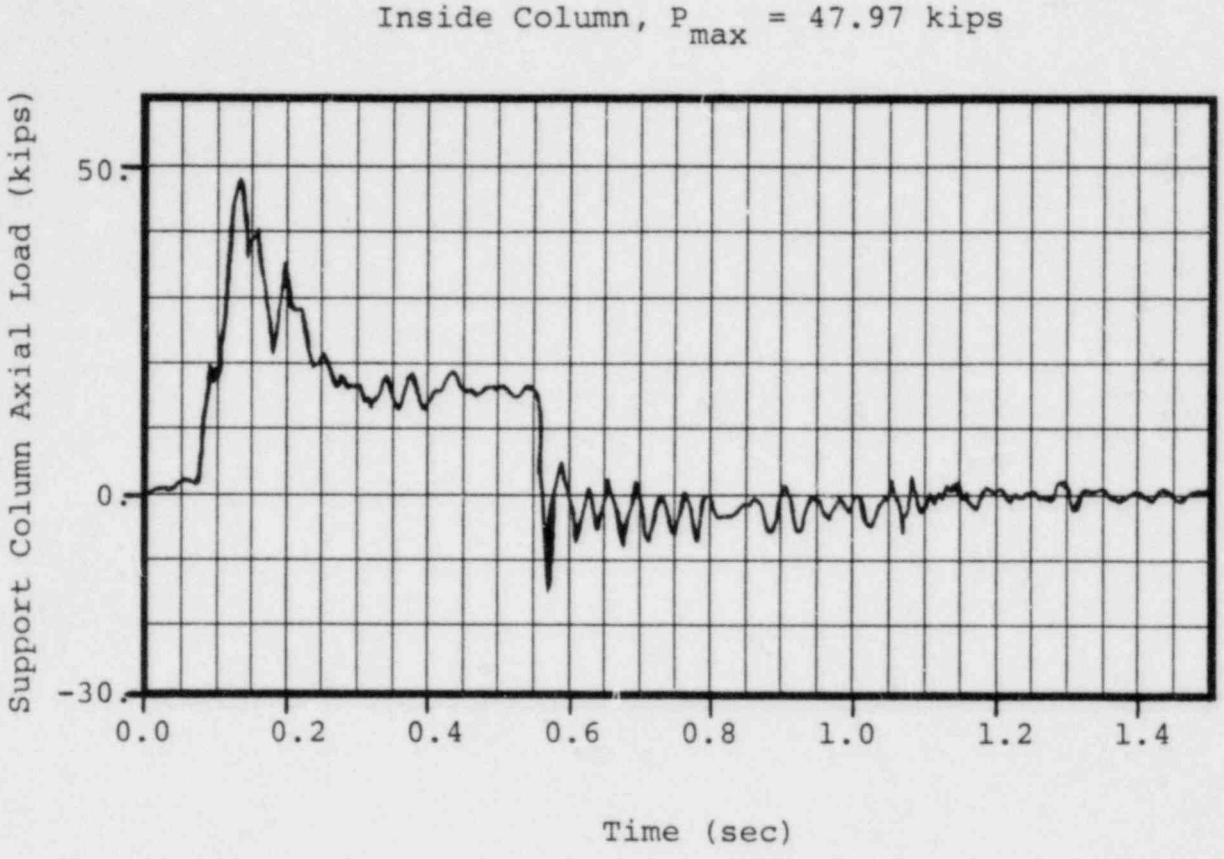

Figure 3-2.5-2

VENT SYSTEM SUPPORT COLUMN RESPONSE DUE TO POOL SWELL IMPACT LOADS - INSIDE COLUMN

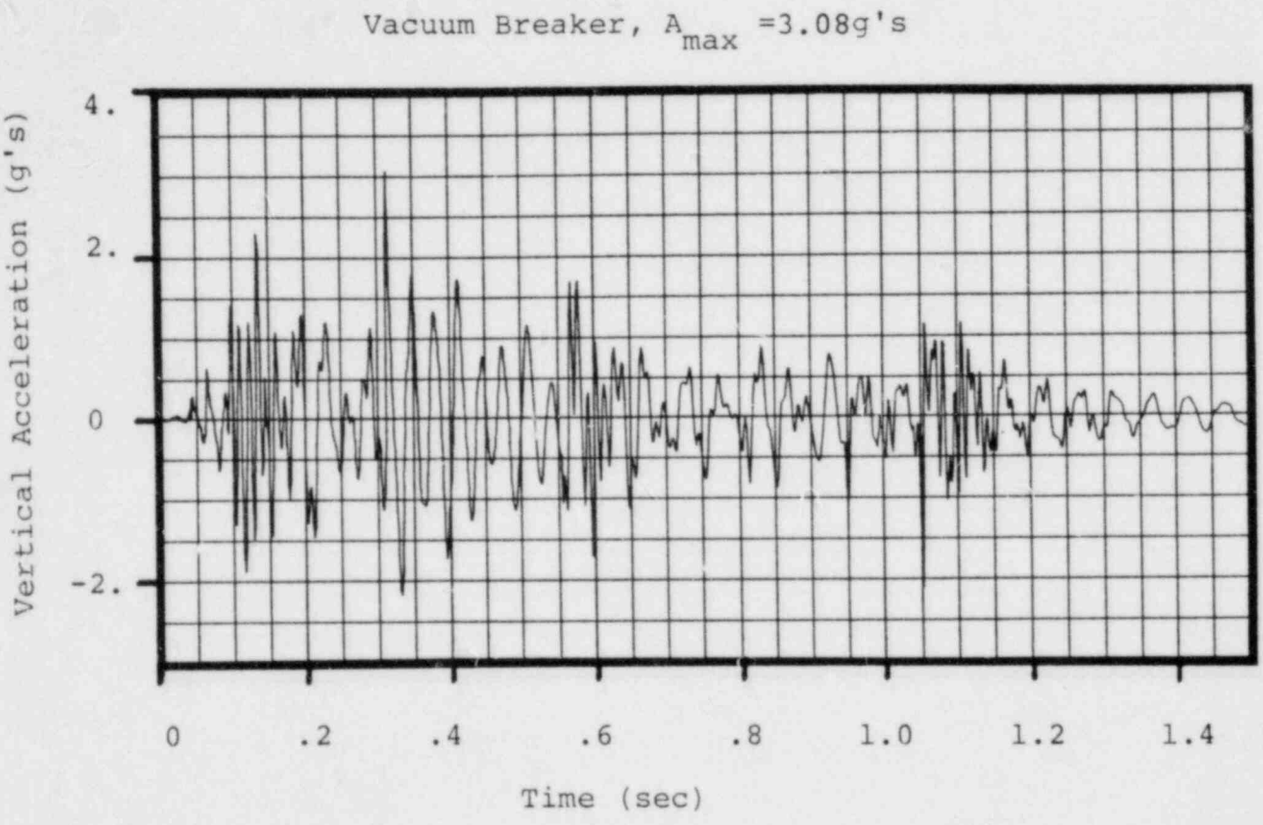

Figure 3-2.5-3

VACUUM BREAKER RESPONSE DUE TO

POOL SWELL IMPACT LOADS

3-2.5.1 Discussion of Analysis Results

The results shown in Table 3-2.5-1 indicate that the largest vent system primary membrane stresses occur for internal pressure loads, vent system discharge loads, pool swell impact loads, DBA condensation oscillation downcomer loads, and chugging downcomer lateral loads. The remaining loadings result in small primary stresses in the vent system major components.

Table 3-2.5-2 shows that the largest vent system support column reactions occur for internal pressure loads, vent system discharge loads, pool swell impact loads, and DBA condensation oscillation loads. The distribution of loads between the inner and outer support columns varies from load case to load case. The magnitude and distribution of reaction loads on the drywell penetrations also vary from load case to load case, as shown in Table 3-2.5-3. Table 3-2.5-4 shows that the differential displacements of the vent line bellows are small for all loadings but thermal loadings.

The results shown in Table 3-2.5-5 indicate that the highest stresses in the vent system components, component supports, and associated welds occur for the SBA II

and the DBA II load combinations. The vent line, vent header, and downcomer stresses for the SBA II and DBA II load combination are less than the allowable limits with stresses in other vent system components, component supports, and welds well within the allowable limits. The stresses in the vent system components, component supports, and welds for the IBA I, DBA I, and DBA III load combinations are also well within the allowable limits.

The results shown in Table 3-2.5-7 indicate that the vent line bellows differential displacements are all well within allowable limits. The maximum displacement occurs for the SBA II load combination.

The loads which cause the highest number of displacement cycles at the vent line bellows are seismic loads, SRV loads, and LOCA related loads such as pool swell, condensation oscillation, and chugging. The bellows displacements for these loads are small compared to the maximum allowable displacement and their effect on fatigue is negligible. Thermal loads and internal pressure loads are the largest contributors to bellows displacements. The specified number of thermal load and internal pressure load cycles is 150. Since the bellows

have a rated capacity of 500 cycles at maximum displacement, their adequacy for fatigue is assured.

The vent system fatigue usage factors shown in Table 3-2.5-8 are computed for the controlling events, which are Normal Operating plus SBA and Normal Operating plus IBA. The governing vent system component for fatigue is the vent header at the downcomer-vent header intersection. The magnitudes and cycles of downcomer lateral loads are the primary contributors to fatigue at this location.

The governing venc system weld for fatigue is the nozzle to gusset weld at the SRV penetration to the vent line. SRV temperature and thrust loads and the number of SRV actuations are the major contributors to fatigue at this location.

Fatigue effects at other locations in the vent system are less severe than at those described above, due primarily to lower stresses and a lesser number of stress cycles.

3-2.5.2 Closure

The vent system loads described and presented in Section 3-2.2.1 are conservative estimates of the loads postulated to occur during an actual LOCA or SRV discharge event. Applying the methodology discussed in Section 3-2.4 to examine the effects of the governing loads on the vent system results in bounding values of stresses and reactions in vent system components and component supports.

The load combinations and event sequencing defined in Section 3-2.2.2 envelop the actual events postulated to occur during a LOCA or SRV discharge event. Combining the vent system responses to the governing loads and evaluating fatigue effects using this methodology results in conservative values of the maximum vent system stresses, support reactions, and fatigue usage factors for each event or sequence of events postulated to occur throughout the life of the plant.

The acceptance limits defined in Section 3-2.3 are at least as restrictive, and in many cases more restrictive, than those used in the original containment design documented in the plant's FSAR. Comparing the resulting

maximum stresses and support reactions to these acceptance limits results in a conservative evaluation of the design margins present in the vent system and vent system supports. As is demonstrated from the results discussed and presented in the preceding sections, all of the vent system stresses and support reactions are within these acceptance limits.

As a result, the components of the vent system described in Section 3-2.1, which are specifically designed for the loads and load combinations used in this evaluation, exhibit the margins of safety inherent in the original design of the primary containment as documented in the plant's FSAR. The intent of the NUREG-0661 requirements, as it relates to the design adequacy and safe operation of the Fermi 2 vent system, is therefore considered to be met.

3-3.0 LIST OF REFERENCES

1. "Mark I Containment Long-Term Program," Safety Evaluation Report, NRC, NUREG-0661, July 1980.

2. "Mark I Containment Program Load Definition Report," General Electric Company, NEDO-21888, Revision 2, December 1981.

3. "Mark I Containment Program Plant Unique Load Definition," Enrico Fermi Atomic Power Plant Unit 2, General Electric Company, NEDO-24568, Revision 1, June 1981.

4. Enrico Fermi Atomic Power Plant Unit 2, Final Safety Analysis Report (FSAR), Detroit Edison Company, Section 3.8, Amendment 12, June 1978.

5. "Mark I Containment Program Structural Acceptance Criteria Plant Unique Analysis Application Guide, Task Number 3.1.3," General Electric Company, NEDO-24583-1, October 1979.

6. ASME Boiler and Pressure Vessel Code, Section III, Division 1, 1977 Edition with Addenda up to and including Summer 1977.